

**Page Denied**

Next 48 Page(s) In Document Denied

sm

Y.A. VASANOV x/, Y.G.JULEV xx/

OPTIMUM CONTOUR OF HEAT REJECTING  
TRIANGULAR FINS WITH MUTUAL IRRADIATION BETWEEN  
FINS AND COOLED BASE SURFACES. THE SYSTEM OF  
PARALLEL STAR - SHAPED RADIATORS. EFFECTS OF THE  
THERMAL RESISTANCE OF COATINGS

x/ Ingeneer, Moscow In-te of Physics and Technics.

xx/ Kandidat of Technics, Moscow In-te of Physics and Technics.

In the present paper the results of the theoretical investigation of the star-shaped radiators are discussed.

The paper consists of the three parts. The first part deals with the one-dimensional problem of the optimum size and number of heat rejection triangular fins radially arranged at the apices of the polyhedral prism with mutual irradiation of the fins and the surface of the cooled prism.

The numerical solution of the problem is obtained with the assumption that the temperature gradient across the fin is negligible in comparison with that of along the fin and surroundings are assumed as a black body of zero temperature. The relationships of dimensionless parameters are given which determine the optimum (with respect to weight) number of fins and their geometry for any combination of the cooled prism temperature and size, amount of the rejected heat, the emissivity of radiating fins and heat conductivity of the fin material.

It is found that the optimum (in the sense of weight) number of radiating fins increases from 4 for black emitting surfaces to about 10-11 for the emissivity of these surfaces of the order of 0.5.

In the second part the thermal radiation characteristics of the infinite system of the four-fin-star-shaped coplanar radiators are calculated taking into account the mutual irradiation of all radiator elements. The problem is solved numerically under the same assumptions as in the first part. The relationships of the dimensionless parameters are given which allow to calculate all the optimal characteristics of the system for any distance between the adjacent radiators of the system. In the third part the problem is discussed taking into consideration the effect of the thermal resistance of the coating which may be used for increasing the emissivity of the radiating surfaces on the thermal radiation characteristics of the four-fin-star-shaped radiators. In addition to the above assumptions it was suggested that the heat rates along the fin in the coating are negligible in comparison with the heat rates along the fin. The given relationships of the dimensionless parameters describe the effectiveness of the coating for any heat conductivity of the latter and the radiator parameters.

§ I. Optimum Contour of Heat Rejecting Triangular Fins  
with Mutual Irradiation between Fins and Cooled Base Surfaces

Let us consider the one-dimensional problem of determination of the optimum size and number of heat rejecting triangular fins radially arranged at the apices of the polyhedral prism taking into account mutual irradiation of the fins and the base surface (Fig.1). In the case of negligible base-surface size such a problem was discussed for the fins of the optimum (Ref.1) and triangular contour (Ref.2).

We shall deal with the thin fins for which the law of thermal radiation and the equation of thermal convection along a fin are true in the form of:

$$\frac{1}{2} Q(x) = -\lambda(L-x) \frac{\alpha}{2} \frac{dT}{dx} \quad (1)$$

$$\frac{1}{2} dQ(x) = -q(x) dx \quad (2)$$

where  $Q(x)$  - the heat flow through the fin section with  $x$ -position

$\lambda$  - the fin material thermal conductivity coefficient.

$\alpha$  - the angle between the side faces of a fin

$q(x) dx$  - the resultant radiation from the fin surface element.

Equations (1) and (2) lead to the following expression for the determination of temperature distribution along a fin:

$$(L-x) \frac{d^2T}{dx^2} - \frac{dT}{dx} - \frac{q(x)}{\lambda \frac{\alpha}{2}} = 0 \quad (3)$$

Consider first the trapezoidal fins of length  $L$ , (Fig.1). In this case the boundary conditions for equation (3) may be written as

a)  $T = T_0$  at  $x = 0$ , b)  $\frac{dT}{dx} = 0$  at  $x = L$ , (4)

When determining  $q(x)$  we shall assume that the fin surface radiating element is at the central plane and the parameters of the surroundings

$\epsilon_{\text{sur}} = 1$  and  $T_{\text{sur}} = 0$ . Then the expression for  $q(x)$  will have the form of (Ref.3)

$$\begin{aligned} q(x) &= B(x) - H_{x-z}(x) - H_{y-z}(x) = \\ &= B(x) - \frac{1}{2} \int_{z_0}^{z_0+2} B(z) \frac{(z_0+z)(z_0+x) \sin^2 \gamma dz}{[(z_0+z)^2 + (z_0+x)^2 - 2(z_0+z)(z_0+x) \cos \gamma]^{3/2}} \end{aligned} \quad (5)$$

$$- \frac{1}{2} \int_{y-z}^{y-z+2} B_1(y) \frac{x y \cos^2 \gamma/2 dy}{(x^2 + y^2 + 2xy \sin \gamma/2)^{3/2}},$$

where  $\gamma = \frac{2\pi}{n}$  is the angle between the central planes of two adjacent fins.

In equation (5)  $B(x)$ ,  $B(z)$ ,  $B_1(y)$  - the effective radiant flows per unit area and time leaving the fin surfaces  $x^*$ ,  $z^*$  and the prism surfaces  $y^*$  are determined by the following relations:

$$B(x) = \epsilon G T^4(x) + (1-\epsilon)[H_{x \rightarrow x}(x) + H_{y \rightarrow x}(x)] \quad (6)$$

$$B(z) = \epsilon G T^4(z) + (1-\epsilon)[H_{x \rightarrow z}(z) + H_{y \rightarrow z}(z)] \quad (7)$$

$$B(y) = \epsilon G T_0^4 + (1-\epsilon)[H_{x \rightarrow y}(y) + H_{y \rightarrow y}(y)] \quad (8)$$

where  $H_{x \rightarrow x}(x)$ ,  $H_{y \rightarrow x}(x)$ ;  $H_{x \rightarrow z}(z)$ ,  $H_{y \rightarrow z}(z)$  - are the heat flows transferred from the adjacent fin and the prism surfaces to the fin which is of interest;

$H_{x \rightarrow y}(y)$ ,  $H_{y \rightarrow y}(y)$  - are the heat flows from the fins to the prism surface.

The relations determining  $H_{x \rightarrow x}(x)$ ,  $H_{y \rightarrow x}(x)$  are evident from equation (5). The heat flow  $H_{y \rightarrow z}(z)$  is determined by the following expression:

$$H_{y \rightarrow z}(z) = \frac{1}{2} \int_{\bar{x}}^{y-z} B_i(y) \frac{z(y-y) \cos^2 \frac{\delta}{2} dy}{[(y-y)^2 + z^2 + 2z(y-y) \sin \frac{\delta}{2}]^{3/2}} \quad (9)$$

The heat flow relations  $H_{x \rightarrow z}(z)$ ;  $H_{x \rightarrow y}(y)$ ;  $H_{y \rightarrow y}(y)$  are obtained from the expressions for  $H_{x \rightarrow x}(x)$ ,  $H_{y \rightarrow x}(x)$ ,  $H_{y \rightarrow z}(z)$ , provided that their variables are interchanged.

Introduce the following dimensionless variables:

$$\bar{T} = \frac{T}{T_0}; \bar{x} = \frac{x}{L}; \bar{z} = \frac{z}{L}; \bar{y} = \frac{y}{L};$$

$$\bar{z}_0 = \frac{z_0}{L}; \bar{L} = \frac{L}{\lambda G T_0}; \bar{H} = \frac{H}{G T_0} \quad (10)$$

After integration with the use of the second boundary condition, the equation (9) in these variables will be written as

$$(\bar{L} - \bar{x}) \frac{d\bar{T}}{d\bar{x}} + N \int_{\bar{x}}^1 [\bar{B}(\bar{x}) - \bar{H}_{x \rightarrow x}(\bar{x}) - \bar{H}_{y \rightarrow x}(\bar{x})] d\bar{x} = 0 \quad (11)$$

$$N = \frac{L_i G T_0^3}{\lambda \frac{d\bar{x}}{dx}} \quad (12)$$

$$\bar{B}(\bar{x}) = \epsilon \bar{T}^4(\bar{x}) + (1-\epsilon)[\bar{H}_{x \rightarrow x}(\bar{x}) + \bar{H}_{y \rightarrow x}(\bar{x})] \quad (13)$$

$$\bar{B}_i(\bar{y}) = \epsilon + (1-\epsilon)[\bar{H}_{x \rightarrow y}(\bar{y}) + \bar{H}_{y \rightarrow y}(\bar{y})] \quad (14)$$

$$\bar{H}_{x \rightarrow x}(\bar{x}) = \frac{1}{2} \int_0^1 \bar{B}(\bar{z}) \frac{(\bar{z}_0 + \bar{z})(\bar{z}_0 + \bar{x}) \sin^2 \frac{\delta}{2} d\bar{z}}{[(\bar{z}_0 + \bar{z})^2 + (\bar{z}_0 + \bar{x})^2 - 2(\bar{z}_0 + \bar{z})(\bar{z}_0 + \bar{x}) \cos \frac{\delta}{2}]^{3/2}} \quad (15)$$

$$\bar{H}_{y \rightarrow x}(\bar{x}) = \frac{1}{2} \int_0^1 \bar{B}_i(\bar{y}) \frac{\bar{x} \bar{y} \cos^2 \frac{\delta}{2} d\bar{y}}{(\bar{x}^2 + \bar{y}^2 + 2\bar{x}\bar{y} \sin \frac{\delta}{2})^{3/2}} \quad (16)$$

$$\bar{H}_{x \rightarrow y}(\bar{y}) = \frac{1}{2} \int_0^1 \bar{B}(\bar{x}) \frac{\bar{x} \bar{y} \cos^2 \frac{\delta}{2} d\bar{x}}{(\bar{x}^2 + \bar{y}^2 + 2\bar{x}\bar{y} \sin \frac{\delta}{2})^{3/2}} \quad (17)$$

$$\bar{H}_{y \rightarrow y}(\bar{y}) = \frac{1}{2} \int_0^1 \bar{B}(\bar{z}) \frac{2(\bar{y}-\bar{z}) \cos^2 \frac{\delta}{2} d\bar{z}}{[\bar{z}^2 + (\bar{y}-\bar{z})^2 + 2\bar{z}(\bar{y}-\bar{z}) \sin \frac{\delta}{2}]^{3/2}} \quad (18)$$

Due to symmetry of the problem,  $\bar{B}(\bar{x}) \equiv \bar{B}(\bar{z})$  at  $\bar{x} = \bar{z}$  the boundary condition for equation (11) will be  $\bar{T} = 1.0$  at  $\bar{x} = 0$

According to equation (5) the heat loss from the surfaces of one fin will be written in the dimensionless variables as

$$q_{fin} = 2L_0 \sigma T_0^4 \int_0^1 [\bar{B}(\bar{x}) - \bar{H}_{x \rightarrow x}(\bar{x}) - \bar{H}_{y \rightarrow x}(\bar{x})] d\bar{x} \quad (19)$$

Since resultant heat flow radiated from the surface of the cooled prism equals to

$$q_{pr} = B_1(y) - H_{x \rightarrow y}(y) - H_{z \rightarrow y}(y) \quad (20)$$

the amount of the heat in the dimensionless variables radiated from prism surface will be determined by the following expression:

$$q_{pr} = L_0 \sigma T_0^4 \int_0^{y_0 - \delta} [\bar{B}_1(\bar{y}) - \bar{H}_{x \rightarrow y}(\bar{y}) - \bar{H}_{z \rightarrow y}(\bar{y})] d\bar{y} \quad (21)$$

Let us find the emission coefficient  $\gamma$  of the system which is the ratio of the heat  $(q_{fin} + q_{pr})n$  radiated by the system to the heat  $q_{ideal}$  which would be radiated by this system if the fin material conductivity were infinitely high and  $\epsilon$  were one ( $R=1.5$ ).

The expression for  $q_{ideal}$  has the form

$$q_{ideal} = 2n(L_0 + \bar{z}_0) \sigma T_0^4 \sin^{\delta/2} \quad (22)$$

and the emission coefficient is determined by

$$\gamma = \frac{1}{2(1+\bar{z}_0) \sin^{\delta/2}} \left\{ 2 \int_0^1 \bar{q}_{res}(\bar{x}) d\bar{x} + \int_0^{y_0 - \delta} \bar{q}_{res}(\bar{y}) d\bar{y} \right\} \quad (23)$$

from which it is seen that this coefficient is a function of the parameters  $N$ ,  $\gamma$ ,  $\bar{z}_0$  and  $\epsilon$ . Thus, the heat radiated by the system equals to

$$q_\epsilon = \gamma q_{ideal} = 2n\gamma L_0 (1+\bar{z}_0) \sigma T_0^4 \sin^{\delta/2}. \quad (24)$$

The solution of the set of equations (11) through (18) and (23) for the triangular fins was derived numerically as an asymptotical one at  $L \rightarrow 1.0$  and  $\delta \rightarrow 0$ .

The relationships between the emission coefficient  $\gamma$  and the dimensionless thermal conduction parameter  $N$  are given in figures 2, 3, 4 and 5 for various values of the parameters  $\gamma$ ,  $\bar{z}_0$  and  $\epsilon$ .

By using the relationships of figures 2 through 5 and having a number of fins and  $\epsilon$  selected, the optimum geometry of triangular fins can be easily determined provided that the temperature  $T_0$ , the prism size  $\bar{z}_0$  and the amount of the radiated heat are known. Really, using the relationships

$\gamma = \gamma(N)$  for selected  $n$ ,  $\epsilon$  and  $\bar{z}_0$  values, one can determine  $\alpha$  from expressions (12) and (24) for a number of  $L$  values and, thus, evaluate the minimum area of a fin. This calculation results are represented in figures 6, 7 and 8 where  $F$  and  $\bar{z}_0$  are the dimensionless variables, related with

physical magnitudes by the following expressions:

$$\bar{F} = \frac{F}{F_{opt}} ; \quad \bar{\Sigma}_o^* = \frac{\Sigma_o}{\frac{q_x}{\epsilon \sigma T_o^4}}, \quad (25)$$

where  $F$  is the total cross-section area of the system of the optimum triangular fins,  $F_{opt} = \frac{q_x}{\lambda G^2 \epsilon^2 T_o}$  is the cross-section area of the optimum fin of minimum weight (Ref.4).

In figure 9 the relationships between  $N_{opt}$  and  $\bar{\Sigma}_o^*$  are given. Using them together with the figures 6, 7, 8 the optimum fin geometry can be determined immediately.

The relations  $\bar{F} = \bar{F}(n)$  at  $\bar{\Sigma}_o^* = 0$ , represented in figures 6, 7 and 8, correspond to the case of the negligible prism size.

In accordance with equation (24), at  $\bar{\Sigma}_o^* = \frac{1}{2n \sin \delta/2}$  a complete degeneration of fins occurs (in this case  $\bar{F} = 0$  and  $\bar{\Sigma}_o^* = \infty$ ).

It is evident that equally with increasing the optimum fin number when the emissivity diminishes the optimum fin number increases with the increase of the parameter  $\bar{\Sigma}_o^*$ .

The dotted curve for the system of the optimum fins equally spaced around a base prism is given in figure 6 (Ref.1). It is seen that at

$\bar{\Sigma}_o^* = 0$  and  $\epsilon = 1.0$  the change of the optimum fins by the triangular fins results in the increase of the fin cross-section by about 6 per cent.

## § 2. Theoretical Investigation of Thermal Radiation Characteristics of Infinite Parallel Star-Shaped Radiator System

Consider the problem of calculation of the thermal radiation characteristics of the infinite radial coplanar radiator system having the heat rejecting triangular fins (Fig.10).

The mathematical model of the radiator system section is shown in figure 10a with the main geometrical parameters.

The governing equation for the problem solution are the energy conservation equations for the arbitrary elements  $dV_1$ ,  $dV_2$  of the transversal and longitudinal radiator fins (Fig.10b)

$$(L-x) \frac{d^2 T_1}{dx^2} - \frac{dT_1}{dx} - \frac{q_{res}(x)}{\lambda \cdot \alpha/2} = 0 \quad (26)$$

$$(L-x) \frac{d^2 T_2}{dx^2} - \frac{dT_2}{dx} - \frac{q_{res}(x)}{\lambda \cdot \alpha/2} = 0, \quad (27)$$

where  $q_{res}(x)$ ,  $q_{res}(z)$  are the resulting radiation flows from the side faces  $dS_1$ ,  $dS_2$  of the elements  $dV_1$ ,  $dV_2$ .

First, consider the trapezoidal fins (Fig.10b). In this case one can write the following boundary conditions for equations (26), (27):

6

$$T_1 = T_0 \text{ at } x=0 \quad (28)$$

$$\frac{dT_1}{dx} = 0 \text{ at } x=L_1 \quad (29)$$

$$T_2 = T_0 \text{ at } z=0 \quad (30)$$

$$\frac{dT_2}{dz} = 0 \text{ at } z=L_2 \quad (31)$$

According to the method of the resulting radiation, expressions describing the flows of the resulting radiation  $q_{12es}(x)$ ,  $q_{21es}(z)$  have the following form:

$$q_{12es}(x) = B_1(x) - H_{x \rightarrow x}(x) - H_{y \rightarrow x}(x) - H_{i \rightarrow x}(x) - H_{j \rightarrow x}(x) - H_{k \rightarrow x}(x) \quad (22)$$

$$q_{21es}(z) = B_2(z) - H_{x \rightarrow z}(z) - H_{y \rightarrow z}(z) - H_{j \rightarrow z}(z) - H_{k \rightarrow z}(z) \quad (23)$$

where

$$B_1(x) = EGT_1^4(x) + (1-E)[H_{y \rightarrow x}(x) + H_{i \rightarrow x}(x) + H_{k \rightarrow x}(x) + H_{j \rightarrow x}(x) + H_{x \rightarrow x}(x)] \quad (24)$$

is the flow of the effective radiation from the side face  $dS_1$  or the element  $dV_1$ ,

$$B_2(z) = EGT_2^4(z) + (1-E)[H_{x \rightarrow z}(z) + H_{y \rightarrow z}(z) + H_{k \rightarrow z}(z) + H_{j \rightarrow z}(z)] \quad (25)$$

is the flow of the effective radiation from the side face  $dS_2$  or the element  $dV_2$  (Fig. 10b),

$H_{x \rightarrow x}(x)$ ;  $H_{y \rightarrow x}(x)$ ;  $H_{i \rightarrow x}(x)$ ;  $H_{j \rightarrow x}(x)$ ;  $H_{k \rightarrow x}(x)$  are the total heat flows radiated from the surfaces denoted by the first letter of the index to the surface  $dS_1$ ,  $H_{x \rightarrow z}(z)$ ;  $H_{y \rightarrow z}(z)$ ;  $H_{j \rightarrow z}(z)$ ;  $H_{k \rightarrow z}(z)$  are the total heat flows radiated from the surfaces "x"; "y"; "j"; "k" to the elemental surface  $dS_2$ .

Similarly, the flow of resulting radiation leaving the base surface equals to

$$q_{32es}(y) = B_3(y) - H_{x \rightarrow y}(y) - H_{z \rightarrow y}(y) - H_{k \rightarrow y}(y) - H_{j \rightarrow y}(y) - H_{i \rightarrow y}(y) \dots \quad (30)$$

where

$$B_3(y) = EGT_0^4 + (1-E)[H_{x \rightarrow y}(y) + H_{z \rightarrow y}(y) + H_{k \rightarrow y}(y) + H_{j \rightarrow y}(y) + H_{i \rightarrow y}(y)] \quad (31)$$

is the flow of the effective radiation from the base surface and

$H_{x \rightarrow y}(y)$ ;  $H_{z \rightarrow y}(y)$ ;  $H_{k \rightarrow y}(y)$ ;  $H_{j \rightarrow y}(y)$ ;  $H_{i \rightarrow y}(y)$  are the total heat flows radiated from the surfaces, denoted by the first letter of the index, to the base surface.

Integration of equations (26) and (27) using the boundary conditions (29), (31) and the dimensionless variables (10) yields the following set of the equations for the radiator:

$$(\bar{\lambda} - \bar{x}) \frac{dT_1}{d\bar{x}} + N \int_{\bar{x}}^{\bar{x}} \bar{q}_{1, \text{res}}(\bar{x}) d\bar{x} = 0 \quad (24a)$$

$$(\bar{\lambda} - \bar{x}) \frac{dT_2}{d\bar{x}} + N \int_{\bar{x}}^{\bar{x}} \bar{q}_{2, \text{res}}(\bar{x}) d\bar{x} = 0, \quad (24b)$$

where

$$N = \frac{\lambda \cdot \sigma T_0^3}{\lambda \cdot \frac{d\bar{x}}{dx}} \quad (24c)$$

$$\bar{q}_{1, \text{res}}(\bar{x}) = \bar{B}_1(\bar{x}) - \bar{H}_{x \rightarrow x}(\bar{x}) - \bar{H}_{y \rightarrow x}(\bar{x}) - \bar{H}_{i \rightarrow x}(\bar{x}) - \bar{H}_{j \rightarrow x}(\bar{x}) - \bar{H}_{k \rightarrow x}(\bar{x}) \quad (24d)$$

$$\bar{q}_{2, \text{res}}(\bar{x}) = \bar{B}_2(\bar{x}) - \bar{H}_{x \rightarrow x}(\bar{x}) - \bar{H}_{y \rightarrow x}(\bar{x}) - \bar{H}_{j \rightarrow x}(\bar{x}) - \bar{H}_{k \rightarrow x}(\bar{x}) \quad (24e)$$

$$\begin{aligned} \bar{B}_1(\bar{x}) = & \epsilon \bar{T}_1^4(\bar{x}) + (1-\epsilon) [\bar{H}_{y \rightarrow x}(\bar{x}) + \bar{H}_{x \rightarrow x}(\bar{x}) + \\ & + \bar{H}_{k \rightarrow x}(\bar{x}) + \bar{H}_{j \rightarrow x}(\bar{x}) + \bar{H}_{i \rightarrow x}(\bar{x})] \end{aligned} \quad (24f)$$

$$\begin{aligned} \bar{B}_2(\bar{x}) = & \epsilon \bar{T}_2^4(\bar{x}) + (1-\epsilon) [\bar{H}_{x \rightarrow x}(\bar{x}) + \bar{H}_{y \rightarrow x}(\bar{x}) + \\ & + \bar{H}_{k \rightarrow x}(\bar{x}) + \bar{H}_{j \rightarrow x}(\bar{x})] \end{aligned} \quad (24g)$$

$$\bar{H}_{x \rightarrow x}(\bar{x}) = \frac{1}{2} \int_0^{\bar{x}} \bar{B}_2(\bar{x}) \frac{(\bar{x}_0 + \bar{x})(\bar{x}_0 + \bar{x}) d\bar{x}}{[(\bar{x}_0 + \bar{x})^2 + (\bar{x}_0 + \bar{x})^2]^{3/2}} \quad (30)$$

$$\bar{H}_{y \rightarrow x}(\bar{x}) = \frac{1}{4} \int_0^{\bar{x}} \bar{B}_3(\bar{y}) \frac{\bar{x} \bar{y} d\bar{y}}{(\bar{x}^2 + \bar{y}^2 + \bar{x} \bar{y} \sqrt{2})^{3/2}} \quad (31)$$

$$\bar{y} = j, \bar{x} = \bar{x}_0 \sqrt{2}; \bar{x}_0 = \frac{\Delta}{\lambda}; \bar{\Delta} = \frac{\Delta}{\lambda_1^2} \quad (40)$$

$$\bar{H}_{k \rightarrow x}(\bar{x}) = \frac{1}{2} \int_0^{\bar{x}} \bar{B}_1(\bar{k}) \frac{(2\bar{x}_0 + \bar{k} + 2)^2 d\bar{k}}{[(\bar{k} - \bar{x}) + (2\bar{x}_0 + \bar{k} + 2)^2]^{3/2}} \quad (41)$$

$$\bar{H}_{i \rightarrow x}(\bar{x}) = \frac{1}{2} \int_0^{\bar{x}} \bar{B}_2(\bar{i}) \frac{(\bar{x}_0 + \bar{i})^2 + (\bar{x}_0 + \bar{i} + 2 - \bar{i})^2 d\bar{i}}{[(2\bar{x}_0 + \bar{i} + 2) \sqrt{2} - \bar{i}] (2\bar{x}_0 + \bar{i} + 2 + \bar{i}) d\bar{i}} \quad (42)$$

$$\bar{H}_{j \rightarrow x}(\bar{x}) = \frac{1}{\sqrt{2}} \int_0^{\bar{x}} \bar{B}_3(\bar{j}) \frac{[(\bar{x}\sqrt{2} + \bar{j})^2 + [(2\bar{x}_0 + \bar{j} + 2)\sqrt{2} - \bar{j}]^2]}{[(2\bar{x}_0 + \bar{j} + 2)\sqrt{2} - \bar{j}] (2\bar{x}_0 + \bar{j} + 2 + \bar{j})} d\bar{j} \quad (43)$$

$$\bar{H}_{x \rightarrow x}(\bar{x}) = \frac{1}{2} \int_0^{\bar{x}} \bar{B}_1(\bar{x}) \frac{(\bar{x}_0 + \bar{x})(\bar{x}_0 + \bar{x}) d\bar{x}}{[(\bar{x}_0 + \bar{x})^2 + (\bar{x}_0 + \bar{x})^2]^{3/2}} \quad (44)$$

$$\bar{H}_{y \rightarrow x}(\bar{x}) = \frac{1}{4} \int_0^{\bar{x}} \bar{B}_3(\bar{y}) \frac{\bar{x}(\bar{y}_0 - \bar{y}) d\bar{y}}{[\bar{x}^2 + (\bar{y}_0 - \bar{y})^2 + \bar{x}(\bar{y}_0 - \bar{y})\sqrt{2}]^{3/2}} \quad (45)$$

$$\bar{H}_{k \rightarrow x}(\bar{x}) = \frac{1}{2} \int_0^{\bar{x}} \bar{B}_1(\bar{k}) \frac{(\bar{x}_0 + \bar{k})(\bar{x}_0 + \bar{k} + 2 - \bar{x}) d\bar{k}}{[(\bar{x}_0 + \bar{k})^2 + (\bar{x}_0 + \bar{k} + 2 - \bar{x})^2]^{3/2}} \quad (46)$$

$$\bar{H}_{j \rightarrow x}(\bar{x}) = \frac{1}{2\sqrt{2}} \int_0^{\bar{x}} \bar{B}_3(\bar{j}) \frac{(\bar{x}_0 - \frac{\bar{j}}{\sqrt{2}})(2 + \bar{j} - \bar{x}) d\bar{j}}{[(\bar{x}_0 - \frac{\bar{j}}{\sqrt{2}})^2 + (\bar{x}_0 + \bar{j} + 2 - \frac{\bar{j}}{\sqrt{2}} - \bar{x})^2]^{3/2}} \quad (47)$$

$$\bar{B}_3(\bar{y}) = E + (1-E) [\bar{H}_{x \rightarrow y}(\bar{y}) + \bar{H}_{2 \rightarrow y}(\bar{y}) + \bar{H}_{k \rightarrow y}(\bar{y}) + \bar{H}_{j \rightarrow y}(\bar{y}) + \bar{H}_{i \rightarrow y}(\bar{y})]. \quad (37a)$$

$$\bar{H}_{x \rightarrow y}(\bar{y}) = \frac{1}{4} \int_0^1 \bar{B}_1(\bar{x}) \frac{\bar{x} \bar{y} d\bar{x}}{(\bar{x}^2 + \bar{y}^2 + \bar{x} \bar{y} \sqrt{2})^{3/2}} \quad (48).$$

$$\bar{H}_{2 \rightarrow y}(\bar{y}) = \frac{1}{4} \int_0^1 \bar{B}_2(\bar{x}) \frac{\bar{x} \bar{y} d\bar{x}}{[\bar{x}^2 + (\bar{y} - \bar{y})^2 + \bar{x}(\bar{y} - \bar{y})\sqrt{2}]^{3/2}} \quad (49)$$

$$\bar{H}_{k \rightarrow y}(\bar{y}) = \frac{1}{2} \int_0^1 \bar{B}_1(\bar{x}) \frac{(2+2\bar{x}+\bar{e}+\bar{k})^2 + [(2+\bar{e}-\bar{x})+(\bar{y}-\bar{y})\sqrt{2}]^2}{[(2+2\bar{x}+\bar{e}+\bar{k})^2 + [(2+\bar{e})+(\bar{y}-\bar{y})\sqrt{2}]^2]^{3/2}} d\bar{x} \quad (50)$$

$$\bar{H}_{j \rightarrow y}(\bar{y}) = \frac{1}{\sqrt{2}} \int_{\bar{j}-\delta}^{\bar{j}+\delta} \bar{B}_3(\bar{j}) \frac{[(2+\bar{e})+(\bar{y}-\bar{y})\sqrt{2}] \cdot [(2+\bar{e})+(\bar{j}-\bar{j})\sqrt{2}] d\bar{j}}{[(2+\bar{e})+(\bar{y}-\bar{y})\sqrt{2}]^2 + [(2+\bar{e})+(\bar{j}-\bar{j})\sqrt{2}]^2}^{1/2} \quad (51)$$

$$\bar{H}_{i \rightarrow y}(\bar{y}) = \frac{1}{\sqrt{2}} \int_0^1 \bar{B}_2(\bar{i}) \frac{(\bar{y}-\bar{y})(2+\bar{e}-\bar{i}) d\bar{i}}{[(2+\bar{e}-\bar{i})+(\bar{y}-\bar{y})\sqrt{2}]^2 + [(2+\bar{e}-\bar{i})^2]^{3/2}} \quad (52)$$

The boundary conditions for equations (26a) and (27a) are

$$\bar{T}_1 = 1.0 \quad \text{at } \bar{x} = 0 \quad (28a)$$

$$\bar{T}_2 = 1.0 \quad \text{at } \bar{x} = 0 \quad (30a)$$

The expressions for the total heat flows which are concluded into the above set of the equations have been obtained on the basis of the formula for the elemental heat flow radiated from the infinitely thin and long strip  $d_3$  to elemental area  $dS$  (Fig. 10c), (Ref. 3).  $dH = B \frac{dS \sin \theta}{2}$  assuming that radiating elements or the fin surfaces are their central planes.

The set of equations (26a), (27a), (28a), (30a), (35a), (37a) together with the boundary conditions (28a), (30) and formulas (52a), (53a), (58) through (52) determines the problem solution completely.

From the results of the problem solution the total radiator-section heat loss data are of the most practical interest. The amount of the heat radiated from one face of a transversal fin (of unit width) is determined by the following expression:

$$Q_{fin} = L, \sigma T_0^4 \int_0^1 \bar{q}_{fin}(\bar{x}) d\bar{x} \quad (53)$$

Similarly, the heat loss from one face of a longitudinal fin equals to

$$Q_{zfin} = L, \sigma T_0^4 \int_0^1 \bar{q}_{zfin}(\bar{z}) d\bar{z} \quad (54)$$

According to equation (50) the amount of the heat, radiated by the prism surface (of unit width) will be written as

$$Q_{spz} = L, \sigma T_0^4 \int_{\bar{j}-\delta}^{\bar{j}+\delta} \bar{q}_{spz}(\bar{y}) d\bar{y} \quad (55)$$

The overall heat loss from a section of the radiator of the unit width equals to

$$Q_z = L, \sigma T_0^4 [ \int_0^1 \bar{q}_{fin}(\bar{x}) d\bar{x} + \int_0^1 \bar{q}_{zfin}(\bar{z}) d\bar{z} + \int_{\bar{j}-\delta}^{\bar{j}+\delta} \bar{q}_{spz}(\bar{y}) d\bar{y} ] \quad (56)$$

To compare the individual radiator section effectiveness with the effectiveness of a similar section of the radiator system, let us express an emission coefficient by the relation

$$\zeta = \frac{Q_z}{Q_{ideal}} \quad (57)$$

where

$$Q_{\text{ideal}} = \sqrt{2} G T_0^4 L, (1 + \bar{\epsilon}_0) \quad (58)$$

According to formula (56) one obtains

$$\zeta = \frac{\int' \bar{q}_{123s}(\bar{x}) d\bar{x} + \int' \bar{q}_{23s}(\bar{x}) d\bar{x} + \int' \bar{q}_{32s}(\bar{y}) d\bar{y}}{\sqrt{2}(1 + \bar{\epsilon}_0)} \quad (57a)$$

It follows from formula (57a) and the set of equations (20a), (21a), (32a) through (52) that the emission coefficient is a function of the parameters  $N, \bar{\epsilon}_0, \bar{\epsilon}, \bar{\ell}, \bar{\delta}, \bar{L}$ . At  $\bar{\ell} \rightarrow \infty$  the emission coefficient  $\zeta$  determines the efficiency of the single radiator section considered in the first section of this paper (§ 1).

If the relations  $\zeta(N, \bar{\epsilon}_0, \bar{\epsilon}, \bar{\ell}, \bar{\delta}, \bar{L})$  are known the overall heat loss from the radiator section is determined by

$$Q_x = \sqrt{2}(1 + \bar{\epsilon}_0) \zeta L G \bar{T}_0^4 \quad (58a)$$

The solution for the case of the triangular heat rejecting fins has been derived as an asymptotical one with  $L = \frac{1}{\bar{\ell}} \rightarrow 1.0$  and  $\bar{\delta} \rightarrow 0$  from the set of equations (20a), (21a), (32a) through (52) together with the boundary conditions (28a), (30a). The solution has been carried out numerically for the general case of the arbitrary distance between the adjacent radiators of the system ( $\bar{\ell} = 0 \pm \infty$ ) in the range of emissivity values  $\bar{\epsilon} = 1.0 \pm 0.75$ .

The emission coefficients are plotted in fig. 11 through 15 as a function of the dimensionless heat conductivity parameter for the various values of the parameters  $\bar{\epsilon}_0, \bar{\epsilon}, \bar{\ell}$ .

The relationships  $\zeta(N)$  at  $\bar{\ell} > 10$  practically agree with the similar relations for the individual radiator, considered in the first section.

Using the relationships given in the figures 11 through 15 and the specified values of  $\bar{\epsilon}$  and  $\bar{\ell}$ , one can find the optimum triangular fins geometry, provided that the fin base temperature  $T_0$ , the overall heat loss from one section  $Q_x$  and the prism "radius"  $\bar{\epsilon}_0$  are known.

When determining the optimum geometry in the case of the following calculation, procedure may be ordered. Setting a number of the values of  $\bar{\epsilon}_0 = \frac{\bar{\epsilon}_0}{L}$  one finds corresponding  $L$  values and  $\zeta$  values, determined by formula (58a).

Furthermore, using the relationships of figures 11 through 15<sup>x)</sup> we determine the values of the dimensionless heat conductivity parameter  $N$ . From formula 12a determine the values of the angle  $\alpha$ .

x) The relationships  $\zeta(N)$  for the intermediate  $\bar{\epsilon}_0$  values can be obtained by the graphical interpolation of the curves, presented in figures 11 through 15.

10

Finally, the area  $F$ , the length  $\ell_1$  and the angle  $\alpha$  are plotted against  $\bar{\epsilon}_0$ , therefrom the optimum fin geometry is determined. In the case of  $\bar{\epsilon}_0 = 0$  the optimum fin geometry is calculated immediately for a number of  $N$  values with  $\hat{y}(N)$  being used (Fig.11 through 15). The results of such calculations of the total optimum triangular fin area are presented in figure 16 where  $\bar{F}$  and  $\bar{\epsilon}_0^*$  are the dimensionless parameters related with the physical magnitudes by expressions (25). For comparison the curves of the one-dimensional minimum area of the triangular fins for the radiator system without the transversal heat rejecting fins are also shown in this figure in dotted lines for the values of the parameter  $\bar{\ell} = 0; 2.0$  and  $\bar{\epsilon} = 1.0; 0.875; 0.75$ .

It is evident from the comparison of  $\bar{F}$  ( $\bar{\epsilon}_0^*$ ) curves that at  $\bar{\ell} = 0$  the system of the radiators with the transversal heat rejecting fins is more advantageous than the system without such fins only when the emissivity  $\bar{\epsilon} = 0.85 \pm 0.9$ . The result obtained in this particular case of the problem confirms G.Z.Grodzovsky's idea: that is, the weight characteristics of a usual panel radiator may be improved at the expense of additional transversal fins installed on the tube. When the dimensionless distance  $\bar{\ell}$  is increased an advantage of the system with the transversal heat rejecting fins over the one without such fins becomes evident. In addition, the charts of figure 16 illustrate clearly the difference between the radiator system and the single radiator weight characteristics.

Relations between the emission coefficient  $\bar{\epsilon}_1$  and the dimensionless heat conductivity parameter  $N$  are shown in figure 17 for various values of the parameters  $\bar{\epsilon}_0$ ,  $\bar{\epsilon}$  and  $\bar{\ell} = 0$  for the radiator system without the transversal heat rejecting fins with the longitudinal triangular fins. The emissivity coefficient  $\bar{\epsilon}_1$  is determined by the formula

$$\bar{\epsilon}_1 = \int_0^{\bar{y}-\bar{\delta}} \bar{q}_{\text{ees}}(\bar{x}) d\bar{x} + \int_{\bar{\delta}}^{\bar{y}} \bar{q}_{\text{ses}}(\bar{y}) dy \quad (59)$$

which expresses the ratio of the total amount of the heat, radiated by the radiator section of unit width (one side of the fin plus the cooled prism surface) to the ideal amount of the heat radiated by the black isothermal fin surface when the incident radiation is absent ( $Q_{\text{ideal}} = L_0 \bar{G} T_0^4$ ).

### § 3. Influence of Coating Thermal Resistance on Heat Radiation Characteristics of Star-Shaped Radiators

Consideration of the coating thermal resistance effect on the radiation efficiency is of great practical interest for both evaluation of the coatings used and selection of the correction factors which must be introduced when theoretical investigation results are used without taking into consideration the thermal resistance of coatings.

The problem of taking into account the coating thermal resistance in the simplest case of the panel radiator with rectangular fins (Fig.18a) was discussed in the reference 6. In the present paper the problem of evaluation of the coating thermal resistance influence is discussed in the general case.

11

or radiation with mutual irradiation of all the construction elements (the heat rejecting triangular fins, the base surfaces) being taken into account (Fig. 18b); this enables more exact selection of the correct factor values.

The radiator scheme with the main geometrical parameters is shown in the figure 1c.

The problem solution is being developed in the one-dimensional statement (thin fins) under the following assumptions:

- a) the heat rejecting fins of the radiator have an identical geometry
- b) the fin material and coating thermophysical properties are independent of a temperature

$$\lambda = \text{constant}, \lambda_1 = \text{constant}, \epsilon_1 = \text{constant}$$

- c) the temperature of the cooled prism is uniform

$$T_o = \text{constant}, t_o = \text{constant}$$

- d) the parameters of the surrounding  $\epsilon_{sur} = 1.0; T_{sur} = 0^\circ K$

- e) the radiating surfaces are grey diffusely reflecting surfaces

- f) the coating temperature gradient in the direction of the fin length as compared to that in the direction of normal to the fin surface is negligible small.

The governing equations used in the solution of the problem are the ones describing law of energy conservation

$$\frac{1}{2} dQ_{\text{accum}} = dQ_{\text{cond}} \quad (60)$$

$$dQ_{\text{cond}} = q_{\text{res}}(x) dS, \quad (61)$$

where

$dQ_{\text{accum}}$  is the amount of the heat accumulated in the element  $dV$  (Fig. 18a) due to net conduction

$dQ_{\text{cond}}$  is the amount of the heat flowing through the coating area  $dS$

$dS$  is the side face of the element  $dV$

$q_{\text{res}}(x) dS$  is the resultant radiation from the side face

By applying Fourier's Law, we can easily transform equations (60), (61) to the form of the equations which describe the temperature profile along the radiator fin

$$\frac{\lambda_1}{\delta} [T(x) - t(x)] = q_{\text{res}}[t(x)] \quad (61a)$$

$$(L-x) \frac{dT}{dx^2} - \frac{dT}{dx} - \frac{q_{\text{res}}[t(x)]}{\lambda \frac{\delta}{2}} = 0. \quad (60a)$$

where

$\lambda; \lambda_1$  are the thermal conductivity coefficient of the fin material and the coating, respectively.

$\delta$  is the coating thickness

$t(x)$  is the temperature of the cooling radiating surface

$T(x)$  is the fin temperature.

12

As above, consider first the trapezoidal fins of  $L_1$  length (Fig. 10a). In this case the following boundary conditions for equation (o3a) are taking:

$$T = T_0 \text{ at } x = 0 \quad (o2)$$

$$\frac{dT}{dx} = 0 \text{ at } x = L_1 \quad (o3)$$

According to the method of the resultant radiation expression for the resultant radiation flow  $q_{\text{res}}[t(x)]$  from the side face  $dS$  of the element  $dV$  is written as follows:

$$q_{\text{res}}(x) = B(x) - H_{z-x}(x) - H_{y-x}(x) \quad (o4)$$

where

$$B(x) = E_1 G t^4(x) + (1-E_1) [H_{z-x}(x) + H_{y-x}(x)] \quad (o5)$$

is the effective radiation flow leaving the side face  $dS$  of the element  $dV$ .

$H_{z-x}(x); H_{y-x}(x)$  are the total heat flows radiated from the surfaces, denoted by the first letter of the index, to the surface  $dS$ .

When deriving the formulas for  $H_{z-x}(x); H_{y-x}(x)$  the assumption is made that the radiating element or the fin surface is in its central plane. Then (Ref. 3).

$$H_{z-x}(x) = \frac{1}{2} \int_0^{L_1} B(z) \frac{(z_0+z)(z_0+x) \sin^2 \frac{x}{2} dz}{[(z_0+z)^2 + (z_0+x)^2 - 2(z_0+z)(z_0+x) \cos \frac{x}{2}]^{3/2}} \quad (o6)$$

$$H_{y-x}(x) = \frac{1}{2} \int_0^{L_1} B(y) \frac{x y \cos^2 \frac{x}{2} dy}{(x^2 + y^2 + 2xy \sin \frac{x}{2})^{3/2}} \quad (o7)$$

In equation (o7)

$$B_1(y) = E_1 G t_0^4 + (1-E_1) [H_{x-y}(y) + H_{z-y}(y)] \quad (o8)$$

is the flow of the effective radiation from the base surface.  $H_{x-y}(y); H_{z-y}(y)$  are the total heat flows radiated from the fin surfaces to the base surfaces or the prism;

$$H_{x-y}(y) = \frac{1}{2} \int_0^{L_1} B(x) \frac{x y \cos^2 \frac{x}{2} dx}{(x^2 + y^2 + 2xy \sin \frac{x}{2})^{3/2}} \quad (o9)$$

$$H_{z-y}(y) = \frac{1}{2} \int_0^{L_1} B(z) \frac{z(y-y) \cos^2 \frac{z}{2} dz}{[z^2 + (y-y)^2 + 2z(y-y) \sin \frac{z}{2}]^{3/2}} \quad (10)$$

It is convenient to transform the set of equations (o3a), (o3b), (o4) through (10) together with the boundary conditions (o2), (o3) into the dimensionless form by introducing the nondimensional variables

$$\bar{x} = \frac{x}{L_1}; \bar{z} = \frac{z}{L_1}; \bar{y} = \frac{y}{L_1}; \bar{t} = \frac{t}{T_0} \quad (11)$$

$$\bar{T} = \frac{T}{T_0}; \bar{H} = \frac{H}{G T_0^4}; \bar{B} = \frac{B}{G T_0^4}; \bar{L} = \frac{L}{L_1}$$

As a result of the transformation and the integration of equation (o3a) together with the boundary condition (o3) the set of the equations will be

13

written in the following form:

$$(L - \bar{x}) \frac{d\bar{T}}{d\bar{x}} + N \int_{\bar{x}}^1 \bar{q}_{res} [\bar{t}(\bar{x})] d\bar{x} = 0 \quad (60b)$$

$$\bar{T} = \bar{t} + N_1 \bar{q}_{res} [\bar{t}(\bar{x})] \quad (61b)$$

where

$$N = \frac{\lambda_1 \sigma T_0^3}{\lambda_2 \frac{d}{dx}} \quad (72)$$

$$N_1 = \frac{\delta \sigma T_0^3}{\lambda_1} \quad (73)$$

$$\bar{q}_{res} [\bar{t}(\bar{x})] = \bar{B}(\bar{x}) - \bar{H}_{x \rightarrow x}(\bar{x}) - \bar{H}_{y \rightarrow x}(\bar{x}) \quad (64a)$$

$$\bar{B}(\bar{x}) = E_1 \bar{t}_o^4(\bar{x}) + (1-E_1) [\bar{H}_{y \rightarrow x}(\bar{x}) + \bar{H}_{z \rightarrow x}(\bar{x})] \quad (65a)$$

$$\bar{H}_{y \rightarrow x}(\bar{x}) = \frac{1}{2} \int_0^1 \bar{B}(\bar{y}) \frac{\bar{x} \bar{y} \cos^2 \frac{\chi}{2} d\bar{y}}{(\bar{x}^2 + \bar{y}^2 + 2\bar{x}\bar{y} \sin \frac{\chi}{2})^{3/2}} \quad (67a)$$

$$\bar{H}_{z \rightarrow x}(\bar{x}) = \frac{1}{2} \int_0^1 \bar{B}(\bar{z}) \frac{(\bar{z}_o + \bar{x})(\bar{z}_o + \bar{x}) \sin^2 \gamma d\bar{z}}{[(\bar{z}_o + \bar{x})^2 + (\bar{z}_o + \bar{x})^2 - 2(\bar{z}_o + \bar{x})(\bar{z}_o + \bar{x}) \cos \gamma]^{3/2}} \quad (66a)$$

$$\bar{z}_o = \frac{z_o}{\lambda_1}, \quad \bar{y}_1 = \frac{y_1}{\lambda_1} = 2\bar{z}_o \sin \frac{\chi}{2} \quad (74)$$

$$\bar{B}_o(\bar{y}) = E_1 \bar{t}_o^4 + (1-E_1) [\bar{H}_{x \rightarrow y}(\bar{y}) + \bar{H}_{z \rightarrow y}(\bar{y})] \quad (68a)$$

$$\bar{H}_{x \rightarrow y}(\bar{y}) = \frac{1}{2} \int_0^1 \bar{B}(\bar{x}) \frac{\bar{x} \bar{y} \cos^2 \frac{\chi}{2} d\bar{x}}{(\bar{x}^2 + \bar{y}^2 + 2\bar{x}\bar{y} \sin \frac{\chi}{2})^{3/2}} \quad (69a)$$

$$\bar{H}_{z \rightarrow y}(\bar{y}) = \frac{1}{2} \int_0^1 \bar{B}(\bar{z}) \frac{\bar{z}(\bar{y}_1 - \bar{y}) \cos^2 \frac{\chi}{2} d\bar{z}}{[\bar{z}^2 + (\bar{y}_1 - \bar{y})^2 + 2\bar{z}(\bar{y}_1 - \bar{y}) \sin \frac{\chi}{2}]^{3/2}} \quad (70a)$$

The boundary condition for equation (60b) is

$$\bar{T} = 1.0 \text{ at } \bar{x} = 0 \quad (62a)$$

The set of equations (60b), (61b), (64a) through (70a) in conjunction with the boundary condition (62a) determines completely the solution of the problem.

The solution of the written set of equations was developed by analogy with the solution of the problems considered in the previous sections of this report. The emission coefficient  $\delta$  was determined by the formula similar to formula (23). From the formula (23) and the above set of the equations it follows that for the case of triangular profile  $\delta$  is a function of the parameters  $N, N_1, z_o, E_1$  and  $\gamma$ .

14

For the case of the four-fin star-shaped radiator with the triangular fins the results of the numerical solution developed in the range of the emissivity  $\epsilon = 1.0 \div 0.75$  and of the values of parameter  $N = 0 \div 0.03$  are shown in figures 19 and 20. The emission coefficient relations  $\beta(\nu)$  at  $N = 0$  correspond to the case of the radiator without coating which has been considered in the first section of this paper.

In the process of the calculation the dimensionless thermal conduction parameter  $N$  has took on the values of 0, 0.25, 0.5, 1.0, 1.5, 2.0, 2.5, 3.0. The relations presented clearly illustrate the influence of the thermal resistance of coatings on the radiation efficiency.

#### БИБЛИОГРАФИЯ

1. ЭРЮБ В.В. "Оптимальная форма теплоотводящих ребер с учетом взаимного облучения". Изв. АН СССР ОТН Энергетика и автомобилика № 6 1962.
2. B.V.KARLEKAN and B.T.CHAO. "Mass minimization of radiating trapezoidal fins with negligible base cylinder Interaction" International Journal of Heat and Mass Transfer v.6.N1. 1963.
3. ЯКОБ М. "Вопросы теплопередачи" ИЛ 1960.
4. ГРОДЗОВСКИЙ Г.Л. "Оптимальная форма теплоотводящих ребер, охлаждаемых излучением". Изв. АН СССР, ОТН. Энергетика и автомобилика. № 6. 1962.
5. SPARROW M., ECKERT E.R.G., IRVINE T.F.Ir. "The Effectiveness of Radiating Fins with Mutual Irradiation" J.the Aerospace Sciences, October, 1961, v.28, N 10.
6. PLAMONDON J.A. "Thermal Efficiency of Coated Fins" Journal of Heat Transfer. vol.84. Series C. №4. 1962.

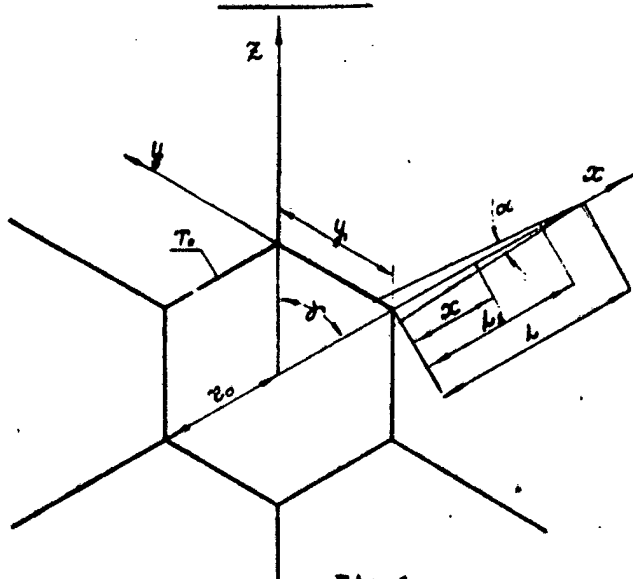


Fig. 1

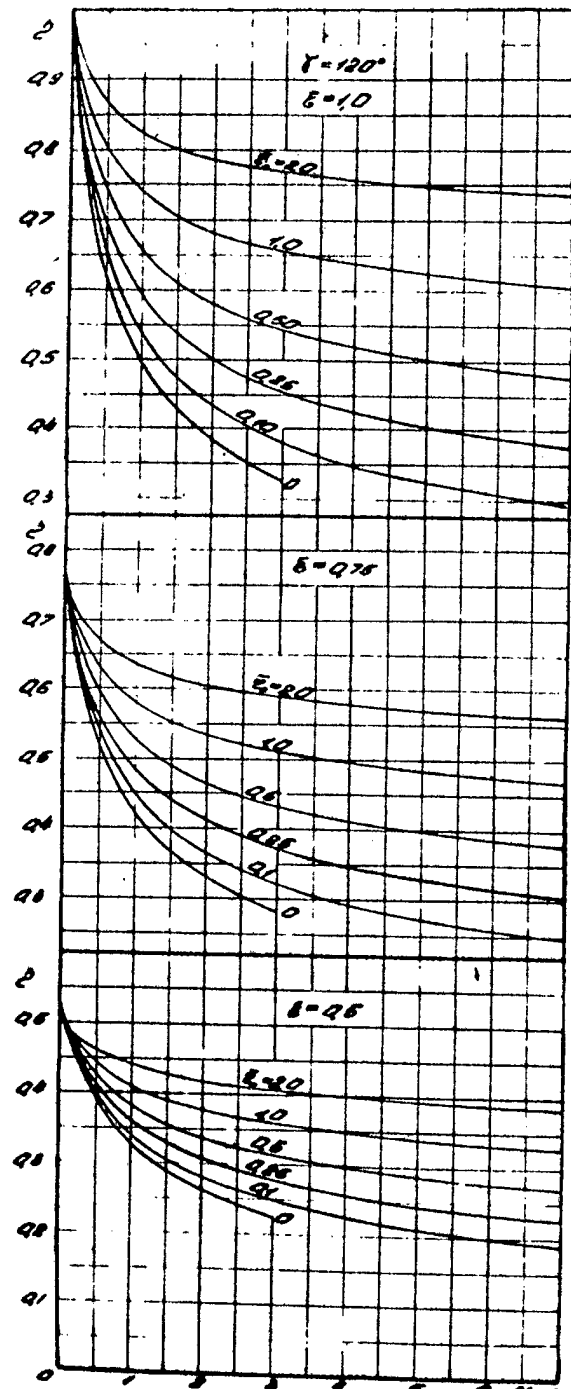


Fig. 2

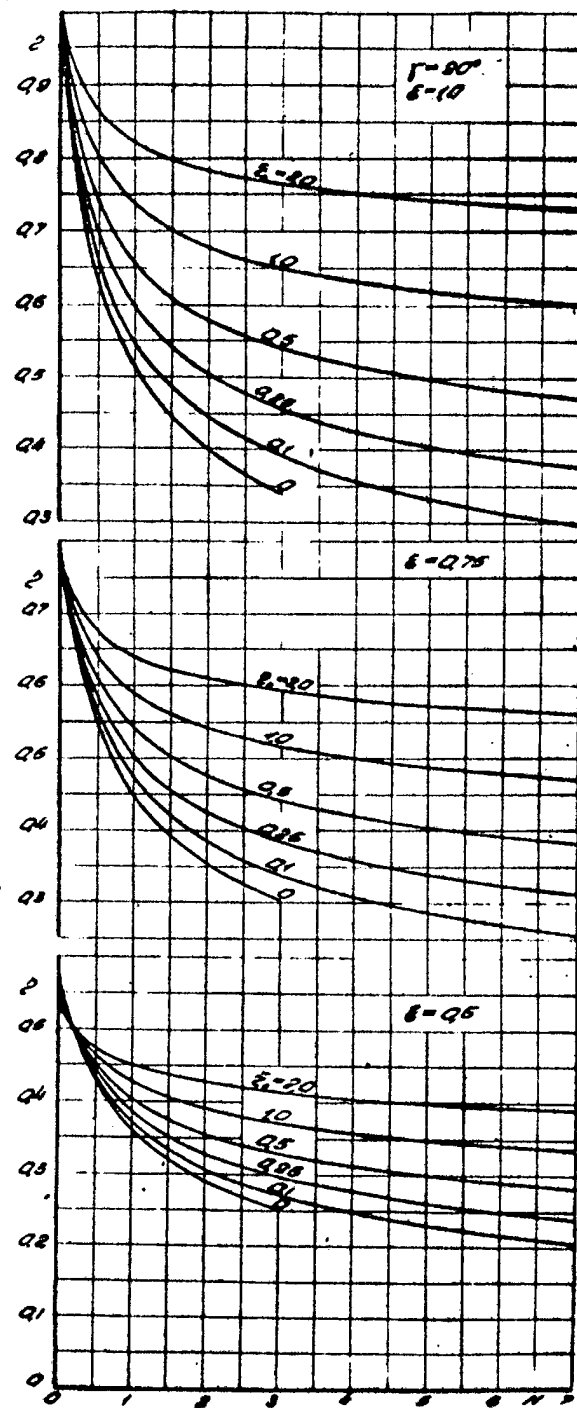


Fig. 3

16

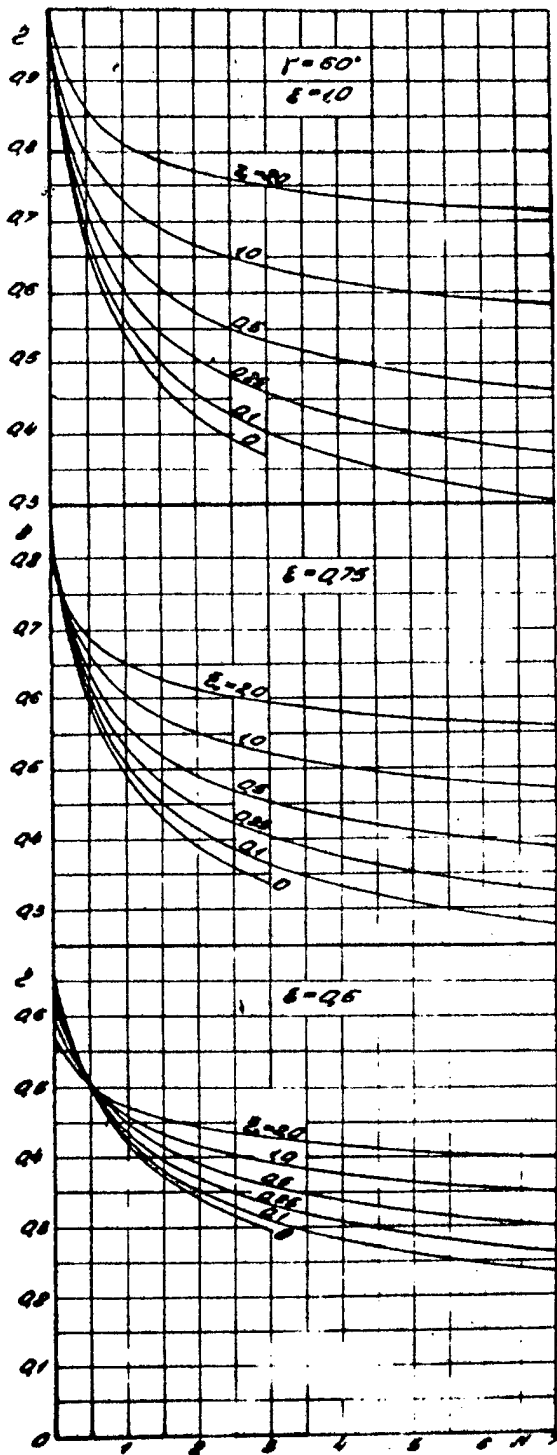


Fig.4

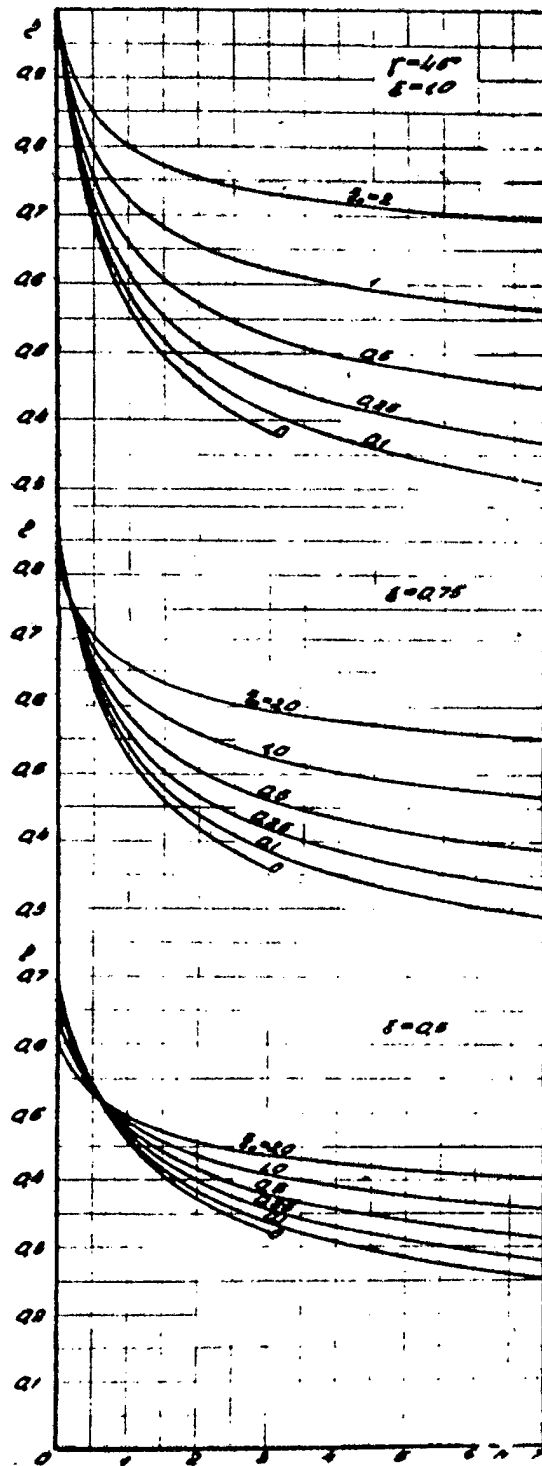


Fig.5

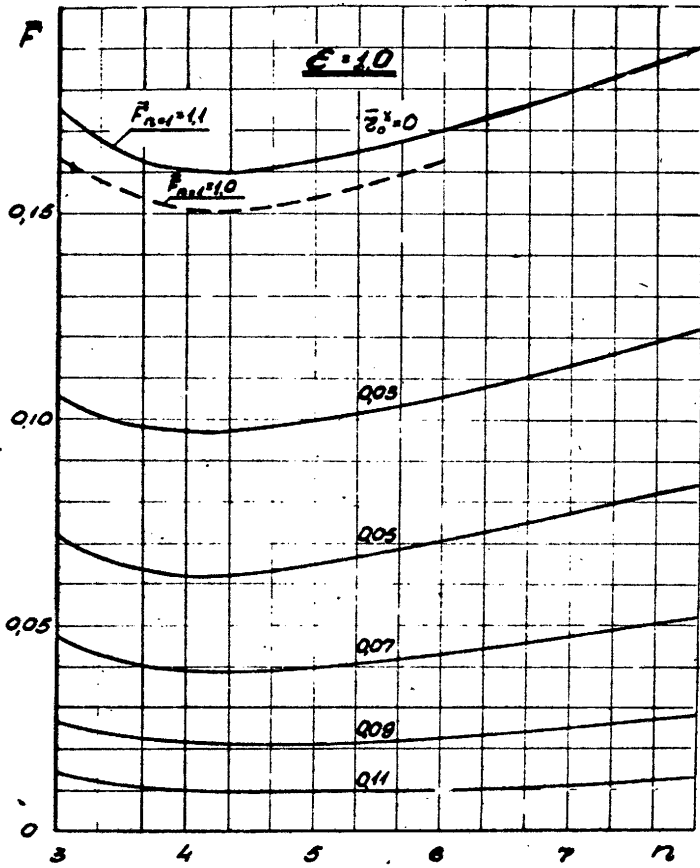


Fig.6

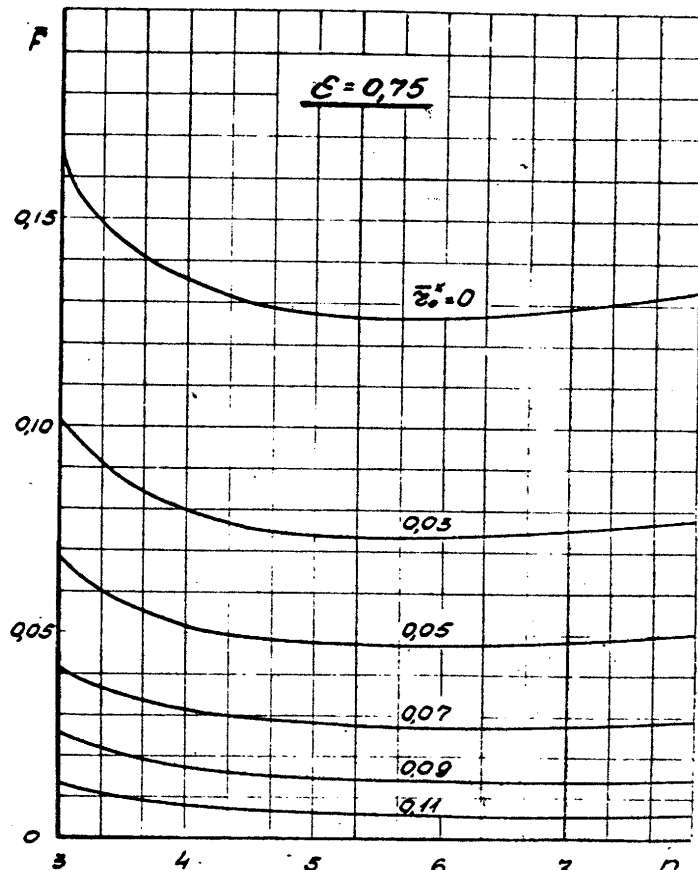


Fig.7

18

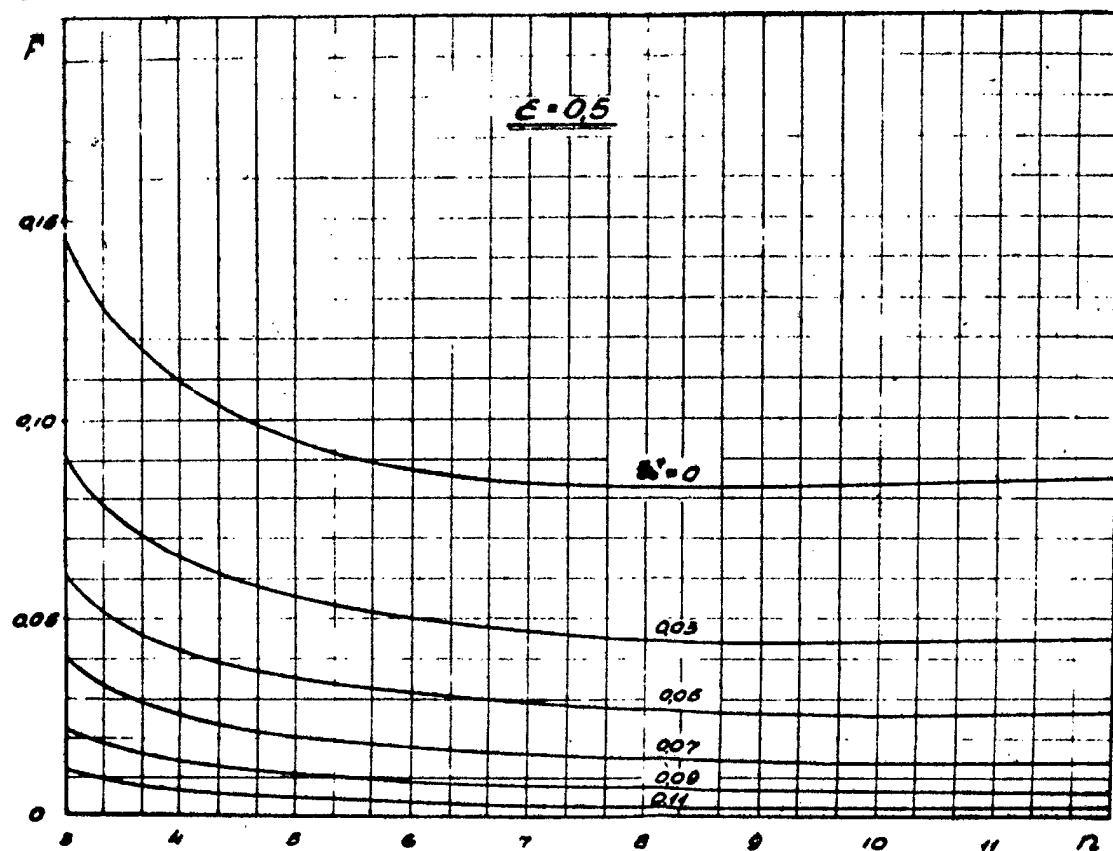


Fig. 8

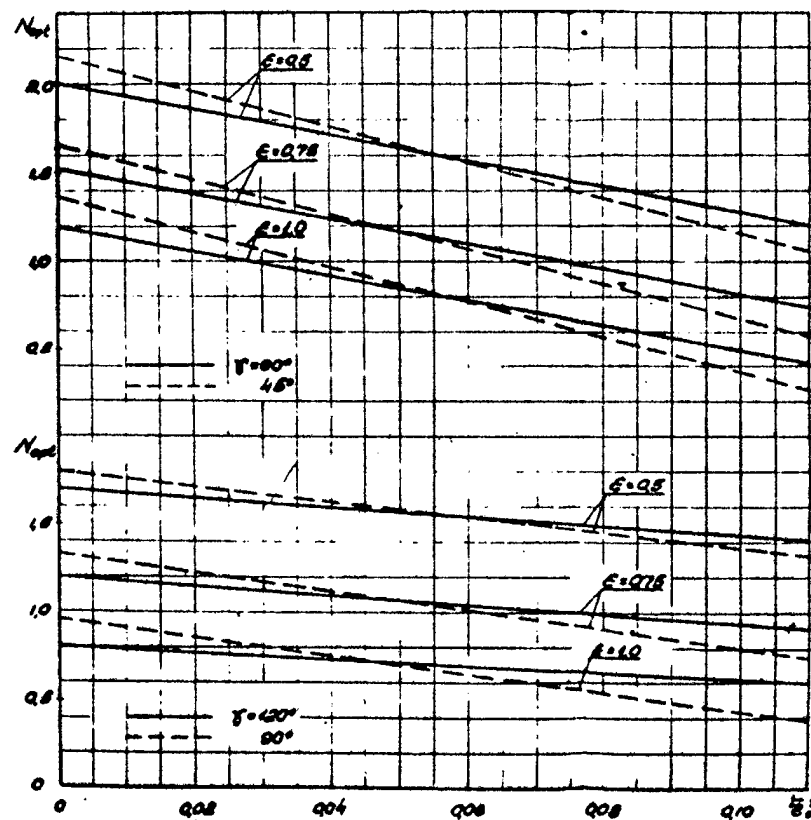


Fig. 9

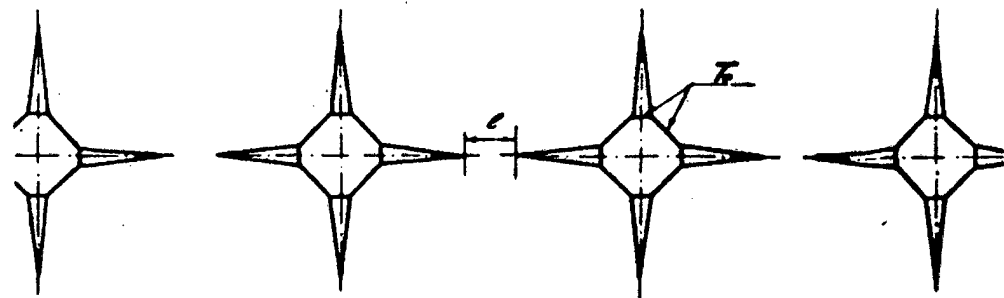


Fig. 10

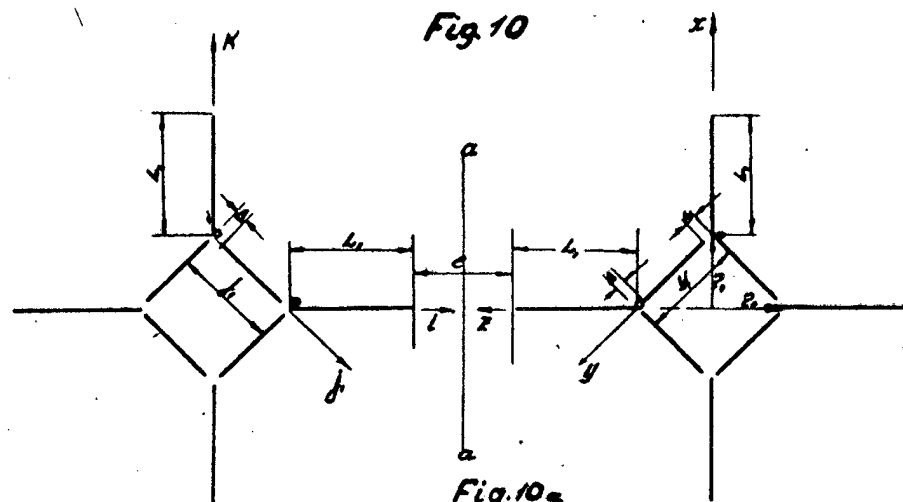


Fig. 10a

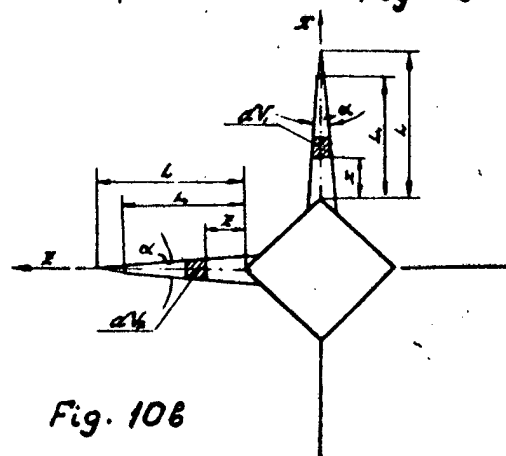


Fig. 10b

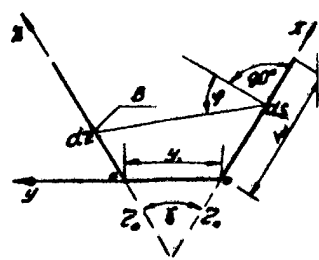


Fig. 10c

B - the effective radiation flow leaving  
the elemental area  $dz$ .

Fig. 10

20

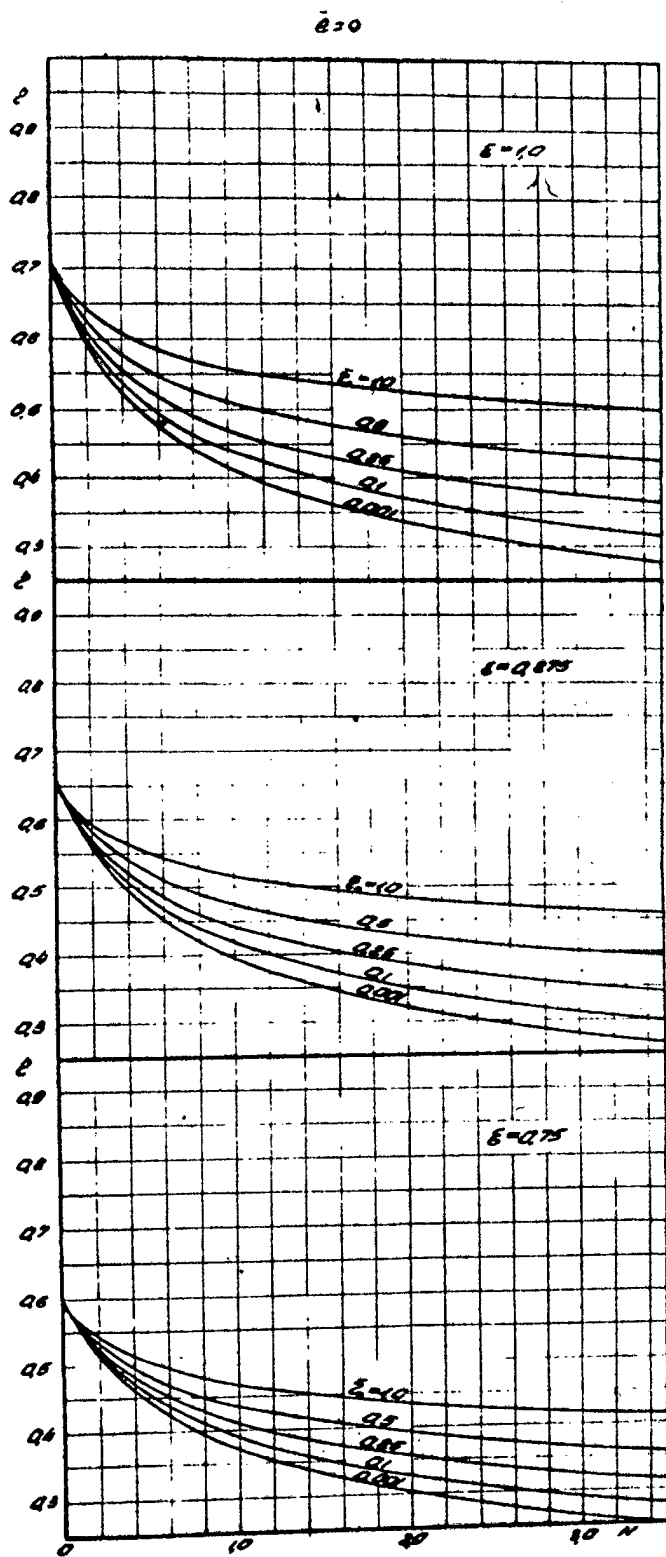


Fig. 11

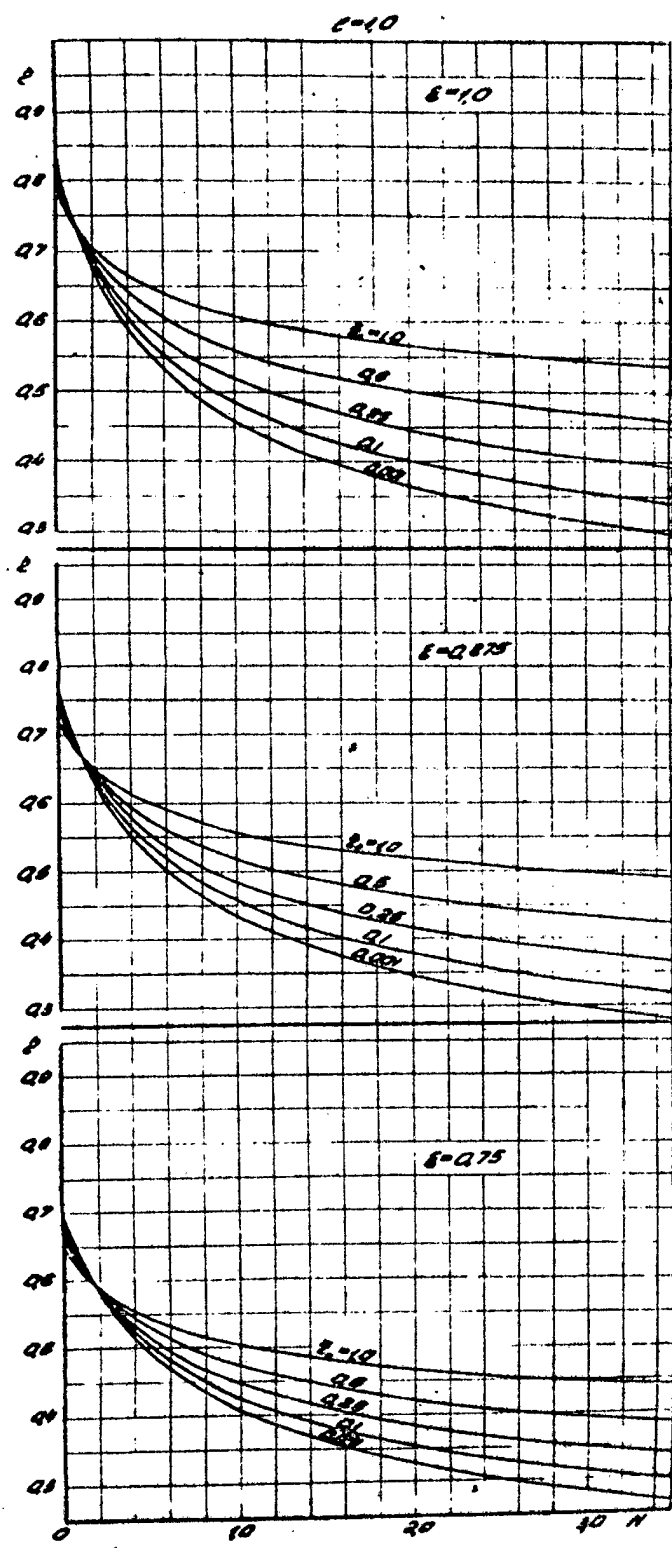


Fig. 12

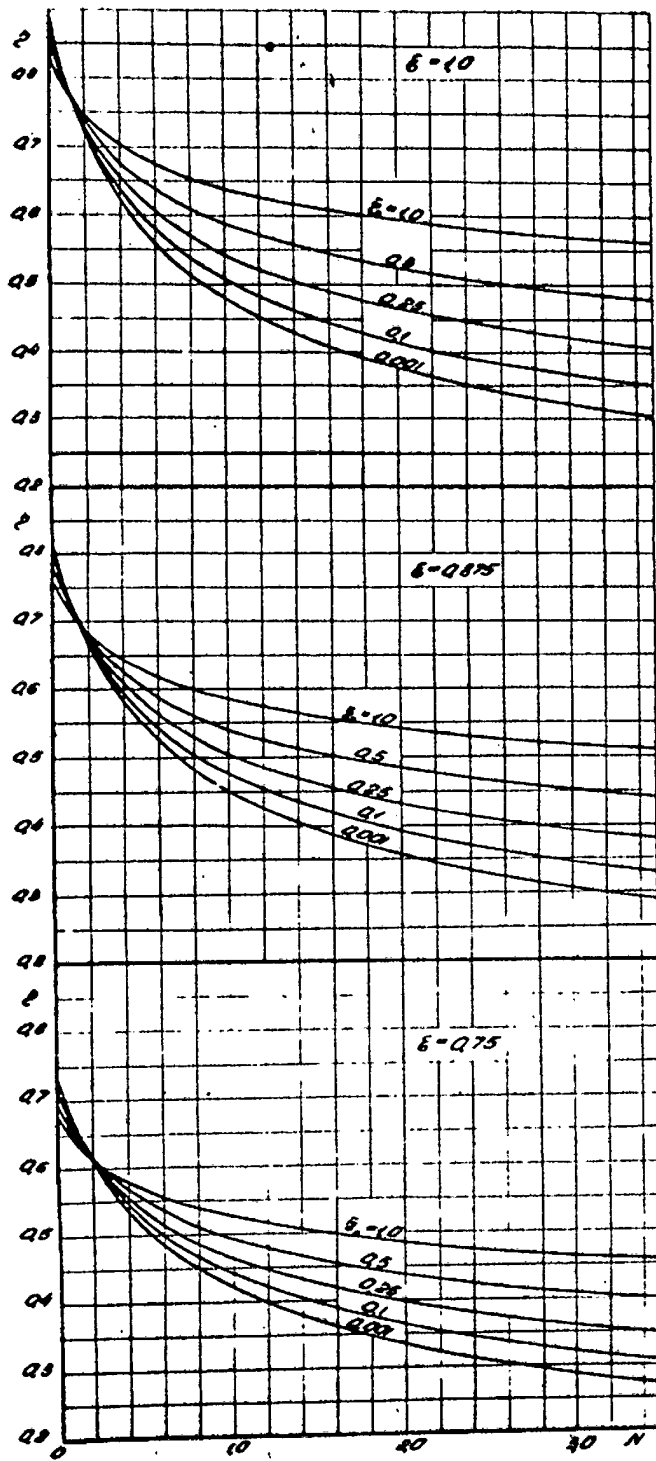
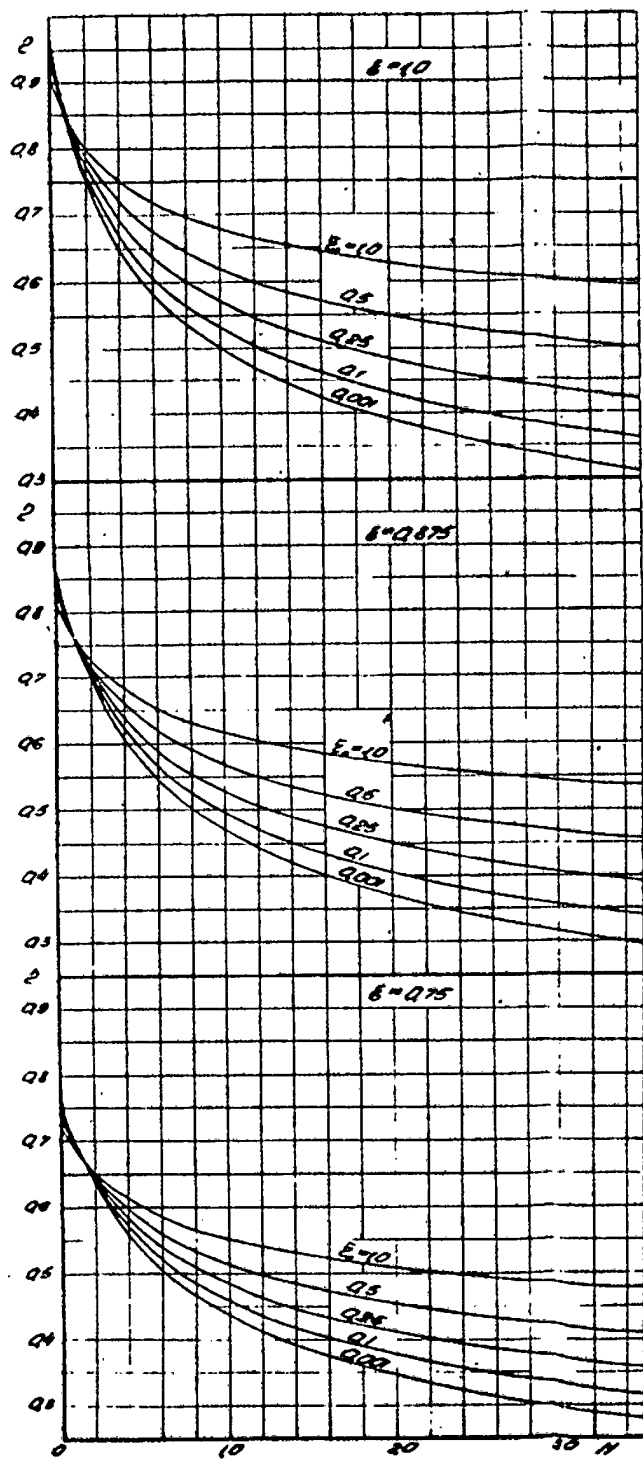
$\bar{E}=2$  $\bar{E}=5.0$ 

Fig. 13

Fig. 14

22

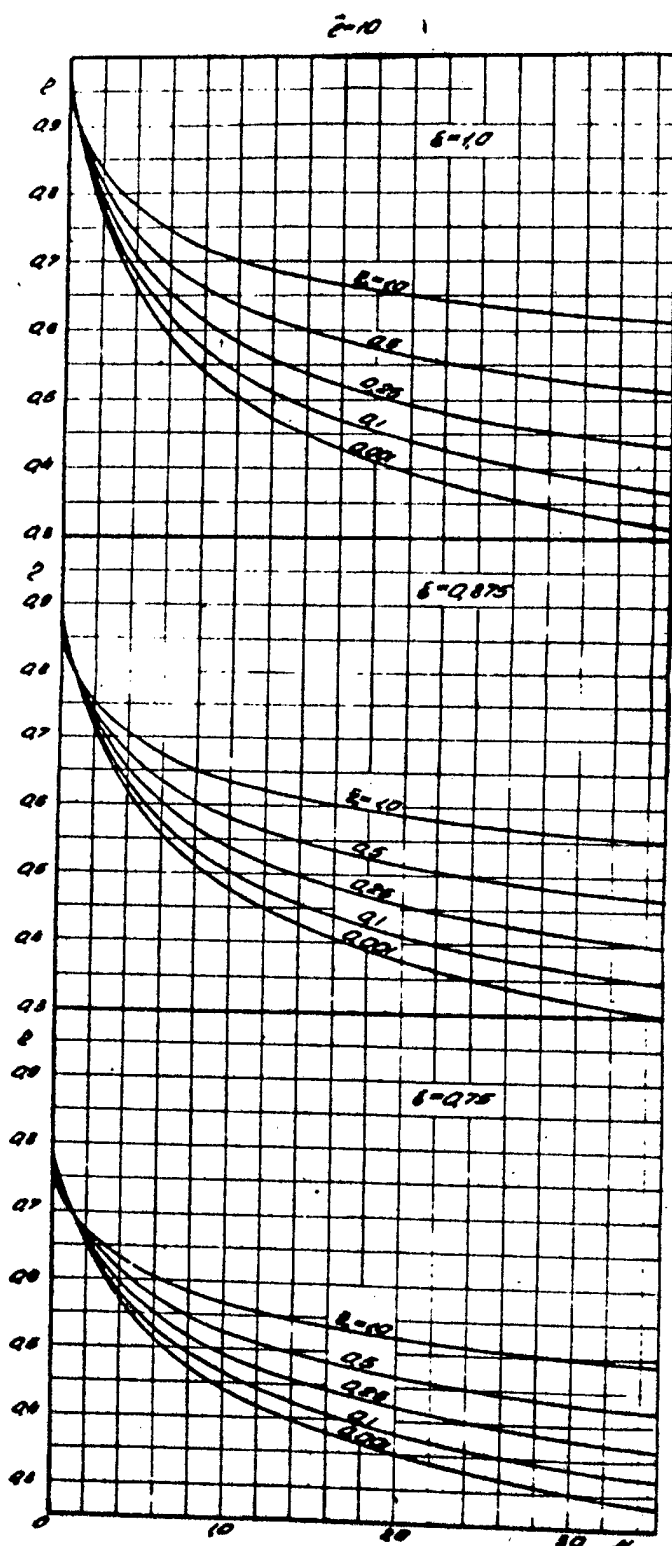


Fig. 15

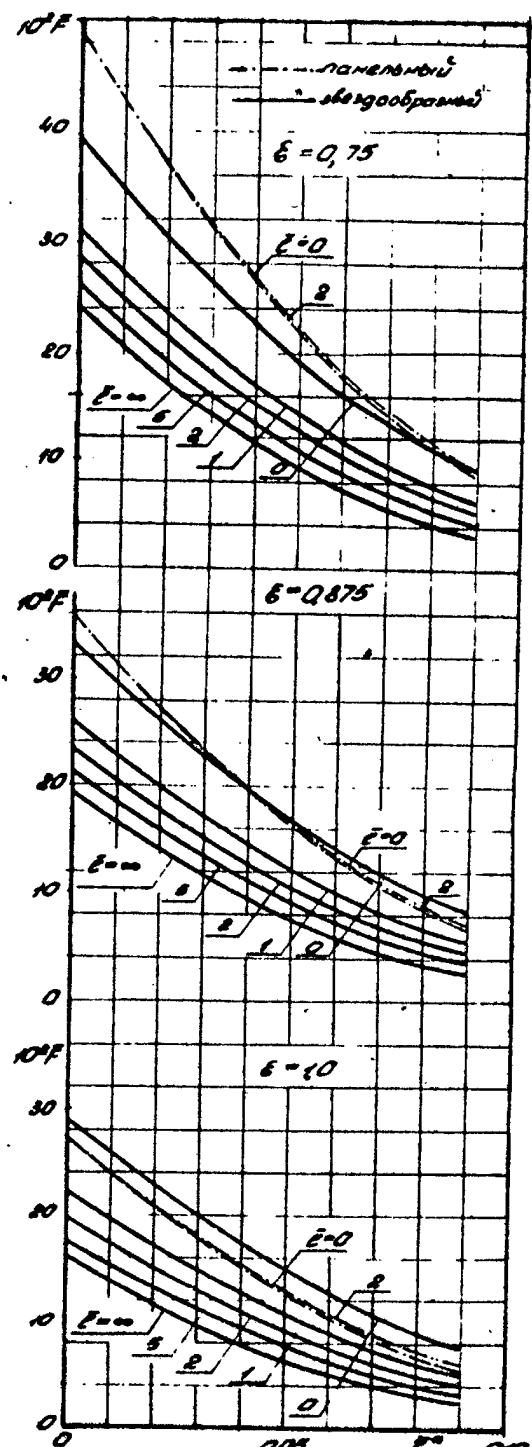


Fig. 16

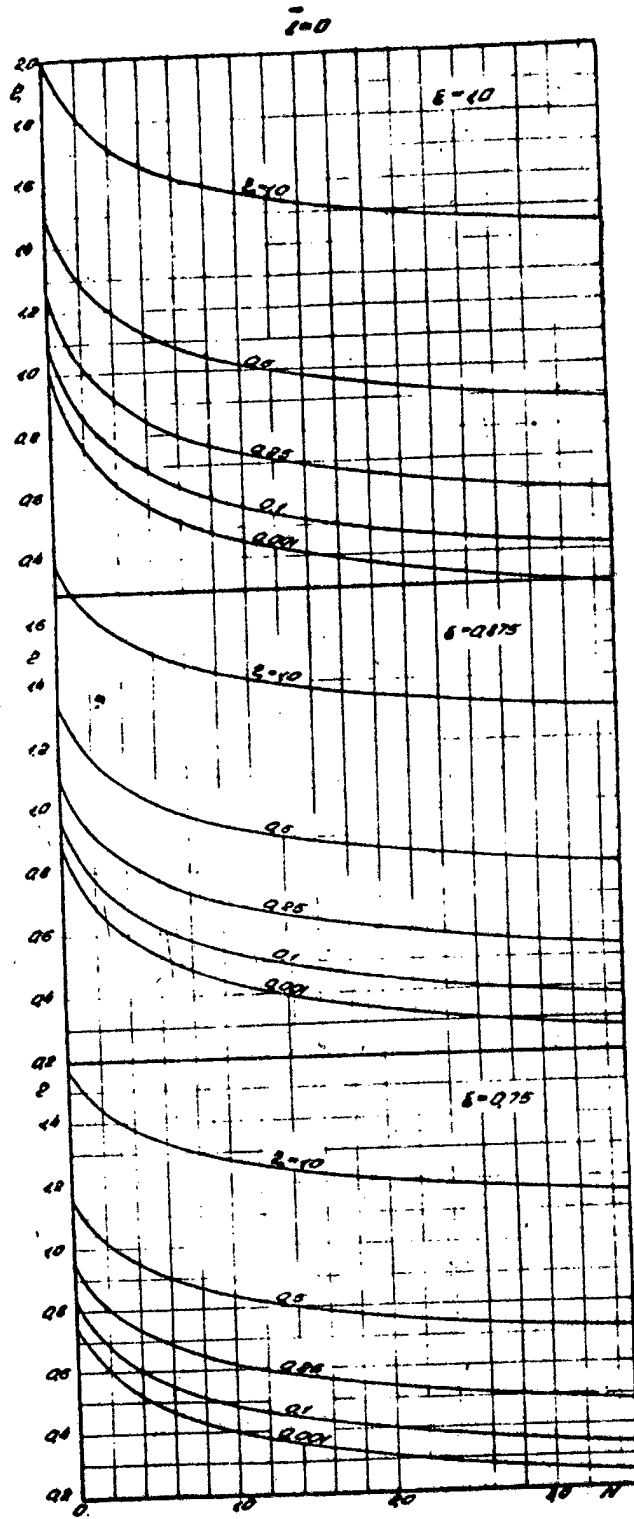


Fig. 17

24

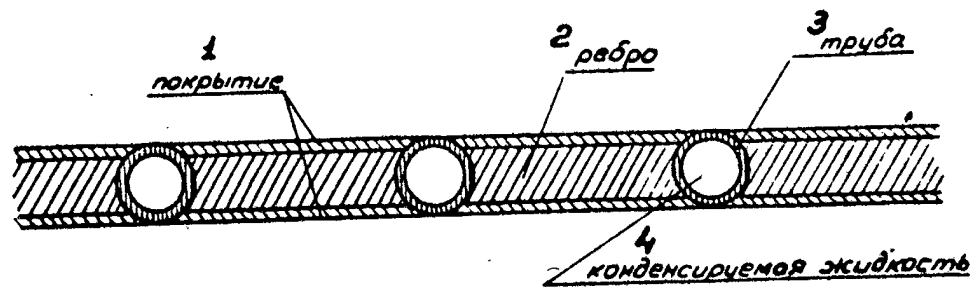


Fig. 18a

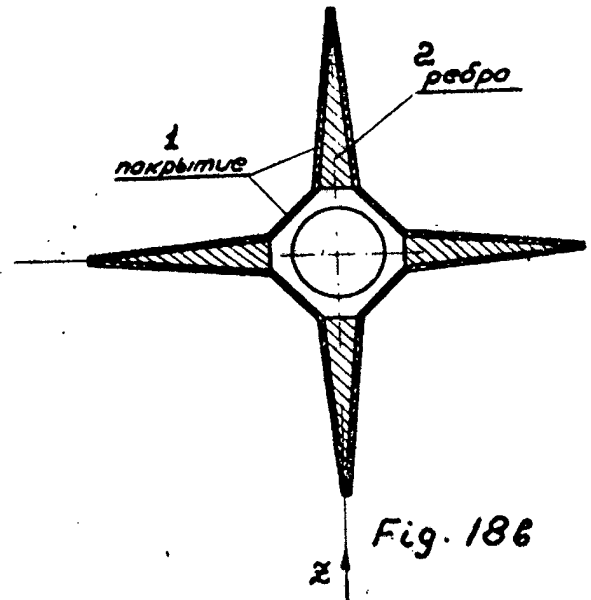


Fig. 18b

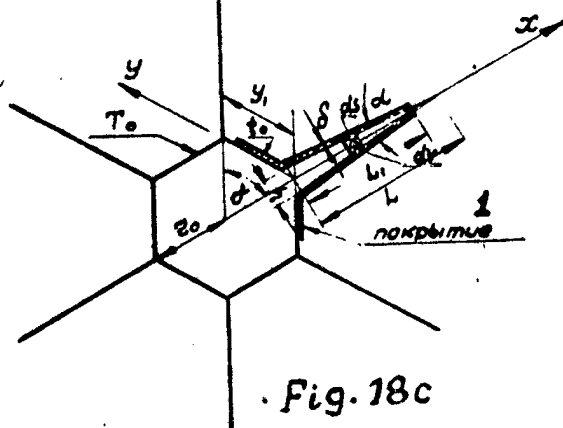


Fig. 18c

Fig. 18

1-coating  
2-fin  
3-tube  
4-condensed fluid

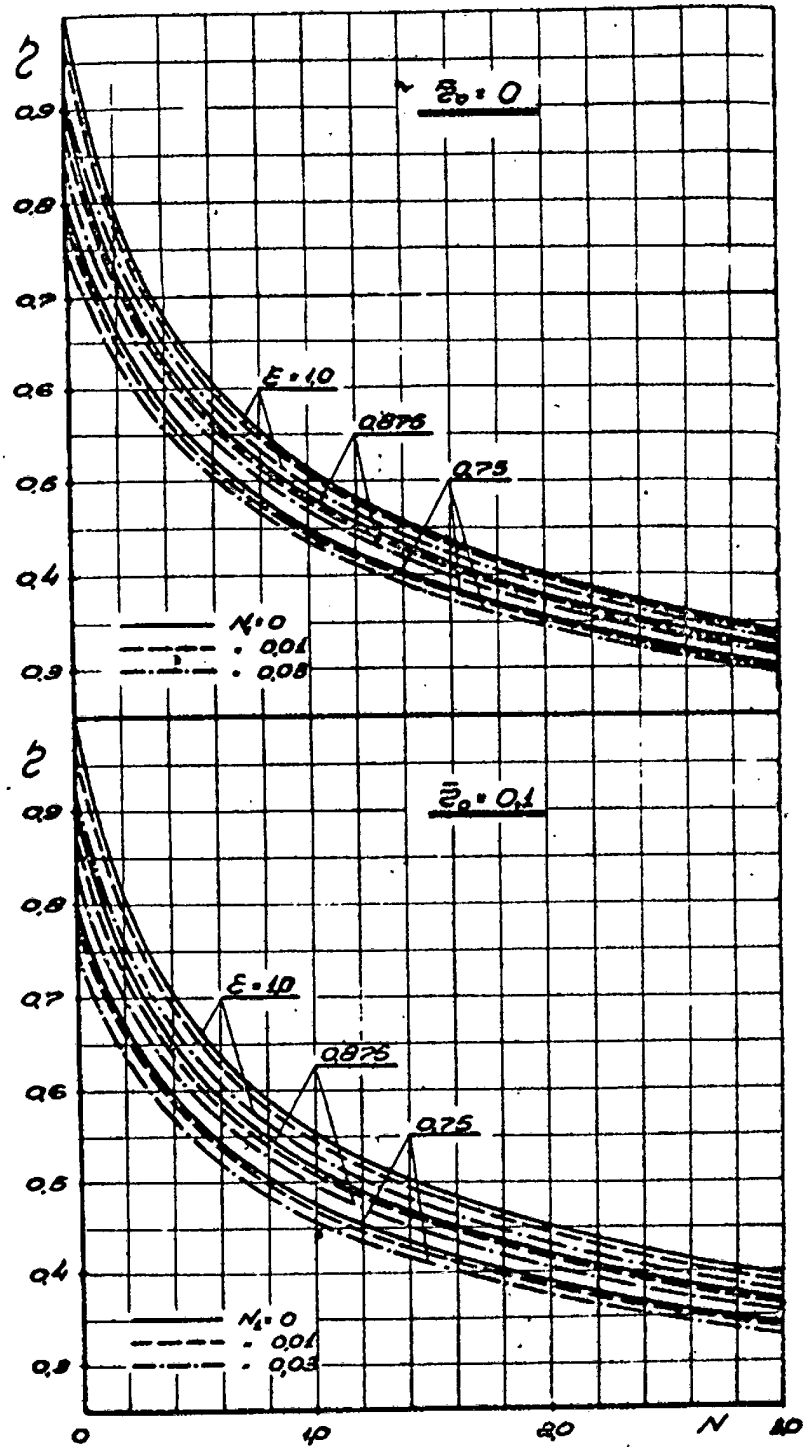


Fig. 19

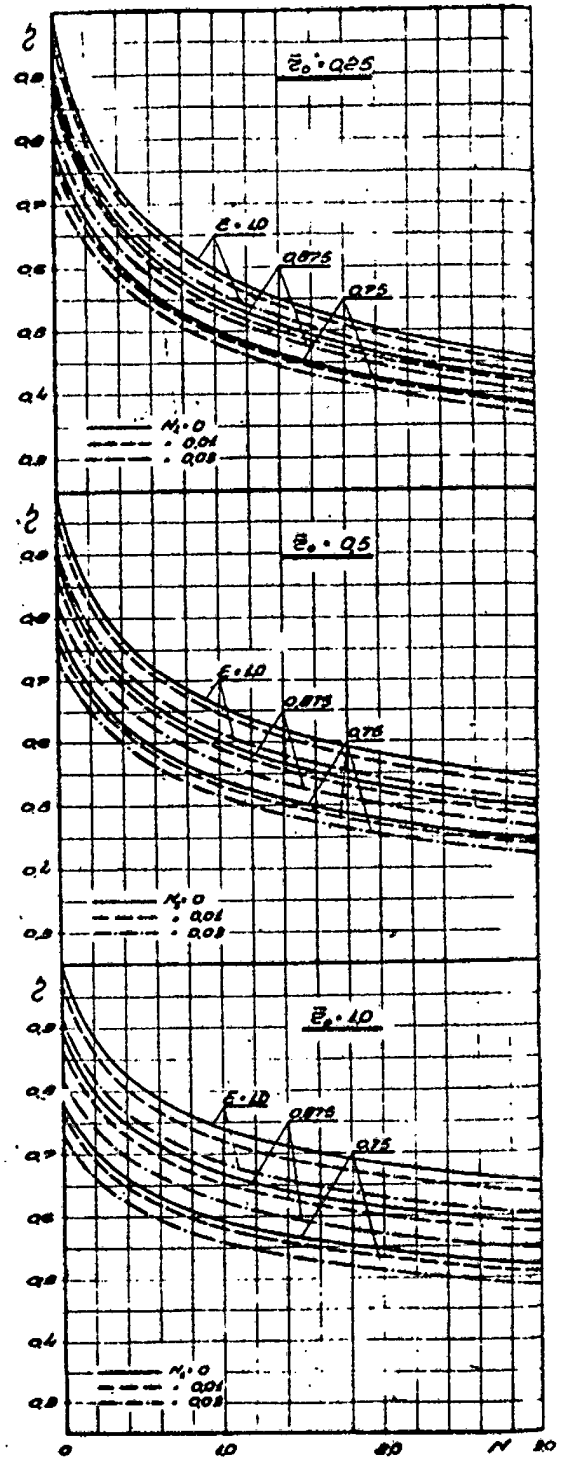


Fig. 20

G.L.GRODZOVSKY<sup>x/</sup>, Y.N.IVANOV <sup>xx/</sup>, V.V.TOKAREV <sup>xx/</sup>

LOW THRUST SPACE FLIGHT MECHANICS

- 
- x/ Doctor of Physics and Mathematics; prof. Moscow In-te of Physics and Technics; editor R.J.Mechanika; Academia of Sciences of the USSR, Baltijskaya 14, Moscow, USSR.
  - xx/ Kandidat of physics and Mathematics, Moscow In-te of Physics and Technics.

### S u m m a r y

The results of more than two hundred investigations are summarized in this paper which have laid the foundation of a new branch of mechanics - low thrust flight mechanics.

It includes the combined solution of the problems associated with selection of optimum weight parameters, the optimum propulsion system control parameters and determination of optimum trajectories for continuously applied propulsive thrust for a case when the weight of the propulsion system is comparable to the launching weight of a vehicle.

The combined solution of the three problems involved is caused by the peculiarities of low thrust propulsion systems: their continuous work and large weight.

The report includes the following sections:

**Introduction.** The physical principles of low thrust and general formulations of optimization problem in space flight mechanics.

**Part I. Space flight mechanics by solar sail.**

1. Basic relationships and formulation of the problem.
2. Interplanetary transfer.
3. Planetary escape.

**Part II. Power-limited flight mechanics.**

4. Optimum weight relationships and elementary movements
5. Ideally controllable propulsion system - optimum weight relationships and optimum power control.
6. Ideally controllable propulsion - system optimum trajectories and vector acceleration programs due to thrust.
7. Uncontrollable propulsion system - optimum weight relationship, optimum trajectories and thrust vector direction programs.
8. Optimum constant and limited thrust acceleration trajectories.
9. Propulsion system controllability limitations.
10. Time limitations for a propulsion system.
11. The number of regulator positions limitations.
12. Optimum combination of power-limited and limited exhaust velocity propulsion systems.
13. Reliability effect in the power-limited propulsion system optimization problem.
14. Correction effect in the power-limited propulsion system optimization problem.
15. Additional weight components for a power-limited propulsion system. Propulsion systems similar to power-limited engines.

**Part III. Low thrust trajectory determination methods.**

16. Analytical solution of dynamics equations.
17. Numerical methods of trajectory determination.

В докладе приведено систематизированное изложение результатов более двухсот исследований, заложивших основу нового раздела механики – механика космического полета с малой тягой.

Предметом этого раздела является совместное решение проблем выбора оптимальных весовых параметров, оптимального управления двигательной системой и определение оптимальных траекторий полета с продолжительно действующей двигательной установкой, вес которой соизмерим со стартовым весом аппарата. Необходимость совместного рассмотрения этих трех составных частей проблемы обусловлена отличительными особенностями двигателей малой тяги: длительным временем работы и большим весом двигательной установки. Доклад включает следующие разделы:

**Введение.** Физические принципы малой тяги и общая формулировка проблемы оптимизации в механике космического полета.

Часть I. Механика космического полета с солнечным парусом.

§ 1. Основные соотношения и формулировка задачи.

§ 2. Перелет между орбитами планет.

§ 3. Выход из сферы притяжения планеты.

Часть II. Механика космического полета с двигателями ограниченной мощности.

§ 4. Оптимальные весовые соотношения для простейших движений.

§ 5. Идеально регулируемая двигательная система – оптимальные весовые соотношения, оптимальное управление мощностью.

§ 6. Идеально регулируемая двигательная система – оптимальные траектории и программы для вектора ускорения от тяги.

§ 7. Нерегулируемая двигательная система – оптимальные весовые соотношения, оптимальные траектории и программы направления вектора тяги.

§ 8. Оптимальные траектории с постоянным и ограниченным ускорением от тяги.

§ 9. Ограничения на регулировочную характеристику двигательной системы.

§ 10. Ограничения на время работы двигательной системы.

§ 11. Ограничения на число положений регулятора.

§ 12. Оптимальное сочетание двигательных систем ограниченной мощности и ограниченной скорости истечения.

§ 13. Учет надежности в задачах оптимизации для двигательных систем ограниченной мощности.

§ 14. Учет коррекции в задачах оптимизации для двигательных систем ограниченной мощности.

§ 15. Учет коррекции в задачах оптимизации для двигательных систем ограниченной мощности.

§ 16. Дополнительные весовые компоненты двигателя ограниченной мощности. Двигательные системы, родственные двигателю ограниченной мощности.

Часть III. Методы построения траекторий с малой тягой.

§ 17. Аналитические решения уравнений динамики.

§ 18. Численные методы построения траекторий.

This paper is devoted to the summarized representation of the results of more than two hundred investigations, which have laid the foundation of a new branch of mechanics - low thrust space flight mechanics, the subject of which is the combined solution of the problems, associated with selection of optimum vehicle weight parameters, of optimum propulsion system control parameters and determination of optimum trajectories for continuously applied propulsive thrust for the case, when the propulsion system weight is comparable with a vehicle launch weight.

Up to present theoretic investigations of the space flight mechanics have been advanced so much that one may speak of certain results of the work done. However material on this subject has been published in the form of hundreds of papers, included in different scientific journals; the present report, and a more detailed survey by the authors /24/, are attempts to summarise the principal aspects of the space flight mechanics. Naturally, the authors have not set a task before themselves to analyse thoroughly all known works in this field, although to give an extensive bibliography was considered to be reasonable. The main emphasis in the paper has been made on the problem of the space flight optimization.

New aspects of the flight mechanics are integrant of the advanced space propulsion systems development. So the established between the XIX-th and XX-th centuries idea of space flight jet propulsion application has encouraged the development of the space flight mechanics (Mesh'erskii, Tsiolkowskii, Lander, Goddard, Hohmann and others) the science, studying motion of space vehicles as mass - variable bodies to determine the maximum payload conditions. In the first stage of the space flight mechanics development the most detailed investigation has been made on the motion of the thermochemically propelled rocket, for which the low specific weight of the propulsion system (the ratio of the propulsion system weight to the maximum developed thrust of the order of the units of percents) (see the below table 1) is characteristic.

For such rockets the neglect of the propulsion system weight has been allowable as a first approximation. and the problem of the flight optimization has been reduced to seeking for the condition of the lowest propellant expenditure to accomplish a prescribed space maneuvers. A reasonable choice of the rocket staging, e.g. the account for the consequently rejected tanks, the weight of which is proportional to the fuel reserve, has not principally changed the cited formulation. On the base of Tsiolkovskii's formula the condition is reduced to minimization of the simple kinematic parameter, called characteristic velocity, which demands consideration of the flight dynamics only: determination of the optimal space trajectories with an indication therein of the optimal phases with respect to application and orientation of the thrust vector. These problems have been represented in detail in the famous basic papers and monographs on rocket dynamics.

The development of advanced space propulsion systems, for example, solar sail, electric jet engines (see below table I) distinguished by their high weight ratio and by great possibilities the exhaust velocity mass

consumption control and others arose new problems of flight mechanics. The prospect of using such propulsion systems is determined by low mass consumption per unit thrust of electric jet and thermonuclear engines (because of high jet velocity) or by the absence of mass consumption for the solar sail. In this connection a new branch of flight mechanics have been developed - the space flight mechanics, studying the combination of the optimal relation between the weight components of a rocket, including the weight of the propulsion system main elements, optimal control and regulation of the propulsion system, and optimal space flight trajectories. The cited basic problem formulation of the space flight mechanics is integrant with the space propulsion system characteristics. Some space propulsion system characteristics are given in the table 1 (ref.94).

To the exclusion of the thermochemical propulsion systems the remaining ones are characterized by a high weight ratio. That is why the need for the combined consideration of the three cited aspects of the problem is due to the distinguished features of the related propulsion systems: the long time of their operation and their large weight.

It should be noted that the low thrust of a number of the discussed in literature propulsion systems (which are origins of the particular investigation advance) is not an outstanding feature of their physical principles, but only provides the assessment of the current possible parameters. That is why the current popular term "low thrust" is highly relative.

The discussed investigations cover a wide range of the flight conditions, for which, besides of the optimal flight dynamics, the selection of the optimal weight parameters is essential. The principal weight parameters considered are: the payload weight  $G_n(t)$ , the propellant weight  $G_m(t)$ ; the power source weight  $G_p(t)$ , accelerator weight  $G_a(t)$  and others. Then the total weight will be:

$$G(t) = G_n + G_m(t) + G_p(t) + \dots \quad (1)$$

Relations between the weight parameters and propulsion system characteristics and the equation of motion form the complete set of equations, describing the vehicle behaviour:

$$G_m = -gq\left(-g\frac{V^2}{2}\right)_{max} = Nod(V); G_p = d(N_0)N_0; G_p = \gamma_{1,2}^{\prime, \prime} P_{max}; P = qV; \ddot{r} = \frac{P}{m} q \vec{t}(t) + \vec{R}(z, t) \quad (2)$$

where  $q$  is mass consumption,  $V$  is an exhaust velocity,  $\gamma$  is power-to-thrust conversion efficiency,  $d$  is a power source specific weight,  $\vec{r}$  is the radius-vector,  $\vec{R}$  is the vector of the acceleration due to gravitational forces,  $\vec{t}$  is a unit vector of the thrust.

To Zander F.A. /85/ (1964) belongs the first serious investigation of the problem of flight with propulsion systems, the weight of which are comparable with a launch vehicle weight. By Zander has been investigated in detail the solar sail flight (fig.1). These investigations were extended in current papers only after 1958.

The solar sail vehicle thrust is produced by radiation pressure from the sun, which is  $P_o = 0.94 \cdot 10^{-6} \frac{\text{kg}}{\text{m}^2}$  at Earth's orbit  $R_o$ . The magnitude  $P$  and direction ( $\vec{n}$ ,  $\vec{p}$ ) depend on the sail setting ( $\vec{n}$ ,  $\vec{e}$ ) (see fig.2) and reflectance :

$$P = \frac{1}{2} P_0 \left( \frac{R_0}{R} \right)^2 S \sqrt{1 + E^2 + 2E \cos(\vec{n} \cdot \vec{e})} \cdot (\vec{n} \cdot \vec{e})$$

$$(\vec{n} \cdot \vec{P}) = \arcsin \frac{(1-E) \sin(\vec{n} \cdot \vec{e})}{\sqrt{1+E^2+2E \cos(\vec{n} \cdot \vec{e})}}$$

$$P_0 = 6,944 \cdot 10^{-6} \frac{\text{Nf}}{\text{M}^2}; R_0 = 0,1495 \cdot 10^{12}$$
(3)

In the papers concerning the solar sail, the idealized case  $E = 1$  is considered:

$$\text{for } E = 1 \quad \vec{P} = P_0 \left( \frac{R_0}{R} \right)^2 \cdot S (\vec{n} \cdot \vec{e})^2 \vec{n}$$
(4)

Then for  $S = \text{const}$ , the weight ingredient of the problem is essentially eliminated and the motion is characterized by the single constant control parameter  $a_0$  (dimension is acceleration); so the only control function is the sail setting angle.

$$q = 0; G_m = 0; G_n = 0; G(t) = G_0 = G_n + g_p S \delta \quad \text{for } S = \text{const.}$$

$$\dot{\Sigma} = a_0 \left( \frac{R_0}{R} \right)^2 (\vec{n} \cdot \vec{e})^2 + \dot{R}; a_0 = \frac{P_0 S}{G_0 + g_p S \delta} \leq \frac{P_0}{g_p S \delta}$$

$$\frac{G_n}{G} = 1 - \frac{a_0 g_p S \delta}{P_0}; \frac{S}{G_0} = \frac{a_0}{g_p P_0} \cdot |\vec{n}(t)| \equiv 1 \quad \left( -\frac{\pi}{2} \leq \vec{n}(t) \cdot \vec{e} \leq \frac{\pi}{2} \right)$$

for  $P_0 \text{lg/cm}^3$ ;  $\delta \sim 2,5 \cdot 10^4 \text{ cm}$ ,  $G_0 \sim 0,4 \text{ cm/sec}^2$

(5)

In a general case ( $\vec{r}, t$ ) there will be no separation of the problem into weight and trajectory domains. Solar - sail - powered interplanetary flight in a central gravitational field of the sun in the cited formulation is studied in references: [85], [133], [138], [163], [225], [226], [144], [207], [188], [189], [28] and others and the equations of planar motion are analysed (see fig. 3)

$$R = r; (\vec{n} \cdot \vec{e}) = \cos \psi; R = -g_0 \left( \frac{z_0}{\Sigma} \right)^2; \dot{\Sigma} = 2\Sigma$$

$$\ddot{z}_x = \frac{v_x^2}{\Sigma} + (a_0 \cos^2 \psi - g_0) \left( \frac{z_0}{\Sigma} \right)^2; \dot{y}_x = \frac{v_y}{\Sigma}; \ddot{v}_y = -\frac{2v_x v_y}{\Sigma} + a_0 \cos^2 \psi \sin \psi \left( \frac{z_0}{\Sigma} \right)^2 \quad (6)$$

at  $\psi = 0$  the solution is the conical sections

$$v_y z = \text{const}; \frac{1}{2} \left( \dot{v}_x^2 + \dot{v}_y^2 \right) - (g_0 - a_0) z_0^2 / \Sigma = \text{const}$$

$$\ddot{v}_x(0) = 0; v_y(0) = \sqrt{g_0 z_0}; \frac{v_x}{v_y} = \frac{a_0}{g_0 - a_0} \quad (7)$$

at  $v_y = \text{const}$ , the solution is the logarithmic spiral

$$z = z_0 \exp(Y \operatorname{tg} \psi); \frac{\sin \psi \cos \psi}{2 - \sin^2 \psi} = \frac{\sin Y \cos^2 Y}{g_0/a_0 - \cos^2 Y}; \psi = \frac{2\Sigma}{v_y} = \text{const} \quad (8)$$

However these particular solutions do not satisfy the boundary conditions; for example, in the circular initial and terminal orbits

$$\text{opt } \psi(t); t = 0; z = z_0; \dot{v}_x = 0; v_y = \sqrt{g_0 z_0}; t = T; z = z; \\ v_{x,0} = 0; v_{y,0} = \sqrt{g_0 \frac{z_0^2}{z_0}}. \quad (9)$$

Exact solutions of the variational problem ( $T_{\min}$  at a given value of  $a_0$ ) are obtained numerically [144], [28]. They are compared with the results of the above cited particular solutions at a prescribed terminal orbital velocity  $v_{x,T} = v_{y,T}$  and at the optimal value of the terminal velocity in the orbit  $v_{y,opt}$  (the problem of misdistance). Comparison shows the great effect of the boundary conditions on the transfer time and on the velocity. The problem of the solar-sail vehicle escape from the planetary gravity field has been studied: (1) in an ecliptical plane, when the speed of the sail rotation is half as high as the rotational speed of the vehicle about the planet, [2027] (see fig 6 and the equation of motion)

$$\ddot{z} - z \dot{\psi}^2 + g_0 \left( \frac{z_0}{\Sigma} \right)^2 = -a_0 \left( \frac{R_0}{R_p} \right)^2 / \sin \left( \frac{1}{2} \psi \right) / \sin \psi$$

$$z \ddot{\psi} + 2z \dot{\psi}^2 = a_0 \left( \frac{R_0}{R_p} \right)^2 / \sin^2 \left( \frac{1}{2} \psi \right) \quad (10)$$

and (2) in the orbit, perpendicular to the ecliptic plane, when the sail

setting is locally optimal with respect to the maximum rate of power increment /128/ (fig.7)

$$\ddot{x}^{(i)} + Q_0 \left(\frac{R_0}{R_p}\right)^2 \cos^2 \alpha^{(i)} \cos^2 \delta^{(i)} + \frac{g_0 t_0^2 x^{(i)}}{\left[\sum_{i=1}^3 (x^{(i)})^2\right]^{1/2}} \quad i=1,2,3 \\ \cos \delta^{(i)} \rightarrow \max(n, V) \quad (11)$$

The second case (see the dotted line in fig.8) guarantees a little shorter time to escape from the gravitational field, however, in both cases the nonoptimal programs of the sail setting have been studied.

From the table II /28/, /202/ it follows that the time to escape from the planetary gravitational field is a considerable part of the interplanetary flight time. In solar sail flight mechanics as a whole only partial conditions of the optimal transfers are investigated.

The other type of the propulsion system, the weight of which is comparable with a launch weight, is a power - limited electrical jet propulsion system. The principal schemes of such propulsion systems are presented in fig.9 taken from Preston - Thomas' work /190/ (1952). The systems consist of the power source  $N_0$  and the accelerator, converting the source energy into kinetic energy of the jet flow at the velocity  $V$  and the thrust  $P$ :

$$P = qV; \frac{1}{2}qV^2 = N \leq N_{\max} \leq N_0 f(V); G_N, G_p, G_m, G_e. \quad (12)$$

The primary energy source can be the Sun or the nuclear system (fig 9). In the range of  $V = 10-100$  km/sec for nuclear systems the propellant consumption  $G$  is unessential /204/

$$\frac{1}{2}G_m V^2 = \alpha c^2 G_e; \alpha \approx 5 \cdot 10^{-4}; \frac{V \text{ km}}{c \text{ sec}} \quad 10^3 \quad 10^2 \quad 10^1 \\ \frac{G_e/G_m}{10^{-2} \quad 10^{-4} \quad 10^{-6}} \quad (13)$$

That is why the weight principal components are  $G_N$ ,  $G_p$  and  $G_m$ . The source  $G_N$  of limited power  $N_0$  determines the main properties and the name of this kind of the propulsion systems.

The specific element of the power source is a radiator for the radiation heat output in a thermoenergetic cycle. The investigations in /16/, /19/, /20/, /22/, /94/, /82/, /97/, /180/, /205/, /228/, /250/ and others have shown the optimal geometry of the heat radiating elements, which provide the minimum weight at the prescribed heat flow  $Q_0$  and the temperature  $T_0$ ; the examples of the optimal shaping of the heat radiating fins are shown in fig (10), (16), (19). Note that the weight of the optimal heat radiating elements is proportional to  $\sim \frac{Q_0}{T_0}$ . Together with the determination of the power unit weight, the total weight of the power source, which depends on the value of the maximal power  $G_N = d(N_0) N_0$ , is determined (see fig.11) /107/.

The characteristics of electrical acceleration, transforming the source energy into the kinetic energy of the oriented jet flow, are considered in detail in a number of works /42/, /49/, /75/, /214/, /220/, and others. In the arc accelerators (fig.12) thermal energy of the propellant heating up to the temperature  $T_0$  is used. The exhaust velocity control may be

accomplished by the input power  $N$  and by the consumption  $q$ :

$$V = A \lambda c \sqrt{\frac{2x}{x+1} g RT_0} \quad T_0 = f\left(\frac{N}{q}\right) \quad (14)$$

Accelerator efficiency  $\eta$  depends essentially on the exhaust velocity (fig.15); the exhaust velocity is bounded by the thermal regimes.

Accordingly, for electrostatic (ion) accelerators (see fig.14) the efficiency  $\eta$  depends essentially on  $V$ , and increase with the exhaust velocity

$$\eta = \frac{V^2}{V+U} \cdot U \sim q$$

Here again the magnitude of the exhaust velocity  $V$  and of the thrust  $P$  can be controlled by varying the electrical parameters.

In general the accelerators permit the power to be converted into thrust with the efficiency, dependent on the exhaust velocity in some velocity range. The mentioned power source and accelerator properties determine the propulsion system characteristics, needed for the flight mechanics analysis, and the thrust control capabilities and weight consumption for thrust realization.

Between the principal parameters of the power - limited propulsion system there are two simple relationships:  $q, V, P, N$ :  $P = qV$

$$N = \frac{1}{2} q V^2 \leq N_{max} \leq N_0(t) \eta(V) \quad (15)$$

therefore the independent parameters are those two, for which it is reasonable to take the explicitly constited ones. Below for the three variants there given full set of equations.

$$V \leq V_{max}, (N, V): P = \frac{2N}{V}; q = \frac{2N}{V^2}$$

$$q \leq q_{max}, (N, q): P = \sqrt{2Nq}; q$$

$$0 \leq q \leq \infty, 0 \leq V \leq \infty: P = \alpha \frac{G}{q}; q = \frac{\alpha^2 G}{2Nq}$$

$$G(t) = G_n + G_N + G_m + G_p; G_N = d(N_0) N_0(t); G_p = \delta(P_{max}) P_{max}, \quad (16)$$

$$G_m = -g \frac{\dot{r}}{V^2} \quad \ddot{r} = \frac{2N_0}{VG(t)} \vec{i} + \vec{R}$$

$$\dot{G}_m = -g \dot{q} \quad \ddot{q} = \frac{\sqrt{2N_0} g}{G(t)} \vec{i} + \vec{R}$$

$$\dot{G}_m = -\frac{\alpha^2 G^2(t)}{2N_0} \quad \ddot{G} = \alpha \vec{i} + \vec{R}$$

$\vec{i}(t)$ ,  $\vec{R}(t)$ ,  $G_N(t)$ ,  $G_p(t)$  and  $q(t)$ , or  $V(t)$ , or  $N(t)$ .

The variational problem requires the determination of the optimal control of the functions, presented in the last line of (16), and furnishing the maximum payload  $\bar{G}_{n max}$  at a specified maneuver and at a specified maneuver time  $T$ . Here in contrast to the classical astrodynamic problems, a weight problem with respect all components must be optimally solved in combination with the dynamic problem.

The weight component role may be illustrated by a number of the simulation problems [15], [16], [111], [114], [154], [175], [190-195], [214], [220], and others. The obvious problem is that of optimal motion with

constant thrust  $P$  in a specified interval of time  $T$  /175/:  
 $N = \text{const}$ ;  $G_N = dN = \text{const}$ ;  $G_p = 0$ ;  $P(t) = \text{const}$   
 $P, T$ ;  $G_n = G_0 - (G_m + G_N) = G_0 - P\left(\frac{g}{V}T + \frac{V}{2}\right)$

$$\max G_n \sim V_{opt} = \sqrt{\frac{2gT}{\Delta}}; \quad G_m = G_N = P\sqrt{\frac{1}{2}gDT} \quad (17)$$

for which the maximum  $G_n$  is reached at  $G_m = G_N$  (see the curve "3" in fig.15). With this problem as an example it is shown [18] that at the related level of the parameters  $\frac{T}{\Delta} \sim 1$  ~~year~~ <sup>kg</sup> ~~kg~~ the influence of the relativistic corrections is unessential.

$$G_n = G_0 - P\left(\frac{gT}{V}\sqrt{1 - \frac{V^2}{c^2}} + \Delta V \frac{1 - \sqrt{1 - \frac{V^2}{c^2}}}{V/c^2}\right)$$

$$V_{opt} = \sqrt{\frac{2gT}{\Delta}} \cdot \frac{1 - \frac{5}{4} \frac{gT}{\Delta c^2}}{1 - \frac{5}{4} \frac{gT}{\Delta c^2}} = \frac{\sqrt{2} \frac{gT}{\Delta}}{1 - \frac{5}{4} \frac{gT}{\Delta c^2}}$$

$$\text{for } \frac{T}{\Delta} \sim 1 \text{ ~~year~~ <sup>kg</sup> ~~kg~~} \quad \Delta \sim 10^{-6} \quad (18)$$

The examples of the optimal weight relationships ("1" -  $P = \text{const}$ , max velocity increment  $\Delta V$ ; "2" -  $P = \text{const}$ , travel along the distance  $L$  at min  $T$ ; 4 - acceleration  $q = \text{const}$ ,  $L$  at min  $t$ , 5 -  $a = \text{const}$ , max  $\Delta V$ ) show the essential influence of the problem type on the solution.

The values of max  $\Delta V$  and min  $T$  for the mentioned simulation problem are given in fig.16. Analysis of the problems, from which power-limited motion investigation started, has shown one feature of the considered optimization - the need for selection of the optimal relation between the weights of the power source and the propellant. The further progress of the simulation problem is the investigation of the optimal flight with an ideally controlled propulsion system [159], [140], [15] and others. When there is no restrictions:

$$0 \leq P \leq \infty; 0 \leq q \leq \infty; 0 \leq V \leq \infty; N(t) \leq N_{\max} = N_0; \quad \gamma = \text{const}$$

$$G_p = 0; \quad G_N(t) \equiv G_N; \quad G(t) = \frac{G_0}{1 + \frac{G_0}{2g} \int_0^t \frac{a^2}{N} dt}$$

$$\bar{G}_n = \frac{G_n}{G_0} = \frac{1}{1 + \frac{G_0}{2g} \int_0^T \frac{a^2}{N} dt} - \bar{G}_N; \quad \text{opt } N(t) = N_{\max} \quad J = \int_0^T a^2 dt \quad (19)$$

$$\text{hpu } G_N = dN_0 (d = \text{const}); \quad \bar{G}_n = \frac{1}{1 + \Phi/\bar{G}_N} - \bar{G}_N; \quad \Phi = \frac{d}{2g} J$$

$$\bar{G}_{n_{\max}} = (1 - \sqrt{\Phi})^2; \quad \bar{G}_{n_{opt}} = \sqrt{\Phi} - \Phi$$

the maximum payload  $\bar{G}_n$  is reckoned as the functional is minimal. Separation of the total problem into a weight and a trajectory ingredients is essential, and justifies the idealization. The mentioned separation retains with the discussed above (see fig.11) nonlinear relationship between the source weight and the maximum power /21/, /24/:

$$\text{at } G_N = d(N_0)N_0 \quad \text{opt} \sim \frac{d G_N(N_0)}{d N_0} \left( \frac{N_0}{G_N} \frac{1}{J^{1/2g}} + \frac{1}{J^{1/2g}} \right) - 1 \quad (20)$$

For power approximation  $\alpha(N_0)$ :

$$\text{at } G_N = \alpha N_0^x; \quad \bar{G}_{n_{\max}} = 1 + \Phi - \sqrt{\Phi} \left( \sqrt{x} + \frac{1}{\sqrt{x}} \right); \quad \Phi = \frac{G_N}{2gN_0} \int_0^T a^2 dt \quad (21)$$

For the thermojet propulsion systems, due to their low specific weight, the problem of the optimal staging is in principle the problem of the optimal tank rejection. For the power-limited propulsion systems, due to high power source, relative weight, the problem of the optimal staging arises in a new formulation, namely the choice of the optimal power source weight decrease, accompanied by proportional maximum power decrease. As is shown in our work [15] for the general case and later in [166] for the particular case  $a = \text{const}$ , at a multistaging power-source elements rejection for the idealized system the weight and trajectory problem ingredients are separated:  $\frac{d G_N(t)}{dt} \leq 0; \quad N_0(t) = \frac{G_N(t)}{a}; \quad N(t) = N_0(t)$

$$G_{n_i} = G_{n_i} + \Delta G_{m_i}; \quad \Phi_i = \frac{d}{2g} \int_{t_{i-1}}^{t_i} a^2 dt; \quad \text{opt } \frac{G_{n_i}}{G_{n_{i+1}}} = \left( \frac{1-\Phi_i}{1+\Phi_i} \right)^2 \quad (22)$$

$$\bar{G}_{n_{\max}} = (1 - \sqrt{\Phi})^2 \sum_{i=1}^n \left( \frac{1-\Phi_i}{1+\Phi_i} \right)^2; \quad \Phi = \sum_{i=1}^n \Phi_i$$

The limited case is that of the infinite number of elements /29/:

$$\text{Opt. } G_N(t); \quad \bar{N} = \frac{N}{N_0}; \quad 1 \geq \bar{N}(t) \geq 0$$

$$\dot{G}_m = - \frac{G^2(t)}{G_N \bar{N}} \frac{d}{2g} a^2; \quad \dot{\vec{r}} = \vec{v}; \quad \dot{\vec{v}} = \vec{a} \vec{t} + \vec{R}$$

$$T_{\min}, \bar{G}_N; \quad (\vec{r}_0, \vec{v}_0); \quad (\vec{r}_s, \vec{v}_s)$$

$$t=0: \bar{G}(0) = \bar{G}_N + \bar{G}_{n_0} + \bar{G}_{m_0} = 1; \quad t_s = T; \quad \bar{G}_{m_s} = 0 \quad (23)$$

$$\text{opt } \bar{G}_N(t) = \begin{cases} \bar{G}_m + \bar{G}_n \\ \text{const} \end{cases} \quad u \min \Phi = \frac{d}{2g} \int_0^T a^2 dt$$

$$\bar{G}_N(t) = \text{const} \quad \text{spu } 1 \geq \bar{G}_N \geq 0,25$$

Data in fig 18 show, that with optimal power-source weight decrease the payload  $\bar{G}_N$  slightly increase at high values  $\Phi$ .

If a part  $\gamma$  of the weight of the rejected power-source elements is used according to Zander's ideas, as a propellant /79/:

$$q_{\Sigma} = q + \gamma \frac{d G_N}{dt}; \quad \gamma(t) \leq \gamma_{\max} \leq 1; \quad \dot{\vec{r}} = -\vec{q}; \quad \dot{\vec{v}} = \vec{v} \quad (24)$$

$$\dot{\vec{v}} = \frac{\sqrt{2g \bar{G}_N \bar{N} (\bar{q} + \gamma \bar{q}_N)}}{\bar{G}_m + \bar{G}_N + \bar{G}_n} \vec{t} + \vec{R};$$

$$\bar{q} = \frac{q}{\bar{G}_N}; \quad \text{opt } \gamma(t) = \gamma_{\max}$$

then the payload can be sufficiently increased (see fig.19). And in this case trajectory and weight ingredients of the problem are separated, which is the main property of the ideally controlled limit thrust propulsion

system.

The solution of the trajectory ingredient of these problems must give the minimum of the functional  $\int \dot{a} dt$  along the trajectory. Such an optimal control has been investigated in [15], [159], [140], [3], [34] and others. The optimal trajectories and the laws for the acceleration-due-to-thrust vector for a planar motion in the field of the two gravitational centers are determined by the solution of the following set of the differential equations [15] (see fig. 20).

$$\text{Opt } \vec{z}(t), \vec{a}(t) : \ddot{\vec{z}} = \vec{a} + R(\vec{z}, t); \quad (\vec{z}(0) = \vec{z}_0; \dot{\vec{z}}(0) = \vec{v}_0; \min J = \int_0^T \dot{a} dt)$$

$$\ddot{z}^{(i)} = a_z^{(i)} + z^{(i)} / y^{(i)} \gamma^2 - \frac{k^{(i)}}{z^{(i)2}} - R^{(i)}; \quad i = 1, 2; \quad k^{(i)} = \gamma M^{(i)}$$

$$z^{(i)} \ddot{y}^{(i)} - a_y^{(i)} - 2 \dot{z}^{(i)} \dot{y}^{(i)} - \psi^{(i)}; \quad y^{(i)} = y^{(i)} + \omega t$$

$$R^{(i)} = \frac{k^{(i)}}{z^{(i)2}} \cos[\psi^{(i)} - \psi^{(i)}]; \quad R^{(i)} = \frac{k^{(i)}}{R^2} \cos \psi^{(i)} - \frac{k}{z^{(i)2}} \cos[\psi^{(i)} - \psi^{(i)}] \quad (25)$$

$$\psi^{(i)} = \frac{k^2}{z^{(i)2}} \sin[\psi^{(i)} - \psi^{(i)}]; \quad \dot{\psi}^{(i)} = \frac{k^{(i)}}{R^2} \sin \psi^{(i)} - \frac{k^{(i)}}{z^{(i)2}} \sin[\psi^{(i)} - \psi^{(i)}]$$

$$\dot{a}_y^{(i)} = \frac{1}{z^{(i)2}} (d_y^{(i)} v_x^{(i)} - 2 a_x^{(i)} v_y^{(i)} + V); \quad \dot{v}^{(i)} = a_y^{(i)} \psi^{(i)} + a_z^{(i)} R^{(i)}$$

$$\dot{a}_x^{(i)} = \frac{1}{z^{(i)2}} \left\{ \frac{1}{2} [(a_x^{(i)})^2 + (a_y^{(i)})^2] + a_x^{(i)} \left[ \frac{(v_x^{(i)})^2}{z^{(i)2}} - \frac{k^{(i)}}{(z^{(i)2})^2} \right] - \lambda - V \frac{v_x^{(i)}}{z^{(i)}} \right\},$$

$$\dot{a}_z^{(i)} = -V \left( a_y^{(i)} \psi^{(i)} + a_z^{(i)} R^{(i)} + \frac{1}{z^{(i)}} a_y^{(i)} \psi^{(i)} \right) - \frac{v_x^{(i)}}{z^{(i)}} \psi^{(i)} a_x^{(i)} R^{(i)} - \frac{2k^{(i)}}{z^{(i)2}} (V - 2 a_x^{(i)} \psi^{(i)})$$

$$(v_x^{(i)} = \dot{z}^{(i)}, v_y^{(i)} = z^{(i)} \dot{y}^{(i)})$$

$$J = \int_0^T \left\{ \left[ \dot{z}^{(i)} - z^{(i)} \dot{y}^{(i)} + \frac{k^{(i)}}{(z^{(i)2})^2} + R^{(i)} \right]^2 + \left[ z^{(i)} \dot{y}^{(i)} + 2 z^{(i)} \dot{y}^{(i)} + \psi^{(i)} \right]^2 \right\} dt$$

In a central field ( $i = 1$ ) the system is simplified [159], [140]:

$$i = 1; \quad k^{(1)} = 0; \quad z = 2z; \quad z \dot{y} = 2y; \quad \dot{z} = a_x + \frac{2z^2}{z} - \frac{k}{z^2}; \quad \dot{y} = a_y - \frac{2z}{z} \dot{z};$$

$$a_x = \frac{1}{z^2} \left[ \frac{1}{2} (a_x^2 + a_y^2) + a_x \left( \frac{2z^2}{z} - \frac{k}{z^2} \right) - \lambda - V \frac{2z}{z} \right];$$

$$\dot{a}_y = \frac{1}{z} (a_y \dot{z} - 2 a_x \dot{z} + V)$$

The parameters  $V$  and  $\lambda$  are the integrals of the set; they play the role of the constants of the isoperimetricity with respect to the angular motion (at  $V = 0$ ,  $\Delta \vartheta$  - opt) and the time of travel (at  $\lambda = 0$ ,  $T$  - opt). The zero radial velocity point  $v_y = 0$  is singular of the node type [12] which is to be accounted for during the computation of the transfer between the circular orbits.

$$v_y = 0 : \quad \frac{1}{2} (a_x^2 + a_y^2) + a_x \left( \frac{2z^2}{z} - \frac{k}{z^2} \right) - \lambda - V \frac{2z}{z} = 0 \quad (21)$$

The related set of the equations is invariant to the transformation, connected with the sign change (therefore the return flight may be replaced by the return flight) and to the transformation, connected with multiplying by  $\ell$ , which permits the variables to be introduced in such a way that the gravitational constant  $K = 1$ :

10

$$\begin{aligned} t &\rightarrow -t; \gamma \rightarrow -\gamma; z_2 \rightarrow -z_2; a_y \rightarrow -a_y; \\ z &\rightarrow \bar{z}_2; t \rightarrow \bar{t}^{\frac{3}{2}} t; v \rightarrow \bar{v}^{-\frac{1}{2}} v; a \rightarrow \bar{a}^{\frac{1}{2}} a; \\ \bar{r} &\rightarrow \bar{r}^{\frac{1}{2}} \bar{r}; \bar{v} = \bar{v}^{-\frac{1}{2}} v; \bar{t} = \frac{t}{z_0^{\frac{3}{2}} / k^{\frac{1}{2}}}; \bar{k} = 1 \end{aligned} \quad (28)$$

For the characteristic phases of the space flight two basic problems are formulated: (1) Orbital transfer (with the specified waiting time  $T_c$  within the influence sphere of the destination planet 2) escape from the gravitational field (by increasing the energy to zero,  $E=0$ )

$$z(0) = z_0; \gamma(0) = 0; v_x(0) = v_{x_0}; z_g(0) = z_{g_0} \rightarrow z(T) = z_g; \gamma(T) = \gamma_g; v_x(T) = v_{x_g};$$

1.  $0 \div 1 \div 0: T_c = \frac{\gamma_g + \gamma_2 - \omega_1 (T_1 + T_2) + 2\pi \bar{n}_1}{\omega_1 - \omega_2}; T_s = T_1 + T_c + T_2$

$$\gamma_1 + \gamma_2 \approx T_1 + T_2$$

2.  $z(0) = z_0; \gamma(0) = 0; v_x(0) = v_{x_0}; z_g(0) = v_{x_g}$  (29)

$$E(T) = \frac{1}{2} (v_x^2 + v_g^2) - \frac{k}{z} = 0$$

$$\delta \gamma = C; \quad 1) \gamma_1 = \gamma_2; \lambda_1 = \lambda_2; 2) \gamma = 0; \frac{a_{x_0}}{a_{x_g}} = \frac{v_{x_0}}{v_{x_g}}$$

$$a_{x_0} - 2a_{x_g}, z_g, z_2, \frac{z}{k} + \dot{a}_{x_0} z_2, \frac{a_{x_0}^2}{k} = 0$$

The optimal conditions for the cited problems are given in the last line of the equations (29). For the optimal transfer between the circular orbits

$$v_{x_0} - v_{x_g} = 0; v_{x_0} = \sqrt{\frac{k}{z_0}}; v_{x_g} = \sqrt{\frac{k}{z_g}}; \quad (30)$$

$$\frac{1}{2} a_{x_0}^2 - \lambda - \sqrt{\frac{k}{z_{g_0}}} = 0; \text{ npu } \lambda = 0 \rightarrow a_0 = a_1$$

In a forceless field the set of the equations is integrated in the final form (157), (159), (140), (155), (2):

$$\text{for } k = 0: \ddot{z} = \ddot{a}; \ddot{a} = 0; \vec{a}(t)_{opt} = \vec{b}_0 t + \vec{b}_1; \quad (31)$$

$$\vec{a}(t) = \frac{1}{6} \vec{b}_0 t^3 + \frac{1}{2} \vec{b}_1 t^2 + \vec{b}_2 t + \vec{b}_3$$

In this case in the simulation problem of the specified velocity increment

$\Delta V$  for the time  $T_c$  near  $\bar{G}_n$  the optimal control corresponds to the law  $\ddot{a} = \text{const}$ :

$$\frac{b_{x_0}}{v_{x_0}} = \frac{b_{x_g}}{v_{x_g}} = \frac{b_{x_0}}{v_{x_0}}, J_{min} = \frac{\Delta V^2}{T} \quad (32)$$

In the problem of the optimal travel between two rest points the linear variation  $a(t)$  is optimal:

$$L, T: a(t)_{opt} = (6L/T^2)(1 - 2t/T); J_{min} = 12 \frac{L^2}{T^3}$$

(33)

II

$$\text{at } (a) = \text{const} \quad J = 16 \frac{\dot{L}^2}{T^3}$$

that gives the functional by  $1/3$  lower than at  $a/a = \text{const}$ . (fig.21).

The set of the equations is integrated in the final form also in the case of the satellite motion around the sphere surface under the influence of the lateral thrust [1], [86]; When the orbit plane turning is caused by low lateral forces, the optimal control corresponds to sinusoidal variation  $a(t)$ :

$$\text{for } r \geq 1 \text{ and } a'' \ll 1 \quad \ddot{\theta} + \theta = ae$$

which gives the functional by 19 per cent lower than at  $a/a = \text{const}$ . (fig.22)

Because of the complexity of the basic set of the equations in a number of works the approximate solution to the variational problem is considered. In the problem of the escape from the gravitational field along the gently sloping spiral with low lateral jet acceleration, in which the condition of gravitational and centrifugal acceleration balance is carried out, there shown the optimality of the motion with the constant tangential acceleration [15], [125], [121], [4]:  $\frac{V_x^2}{\epsilon} \approx \frac{k}{r_0^2}$ ;  $\dot{r}_x = V_x$ ;  $\dot{V}_x = a_x$ ;  $V_y = a_y - \frac{V_x \dot{r}_x}{r}$

$$V_x = 2\sqrt{\frac{r_0^2}{k}} a_y; V_y = \sqrt{\frac{k}{r_0}} Q; r = \frac{r_0^2}{Q}; Q = 1 - \frac{5a_y dt}{\sqrt{k/r_0}}$$

$$V_{x_0} = 2\sqrt{\frac{r_0^2}{k} a_y}; \tau \sim \sqrt{\frac{4\pi k}{a_y}}; V_x \sim a_y; a_x \sim a_y^2 \quad (25)$$

$$J = \int a^2 dt = \int a_y^2 dt \quad (a_x \ll a_y)$$

$$\text{Opt } a_y = \text{const}$$

In fig.23 [140] the examples of such motions are shown, and in fig.24 there shown the required values of the functional for the earth gravitational field.

For the approximate solution of the optimal orbital transfer problem the technique, based on the application of the proposed by Emeev T.M. "transporting" coordinate system, is effective, where as a basic trajectory the Kepler's one is used  $x^0(t)$ ,  $y^0(t)$  [31/15]:

$$x^0(t), y^0(t); x = x^0 + \bar{x}, y = y^0 + \bar{y}; z = \bar{z}$$

$$\dot{x} = a_x; \ddot{x} = a_y; \ddot{\bar{x}} = a_z; \dot{a}_x = 0; \dot{a}_y = 0; \dot{a}_z = 0$$

$$\bar{x}(0) = \bar{y}(0) = \bar{z}(0) = \bar{x}(T) = \bar{y}(T) = \bar{z}(T) = 0 \quad (26)$$

$$\dot{\bar{x}}(0) = \dot{x}_0 - \dot{x}^0 \dots$$

$$\dot{\bar{x}}(T) = \dot{x}_T - \dot{x}^T \dots$$

The examples of the application technique of the optimal Earth - Mars transfer are shown in fig.25.

The exact optimal trajectories and the laws of jet acceleration control are found by the numerical integration of the above shown set of the equations. In the problem of escape from the gravitational field at relatively high jet accelerations [206] the variation of  $a_x$  and  $a_z$  is of oscillating character (fig.26). Dimensionless variables permit to obtain the universal relationship between the functional and the time of escaping from the field [34] (fig.27).

Accordingly, the computation of the optimal trajectories and laws  $a(t)$  for orbital transfers is made; a number of examples for the optimal

12

Earth-Mars transfer between the circular co-planar orbits /54/ are given in fig.28. The family of the curves of the optimal values of the functionals  $\mathcal{J}$  with respect to two parameters: the angular movement and the time of transfer  $T$  - permits to determine all the parameters of the optimal transfer (fig.29).

The relationship between the functional, the different dates of the launch and the flight time  $T$  is presented in fig.20 with an account for the ellipticity of the co-planar Earth's and Mars' orbits. The interception points of the two families of curves the points of nonuniqueness of the solution to the boundary value problem, in which the transfer time  $T$ , the initial and final coordinate values and the velocities and the functional values coincide, - are of interest (see the example in fig.31).

In the problem of the orbital transfer with return and with a specified time  $T$  of the flight about the destination planet the optimal conditions for both forward and return flight trajectories are (as it was indicated above) the equalities of the parameters  $\lambda$  and  $\lambda$  along the both trajectories. This condition is satisfied by symmetrical transfers, however, the examples of asymmetrical transfer optimality have been proved (see, for example fig.32 /16b/. The influence of the  $Z$ -component of the Earth-Mars -Earth transfer /16b/ (fig.33) on the total functional appeared to be gentle, although along the flight stages the functional is essentially different

	Three-dimensional motion - elliptical orbits	TWO - dimensional motion - circular orbits
$S - M$ $T_1 = 1840$	$\mathcal{J}_1 = 6,58$	12,91
$M - S$ $T_2 = 3120$	$\mathcal{J}_2 = 24,99$	19,02

### 3 - M 3

$$T_8 = 5440, T_6 = 480 \quad \mathcal{J}_1 = \mathcal{J}_2 = 31,57 \quad 31.93$$

By the certain optimal laws of the jet acceleration  $a(t)$  control along the trajectory there can be determined also the remaining parameters: the thrust control  $P(t)$ , consumption control  $q(t)$  exhaust velocity control  $V(t)$ , the vehicle weight variation  $W(t)$  along the trajectory:

$$\begin{aligned} \text{opt } a(t) \sim N, P, q, uV : \quad N = \frac{Gn}{2} : \quad \frac{Gn}{G_0} = \sqrt{\Phi} - \Phi, \\ \Phi = \Phi(T), \quad \Phi(t) = \frac{d}{dt} \int_0^t a^2 dt \\ P(t) = G(t) \frac{a(t)}{g}, \quad q(t) = G^2(t) a^2(t), \quad g^2 N \\ V(t) = 2 Ng/G(t)a(t); \quad G(t) = G_0 / \left( 1 + \frac{G_0 \Phi(t)}{Gn} \right) \end{aligned} \quad (18)$$

The example shown in fig.34 for the Earth - Mars - Earth mission /16b/ suggests that considerable exhaust velocity control is necessary for the optimal program.

As a whole the consideration of the ideally - controlled propulsion system permitted to determine the upper boundary of the pertinent class propulsion system possibilities. To evaluate the maximum deterioration of

the characteristics, caused by the restrictions on the regulation, another limit case is considered - the power limited unregulated propulsion system: the system with constant thrust, consumption, exhaust velocity, but with the possibility of thrust cut-off [30] and others.

$P = \text{const}$ ,  $g = g_0$ ;  $V = V_0$  ( $N = \text{const}$ );  $G_{\Sigma} = G_m + G_N$

$$\dot{G}_{\Sigma} = g_0 \delta; \dot{\Sigma} = \bar{\Sigma}; \dot{V} = \frac{\sqrt{G_m g_0 \delta}}{\dot{\Sigma} + R};$$

$$\begin{array}{l|l} \dot{G}_{\Sigma} + G_N & \delta = 1 \\ \dot{G}_N = 0; \dot{g}_0 = 0 & \delta = 0 \end{array} \quad (39)$$

$$\delta(t), \dot{\Sigma}(t) \rightarrow G_{\Sigma}(0) + G_N = 1; \dot{\Sigma}(0) = \bar{\Sigma}_0; \dot{V}(0) = \bar{V}_0;$$

$$\dot{\Sigma}(T) = \bar{\Sigma}, \dot{V}(T) = \bar{V}$$

for max  $G_{\Sigma}(T)$

For the particular variational problem solution it is necessary to formulate such controls  $\delta(t)$  and  $\dot{\Sigma}(t)$  and choose such values of the constant parameters  $\bar{G}_N$  and  $q$ , which provide  $\dot{G}_u \max$ . The weight and trajectory ingradient of the problem are not separated.

The problem is essentially simplified for the homogenous gravitational field, for which the solution for the optimal thrust direction is following [30], [38], at  $R(\vec{r}, t) = \text{const}$ , opt  $\dot{\Sigma}(t) = \frac{\bar{E}_1 - \bar{E}_2 t}{\sqrt{6_1^2 - 26_2^2 \cdot 6_1 t + 6_2^2 t^2}}$ ,

$$\Phi_L = \frac{d}{2g} \frac{12L^2}{T^3} \quad (40)$$

For the motion between the two rest points the optimal solution depends on the functional  $\Phi_L = \frac{d}{2g} \frac{12L^2}{T^3}$  (see fig.35). The optimality or one coasting are at the trajectory center of the duration  $1/3 T$  is shown.

The results of the numerical solution to the problem of the optimal orbital transfer Earth-Mars with  $P = \text{const}$ . [165] are presented in fig.36. The comparison of the functional value for the regimes  $P_{\text{opt}} = \text{var}$ ,  $P = \text{const}$  with power on and off [165] is illustrated in fig.37.

The introduction of the direct restrictions on the propulsion system parameters (the particular case is  $P = \text{const}$ ) makes the solution to the optimization problem much more complex, since in this case the trajectory and weight ingradient of the problem are not separated. The mentioned difficulties do not exist, if the restrictions are imposed on the acceleration  $a$  due to thrust; however these conditions account for the restrictions, imposed on the propulsion system parameters (consumption and jet velocity), only in indirect manner. The solution of the weight ingradient of the problem [19] (see above) entirely extended to the case of the limited acceleration; the trajectory optimization problem consists as previously of providing the minimum of the functional  $J = \int_a dt$ .

In the case of constant  $a(t) = Q_0$  the problem of minimum is equivalent to that of minimum  $T$  at specified value or , the latter for-

14

mulation is used for the problem solution in a central field /51/, /58/.

[126] (fig.38).

$$a(t) = a_0 = \text{const} ; \quad \dot{\gamma} = a_0^2 T ; \quad \dot{z} = v_0 \sin \psi ; \quad \dot{\varphi} = -\frac{v_0}{r} \cos \psi ;$$

$$\ddot{v} = a_0 \sin(\psi - \vartheta) - \frac{1}{r^2} v \sin \psi \quad (41)$$

$$\dot{\psi} = \frac{a_0}{v} \cos(\psi - \vartheta) + (1 - \frac{v_0^2}{r^2}) \cos \psi / r^2 v$$

For near-orbits transfer /126/ : at  $t_1 \approx 1$ ;  $a_0 \ll 1$ .

$$\text{Opt } C_{tg} \gamma = \frac{\sin(t+t_0)}{2 \cos(t+t_0) + c_0} . \quad (42)$$

The comparison between the approximate (dotted line) and exact (continuous line) programs (t) for the example of Earth-Mars mission at  $a_0 = 0,1 \text{ cm/sec}^2$  ( $T = 186 \cdot 24 \text{ hours}$ ) is given in fig.39. Here the value  $\gamma = 16,1 \text{ m}^2/\text{sec}^3$ , instead of the value  $6,6 \text{ m}^2/\text{sec}^3$  is representative according to the optimal solution.

The possibility of the power off:

$$a(t) = a_0 \left| \begin{array}{l} \dot{\gamma} = a_0^2 \delta ; \quad \dot{z} = \vec{v} ; \quad \vec{v} = a_0 t \delta + \vec{R} ; \quad \text{at min } \gamma(T) \\ a(t) = 0 \quad | \vec{i}(t) \cup \delta(t) ; \quad \gamma(0) = 0 ; \quad \dot{z}(0) = \vec{z}_0 ; \quad \vec{v}(0) = \vec{v}_0 ; \quad \vec{z}(T) = \vec{z}_T ; \quad \vec{v}(T) = \vec{v}_T \end{array} \right.$$

$$\text{at } \vec{R} = 0 ; \quad L, T : \quad \gamma_{\min} = 13,5 \frac{L^2}{T^3} \quad (43)$$

$$\left( \gamma_{\text{opt}} = 12 \frac{L^2}{T^3} ; \quad \gamma_{a=\text{const}} = 16 \frac{L^2}{T^3} \right)$$

improves considerably the functional of the problem in this case. For the motion between the rest points  $\gamma = 13,5$  /3/ (see the dotted line in fig.21 and compare with (33)) and a coasting arc takes  $1/3$  of the total time; for the problem of the orbit plane turning (see the dotted line in fig.22) the departure from the optimal functional  $\sim 8$  per cent and the coasting arc covers the arc  $\pm 23,2^\circ$  [23]. The comparison for the example of the Earth-Mars mission is given in fig.40 /168/. The problem of the approximation of the complex optimal law of limited-power propulsion system control by a simple stepwise law is investigated in detail in [33].

The ideally regulated and unregulated propulsion systems, considered above, represent the upper and lower criteria of the power - limited regulated propulsion system capabilities. As has been noted above, in a real accelerator, when the jet velocity being regulated in a certain range, the efficiency depends on  $N(t)$ ;  $N(t) \leq N_{\max}(V) \leq N_0$ ;  $0 \leq V_{\min} \leq V(t) \leq V_{\max} < \infty$

$$G_N = \alpha N_0 (d + \text{const}) ; \quad N_{\max}(V) = N_0 \gamma(V) ; \quad \bar{N} = \frac{N}{N_{\max}} : \quad (44)$$

$$16 \quad \dot{G}_x = -\frac{g}{\omega} G_N \bar{\epsilon}(V) \frac{\bar{N}}{V^2}; \quad \dot{\bar{\epsilon}} = \bar{U}; \quad \dot{\bar{U}} = \frac{\frac{g}{\omega} G_N}{G_x \cdot G_N} \bar{\epsilon}(V) \frac{\bar{N}}{V} \bar{\epsilon} + R; \quad \dot{G}_N = 0$$

15

$$G_x = G_m + G_n / V(t), \quad \bar{\epsilon}(t) \text{ and } \bar{N}(t) \sim \max G_x(T) \quad (44)$$

$$G_x(0) + G_N(0) = 1, \quad \bar{\epsilon}(0) = \bar{\epsilon}_0, \quad \bar{U}(0) = \bar{U}_0; \quad \bar{\epsilon}(T) = \bar{\epsilon}_T, \quad \bar{U}(T) = \bar{U}_T$$

For the written set of the equations the optimal controls  $V(t)$ ,  $\bar{\epsilon}(t)$ ,  $\bar{N}(t)$  and opt  $G_N$ , providing  $\bar{G}_n \max$ , are determined. As an example, the following simplest regulating characteristic  $\bar{\epsilon}(V)$  is considered:

$$\begin{aligned} \bar{N} &= 1 / \bar{\epsilon}(V) = \begin{cases} 1 & \text{at } V_{\min} \leq V \leq V_{\max} \\ 0 & \text{at } V \leq V_{\min}; V \geq V_{\max} \end{cases} \\ \bar{N} &= 0 / \bar{\epsilon}(V) = \begin{cases} 1 & \text{at } V_{\min} \leq V \leq V_{\max} \\ 0 & \text{at } V \leq V_{\min}; V \geq V_{\max} \end{cases} \end{aligned}$$

which in limit cases transforms into ideally regulated and unregulated systems (fig.41). The presence of the arcs with  $V_{opt}(t)$ ,  $V = V_{\max}$  and  $\bar{N} = 0$  is seen in (fig.42). In fig.42 indicated the programm of optimal restricted-exhaust velocity control for the example of the Earth-Mars mission. Another kind of restrictions, that is imposed on the time or the propulsion system operation, is considered in [30].

With long time of the propulsion systems operation the problem of reliability becomes of especial importance. The relation of the reliability problem to the choice of the optimal trajectory and weight parameters has been investigated in detail in [7], and accordingly, the account for the trajectory correction in the problems of the weight parameters optimization for the power-limited propulsion systems has been considered in [78].

In conclusion it may be noted, that the propulsion system contrasting, contained in a number of works, is not always scientifically justified. It is more correct to investigate [121], [32] the optimal combination and the domains of the reasonable application of the various propulsion systems.

As an example in fig.44 [121] for the two simulation problems (velocity increment flight along the distance L) there presented data of power-limited propulsion systems combination with limited jet velocity. The shaded domain, where this combination is reasonable, corresponds to the payload proximity for each of the propulsion systems.

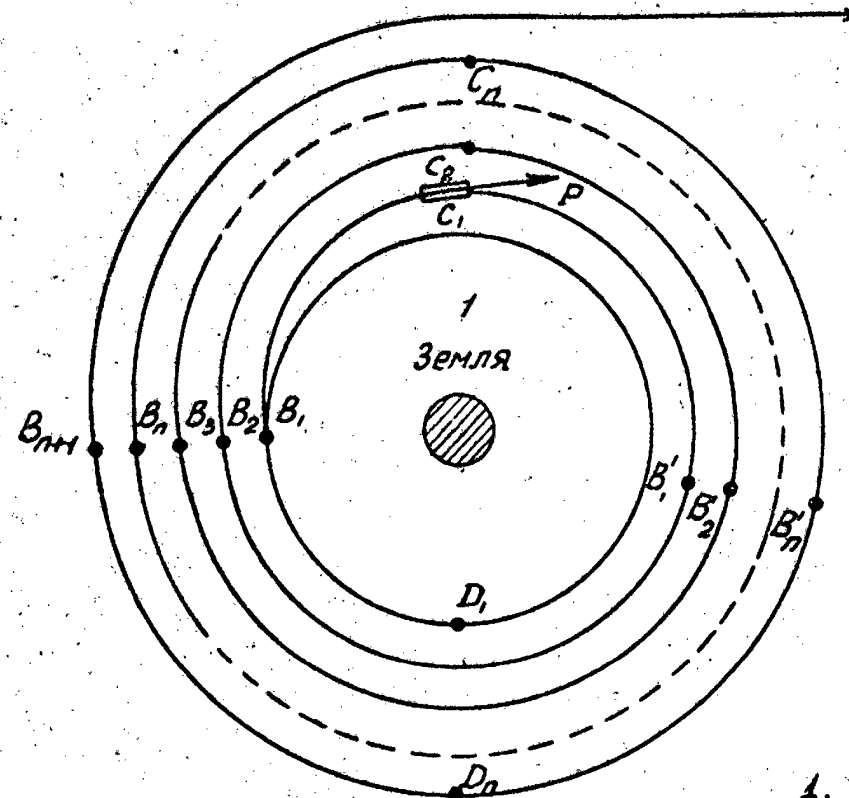
The indicated data deal briefly only with the formulating and resulting aspects of the basic carried out works; the statement of the essential investigations by the methods of the variational problem solution see in Part IV of our survey [24].

Table 1

Propulsion system type 1	Principal scheme 2	Jet composition 3	Exhaust velocity $V [m/sec]$ 4	Specific weight of the propulsion system (propulsion system weight divided by maximum thrust) $\mathcal{T} = G_{g,y} / P_{max}$ 5	Acceleration due to thrust (thrust divided by the vehicle mass) $a [m/sec^2]$ 6
Thermal jet engines	Chemical combustion chamber	Gaseous combustion products	up to $4.5 \cdot 10^3$	$10^{-2}$	$10^{-5} \cdot 10^{-2}$
	Solid nuclear propellant reactor	Dissociated gas	$8 \cdot 10^2 - 1.2 \cdot 10^4$	$10^{-1}$	$1 \cdot 100$
	Liquid nuclear propellant reactor	Dissociated gas	$1.2 \cdot 10^4 - 2 \cdot 10^4$	$10^{-1}$	$1 \cdot 100$
	Gaseous nuclear propellant reactor	Plasma	$2 \cdot 10^4 - 7 \cdot 10^4$	$10^{-1}$	$1 \cdot 100$
Electrical jet engines	Arc heater	Plasma	up to $2.5 \cdot 10^4$	$10^3$	$10^{-3} \cdot 10^{-2}$
Power limited engines	Electrostatic accelerator	Plasma	$5 \cdot 10^4 - 10^6$	$10^3$	$10^{-5} \cdot 10^{-2}$
	Electrodynamic accelerator	Plasma	$5 \cdot 10^4 - 10^6$	$10^3$	$10^{-5} \cdot 10^{-2}$
Solar sail	Mirror surface reflecting solar rays	Photons or the solar radiation	$3 \cdot 10^{-8}$	$10^4$	$10^{-5} \cdot 10^{-2}$

Table II

Planet	Mercury	Venus	Jupiter	Saturn	Uranus	Neptun	Pluto	
T, years	0.53	0.45	6.6	17	49	96	145	
Payload, $G_n, m$	Mass of the unit sail area, $\rho \delta, g/cm^2$	Sail demensions		Total vehicle weight, $G_0, m$	Initial acceleration due to solar pressure $a_0, cm/sec^2$	Duration of the maneuver $T, 24 hours$	Radius of the initial circular orbit, $Z_0, km.$	Maximal departure of the trajectory till the take off instant, km
		Area, $S_0, m^2$	Equivalent circle diameter, m					
0.1	$10^{-4}$	$10^6$	$1.12 \cdot 10^3$	1.1	0.85	54	$7.25 \cdot 10^3$	$4.2 \cdot 10^5$
0.1	$2 \cdot 10^{-4}$	$10^6$	$1.12 \cdot 10^3$	2.1	0.44	112	$7.25 \cdot 10^3$	$6.1 \cdot 10^5$
0.1	$3 \cdot 10^{-4}$	$10^6$	$1.12 \cdot 10^3$	3.1	0.3	119	$7.25 \cdot 10^3$	$7.62 \cdot 10^5$
0.1	$10^{-4}$	$2.46 \cdot 10^5$	$0.56 \cdot 10^3$	0.348	0.67	73	$7.25 \cdot 10^3$	$4.78 \cdot 10^5$
0.1	$10^{-4}$	$10^5$	$0.356 \cdot 10^3$	0.2	0.46	105	$7.25 \cdot 10^3$	$5.87 \cdot 10^5$



1. Earth

Fig.1

1. Sail 2. Solar rays

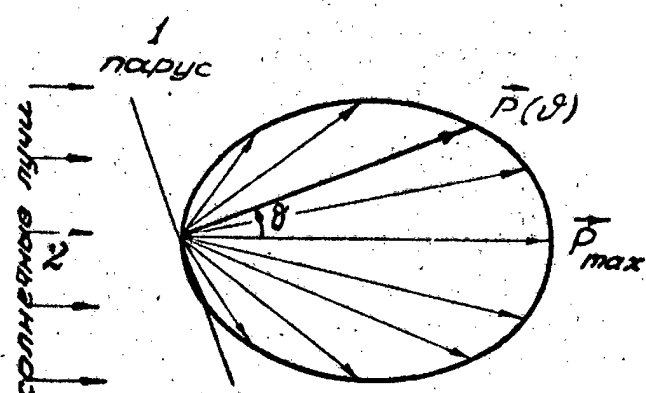


Fig.2

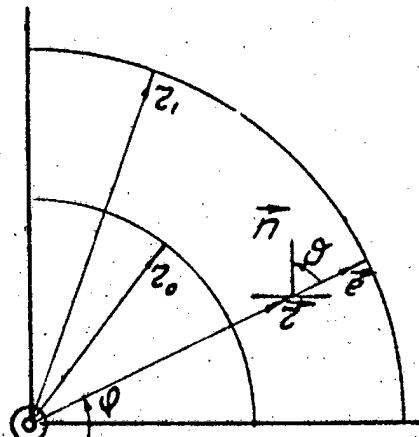
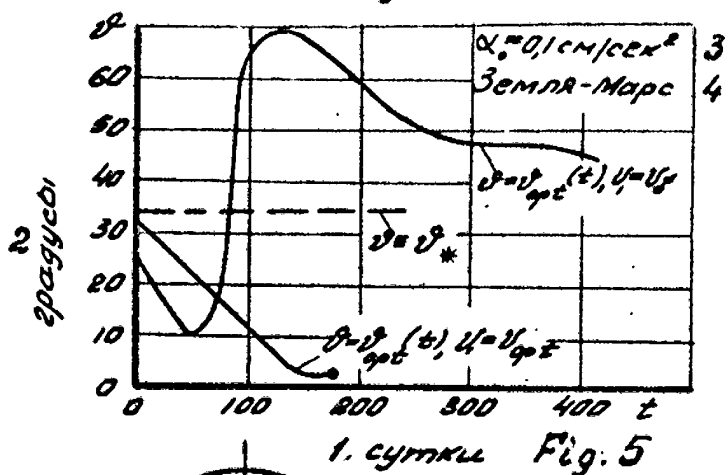
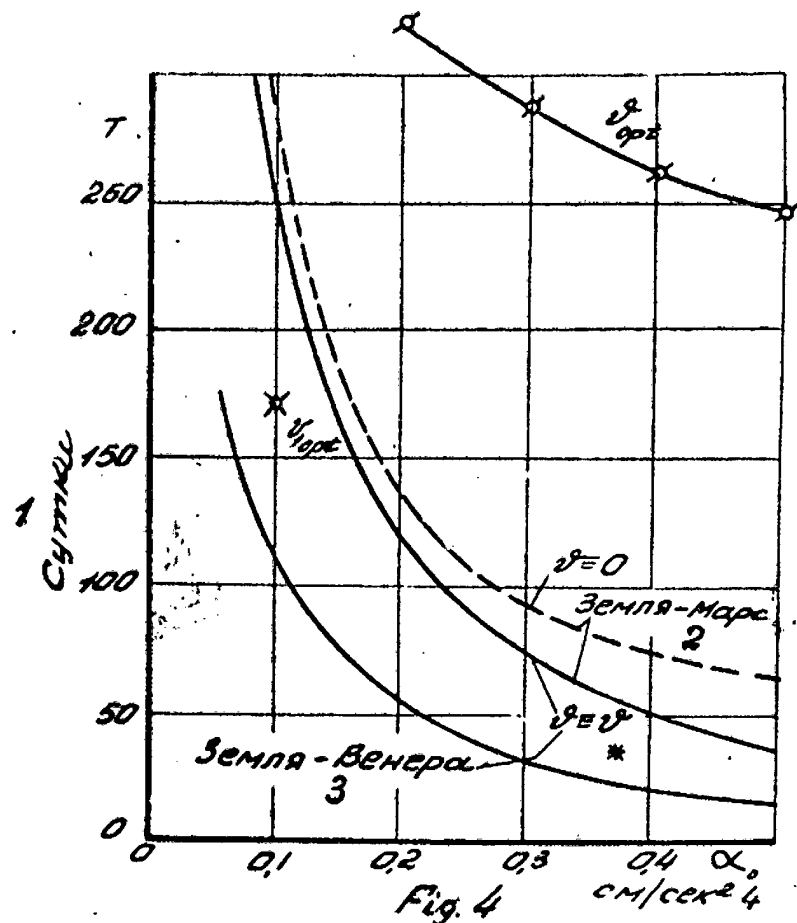
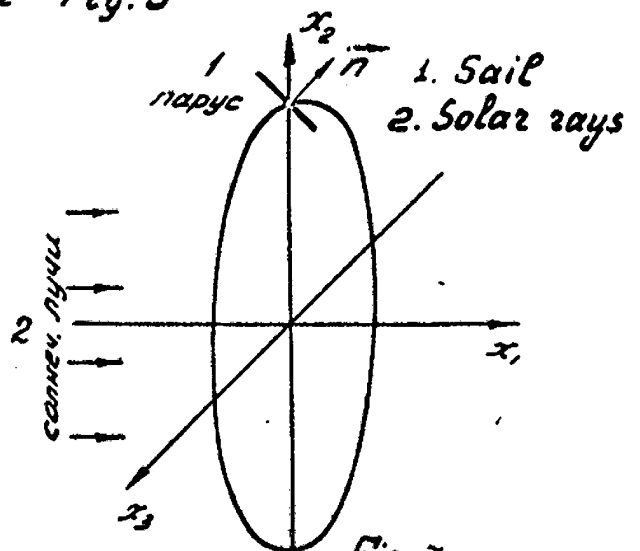
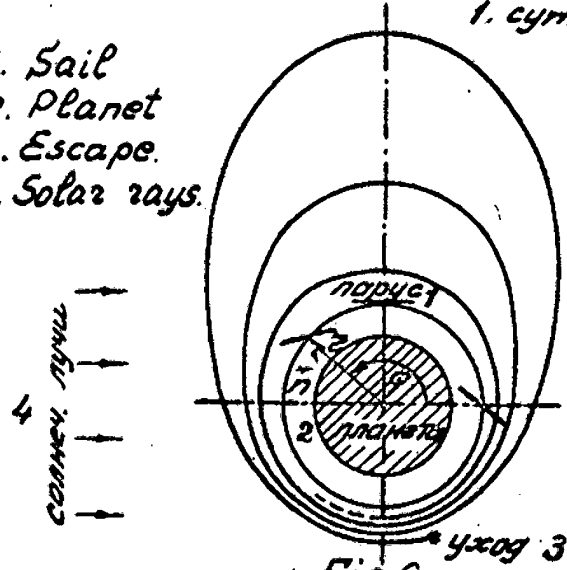


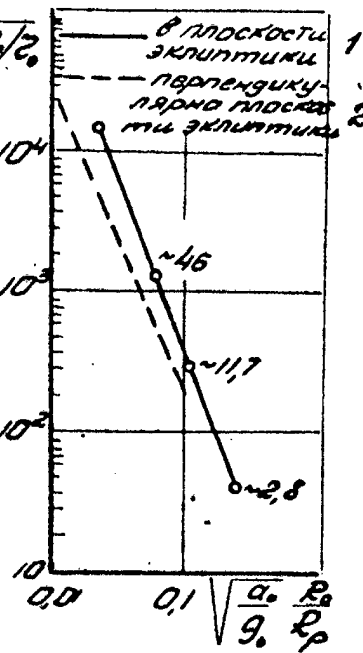
Fig.3



1. Sail
2. Planet
3. Escape.
4. Solar rays.



1. Photo or thermo-element.
2. Vapour vessel.
3. liquid.
4. Radiator
5. Turbine
6. Ionization chamber.
7. Electric generator.
8. Nuclear reactor.
9. High pressure vapour..
10. Turbine
11. Liquid.
12. Radiator.
13. Low pressure vapour
14. Electric generator.



1. In ecliptic plane.
2. Perpendicular to the ecliptic plane.

Fig. 8

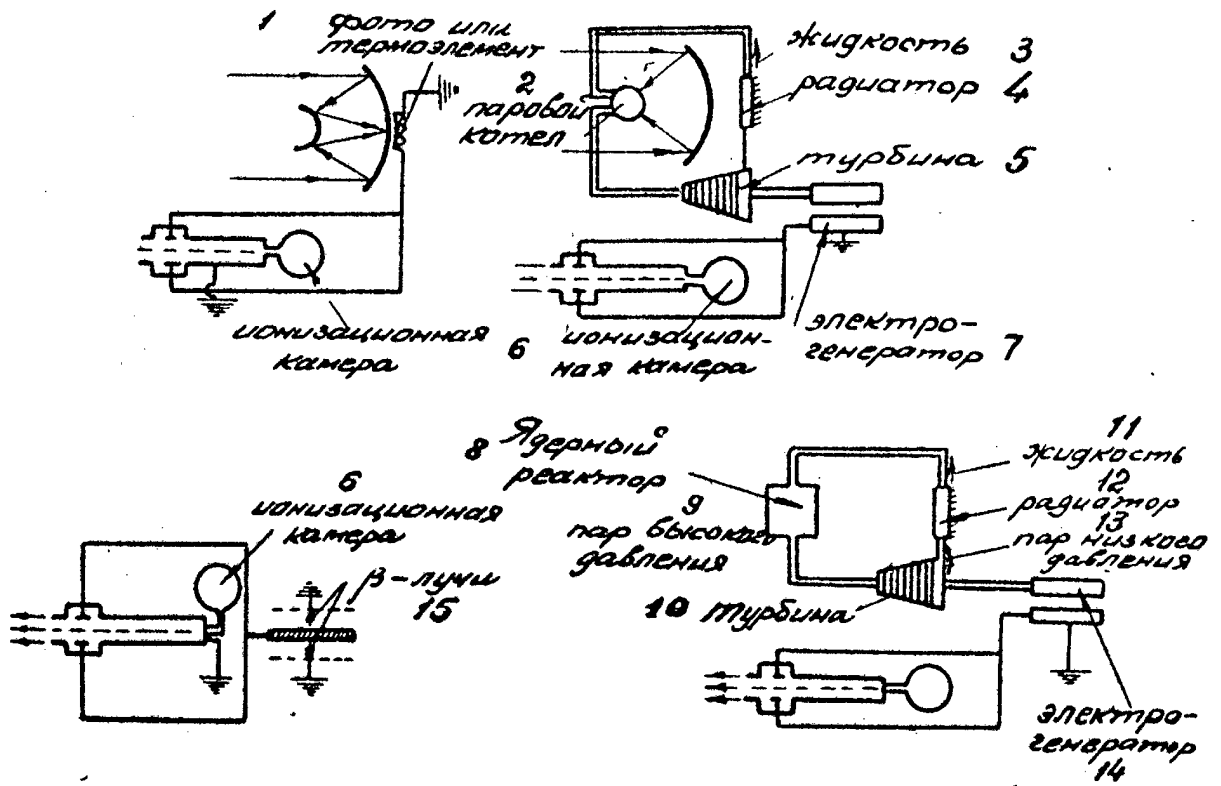
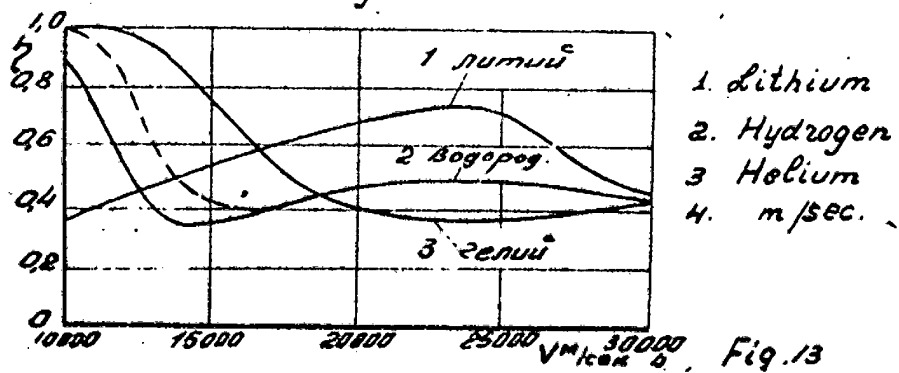
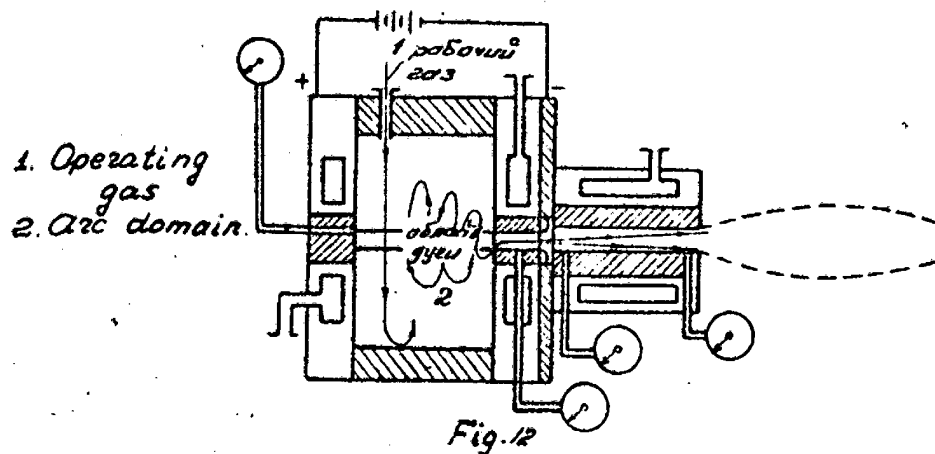
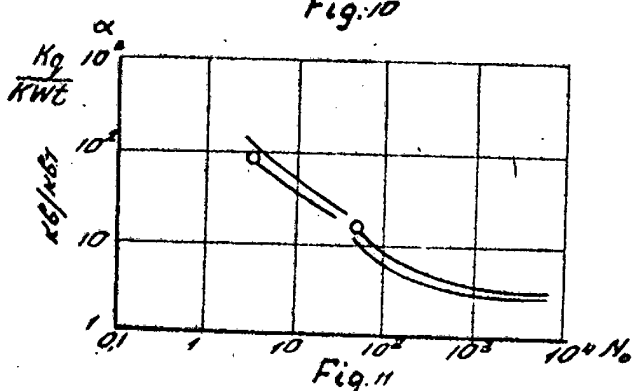
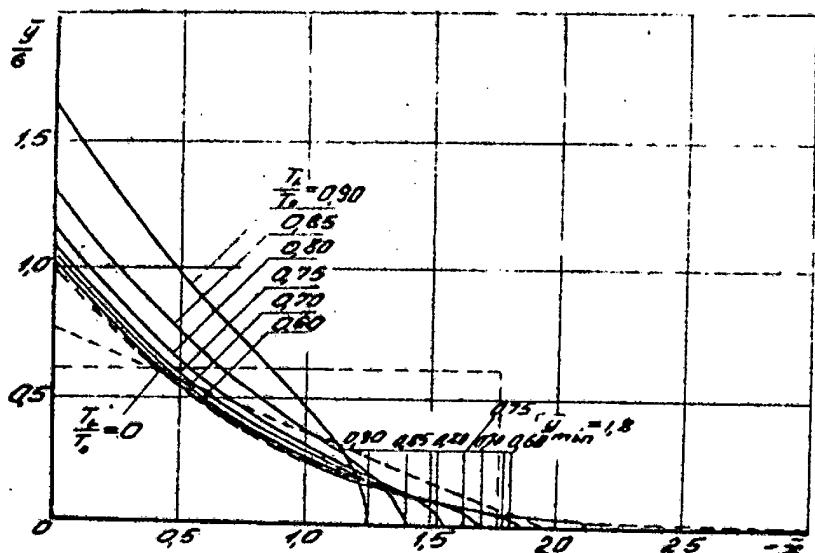
15.  $\beta$ - rays

Fig. 9



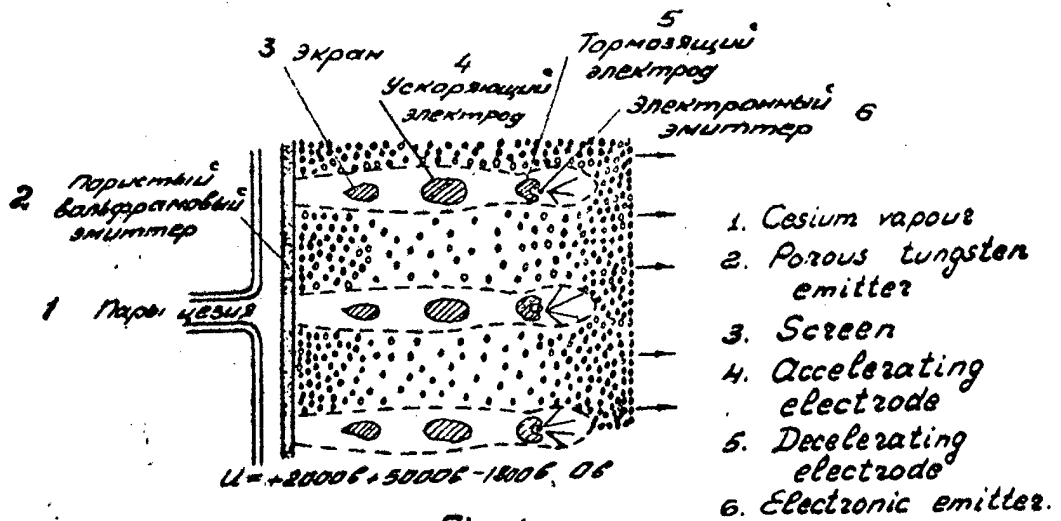


Fig. 14

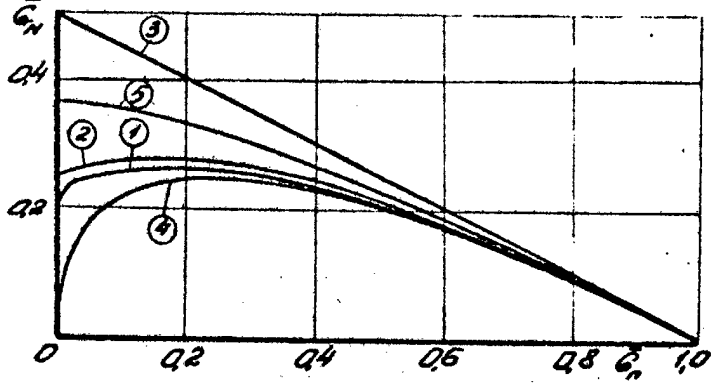
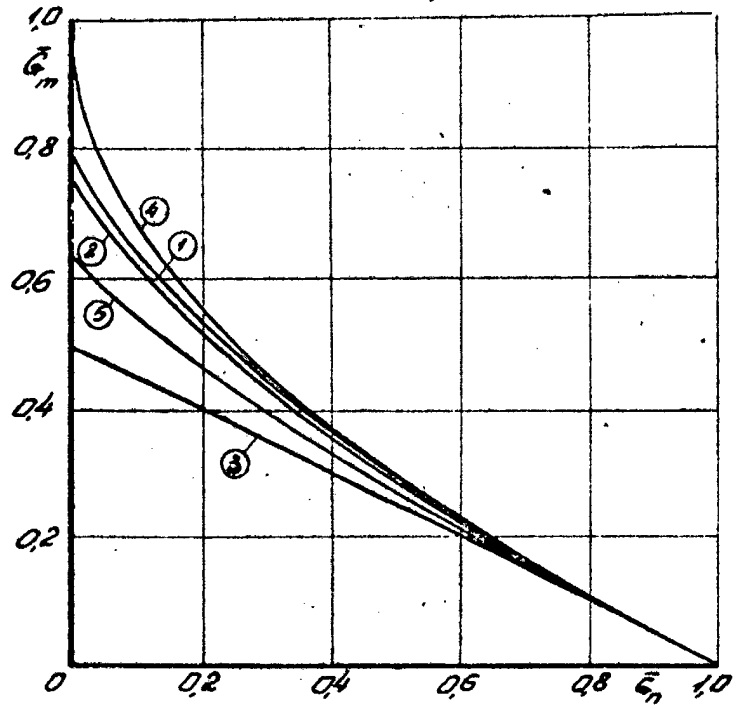


Fig. 15

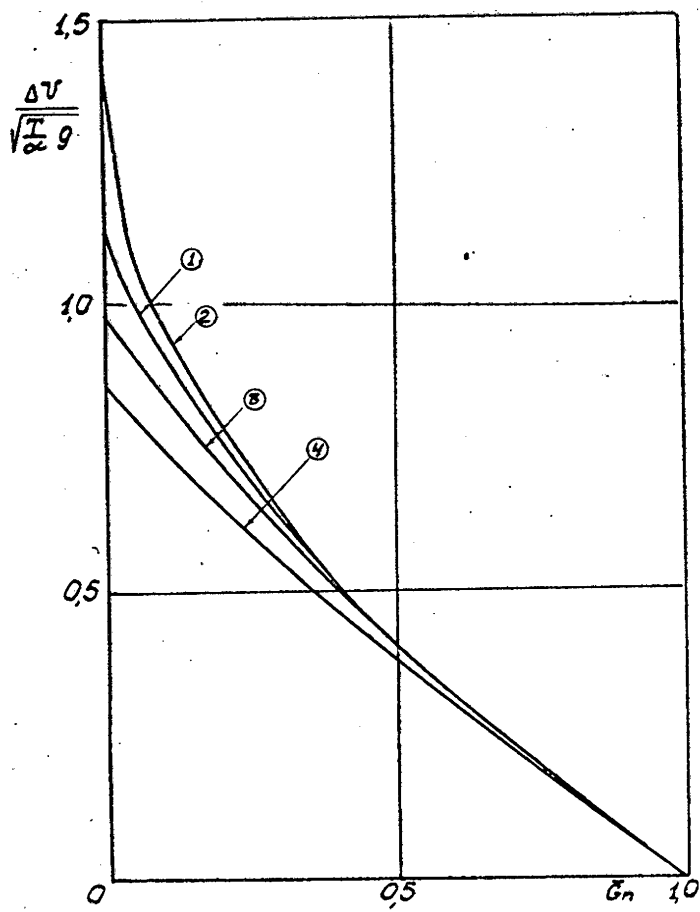
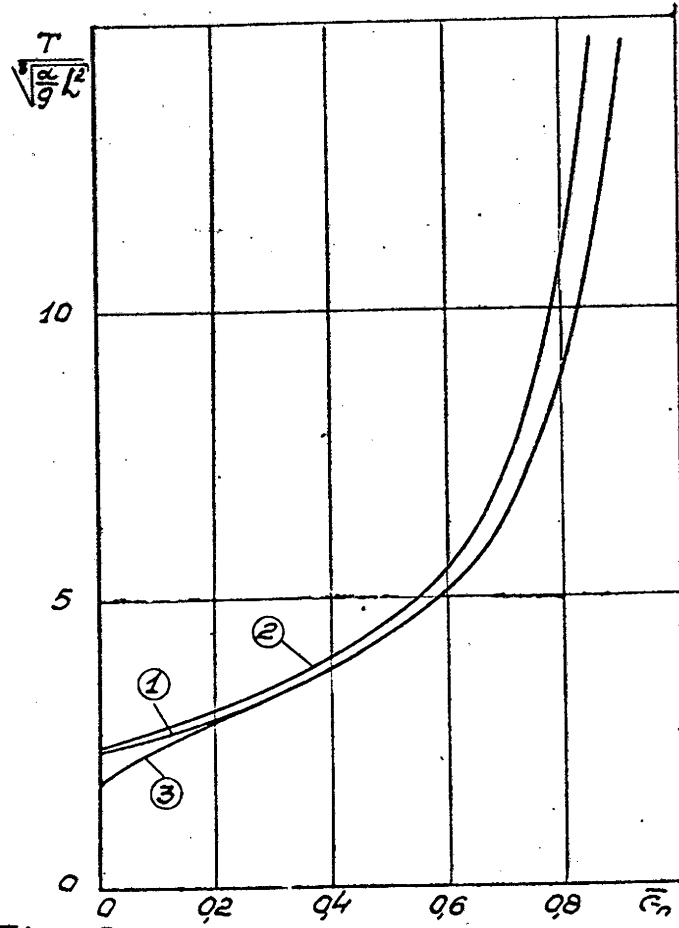


Fig. 16



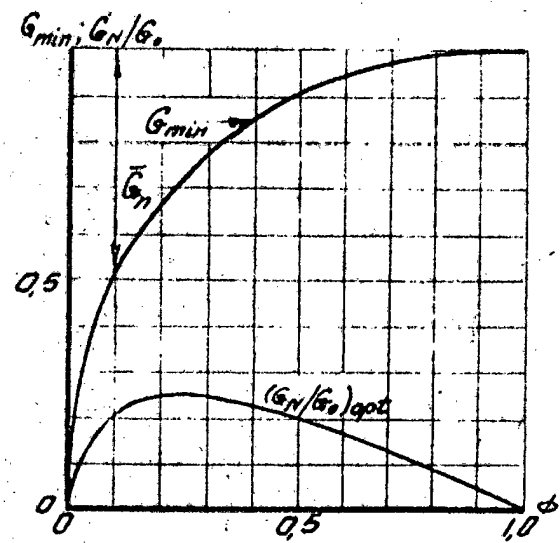


Fig. 17

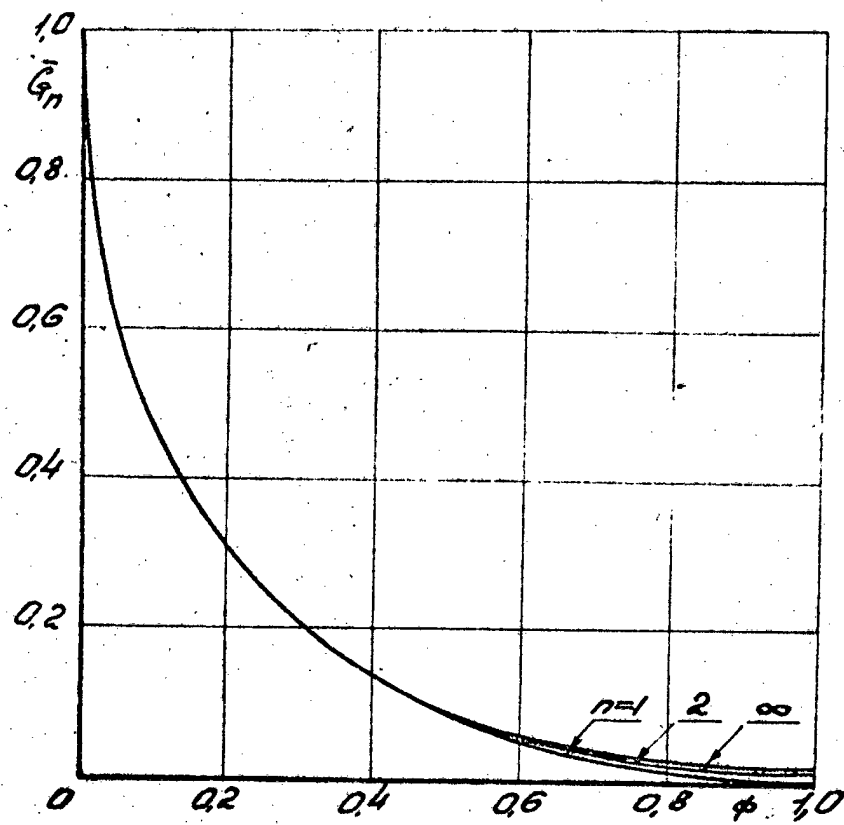


Fig. 18

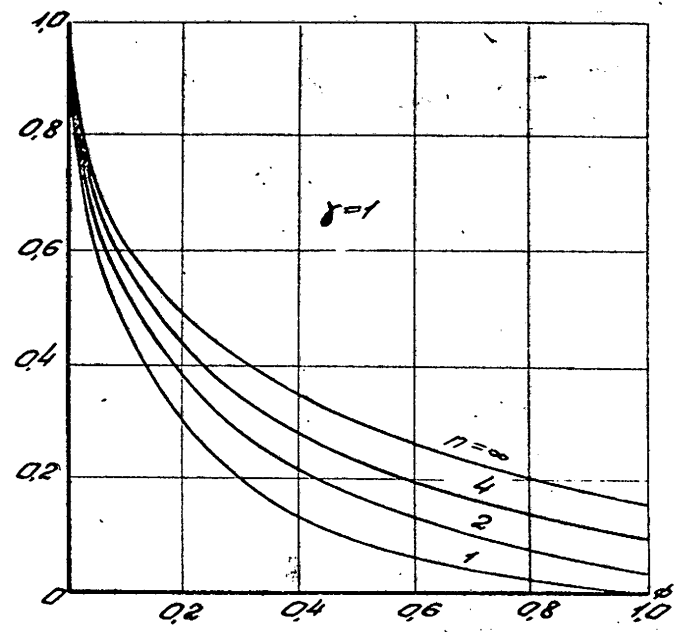
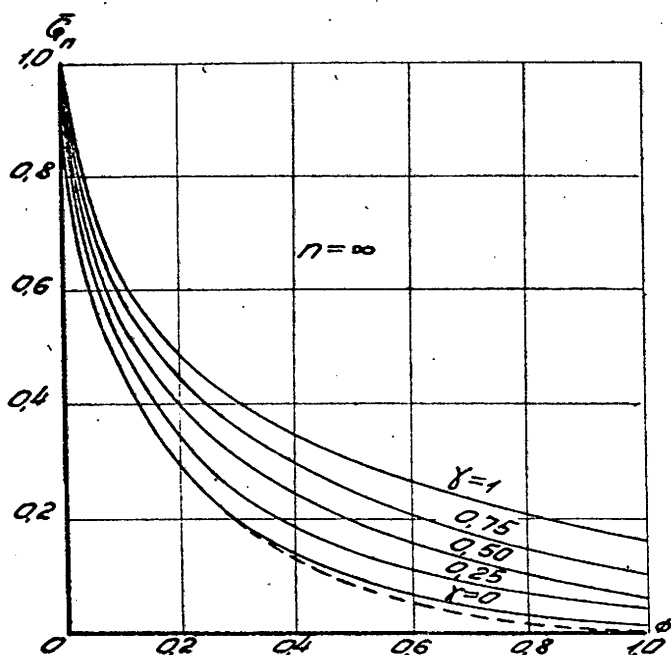


Fig.19

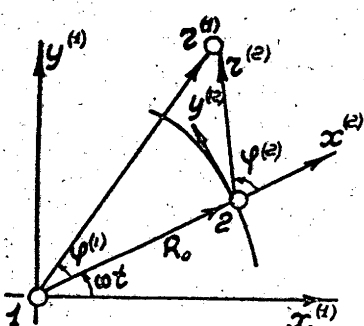


Fig. 20

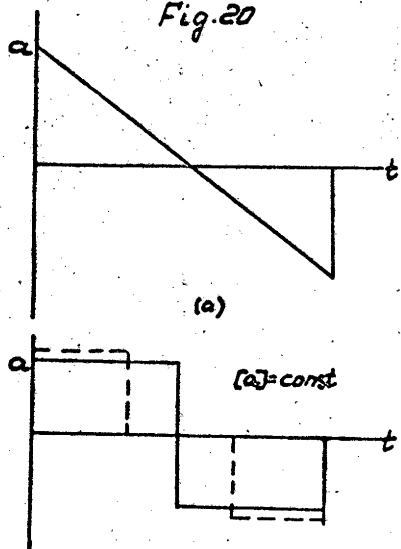


Fig. 21

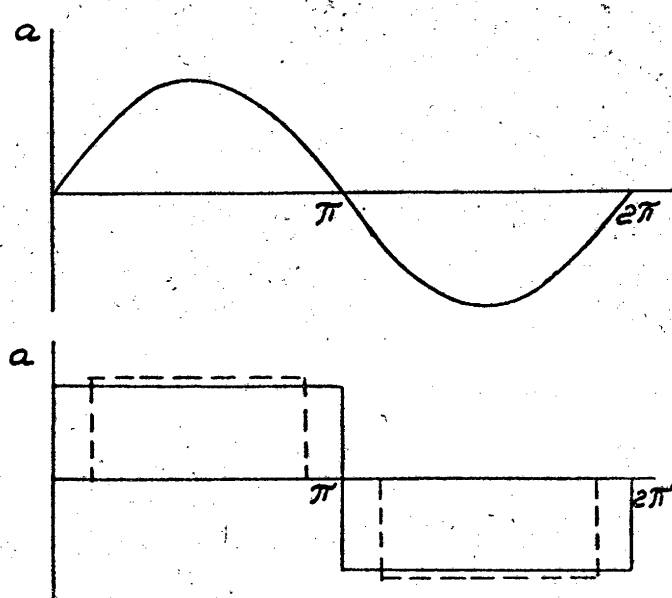


Fig. 22

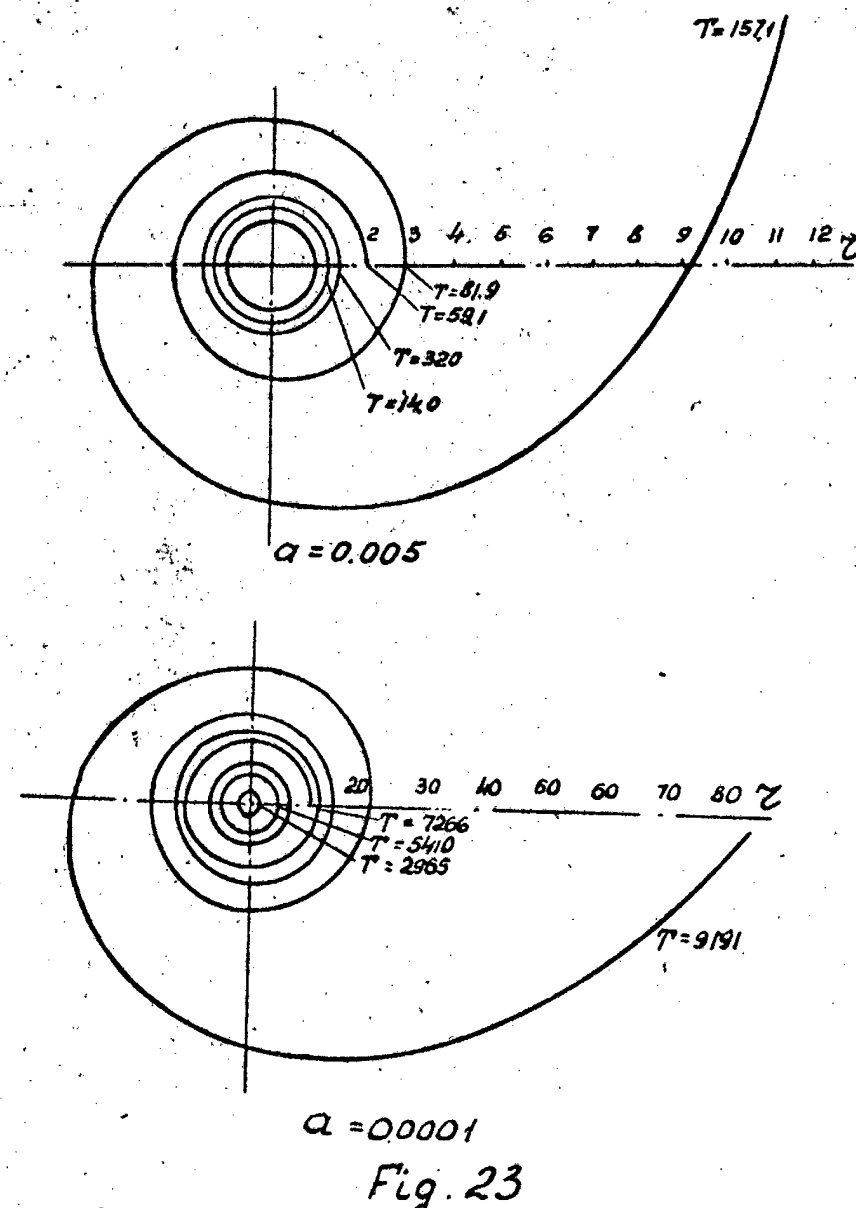


Fig. 23

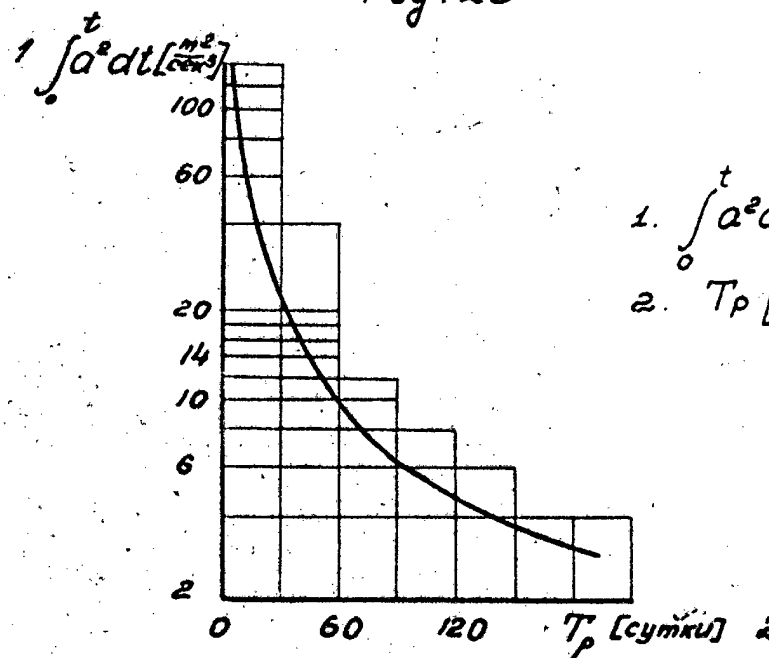


Fig. 24

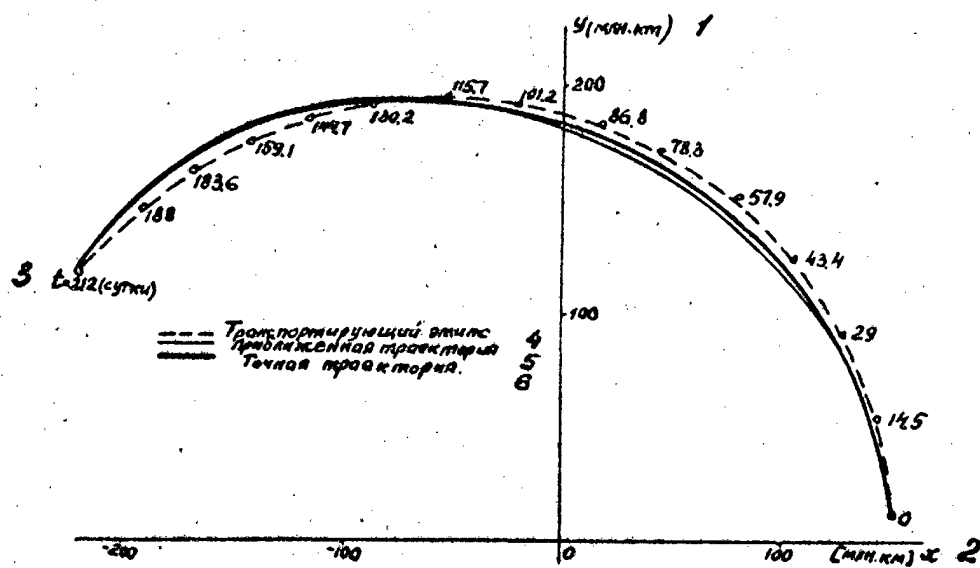
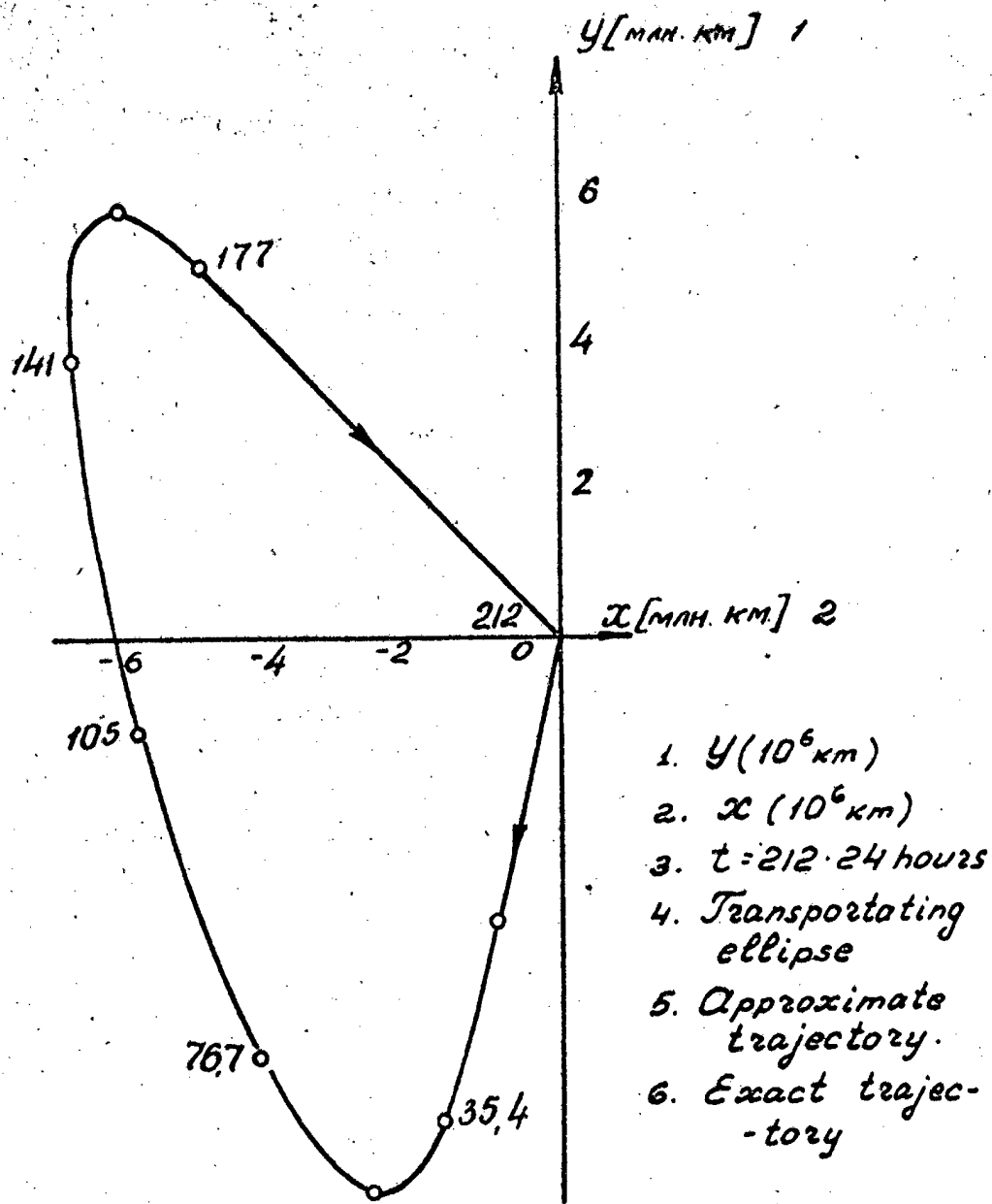


Fig. 25

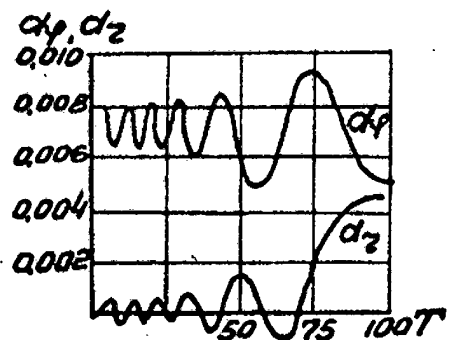


Fig. 26

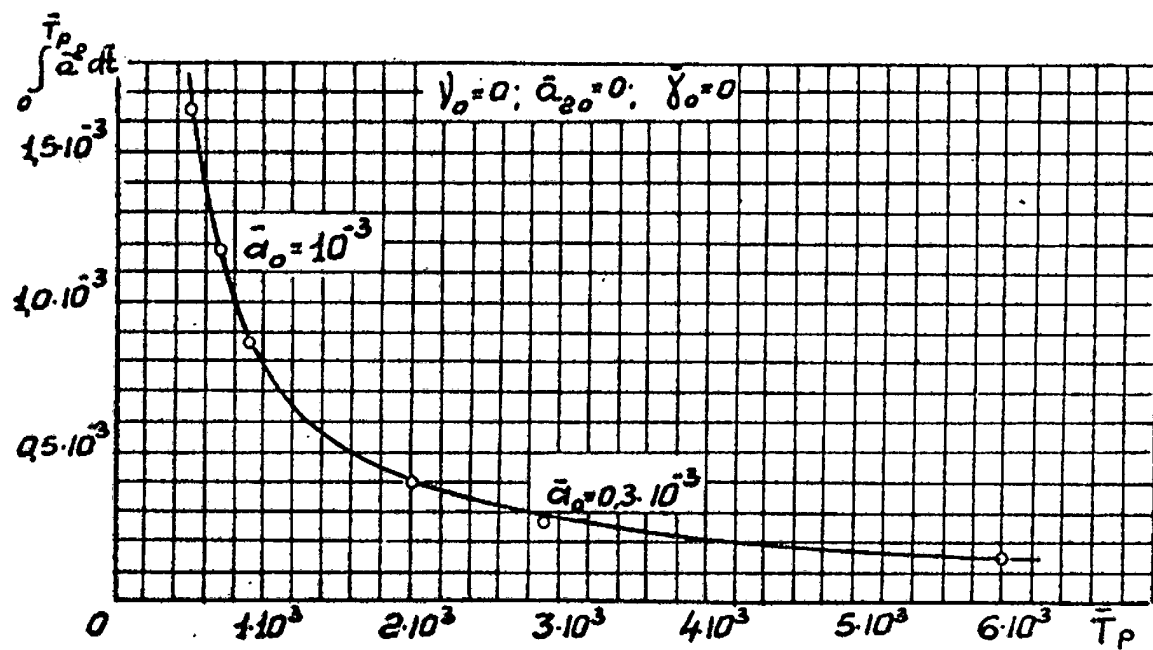


Fig. 27

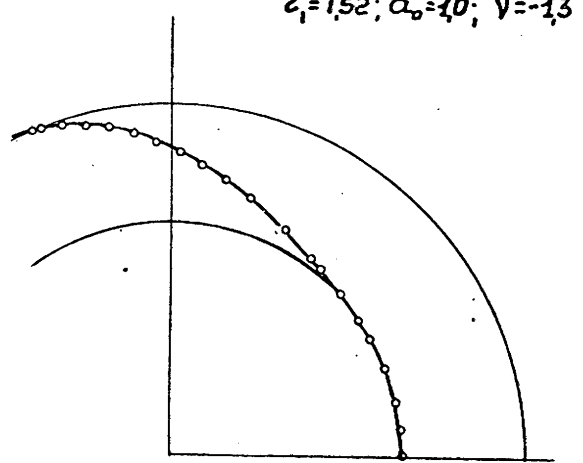
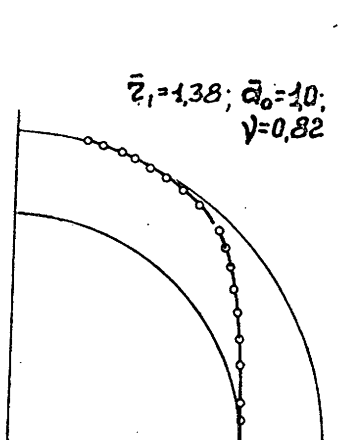
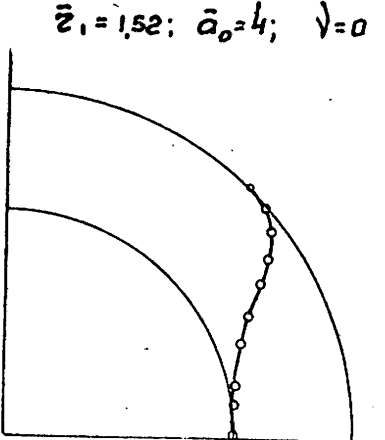
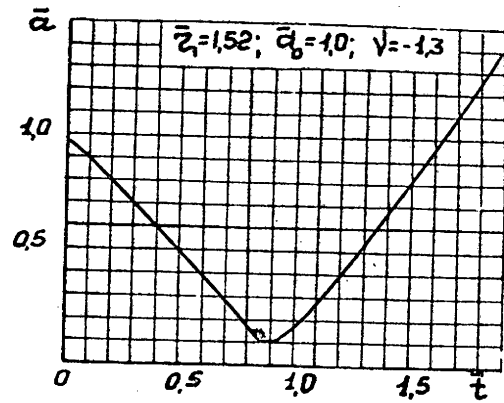
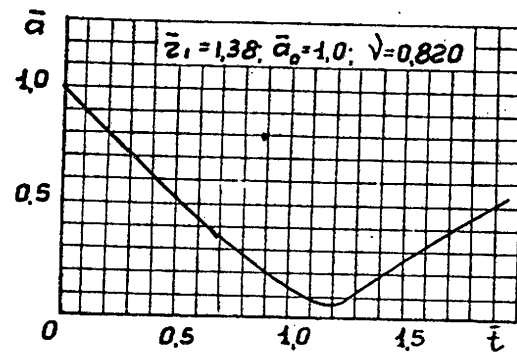
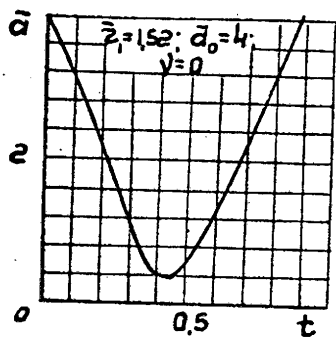


Fig. 28

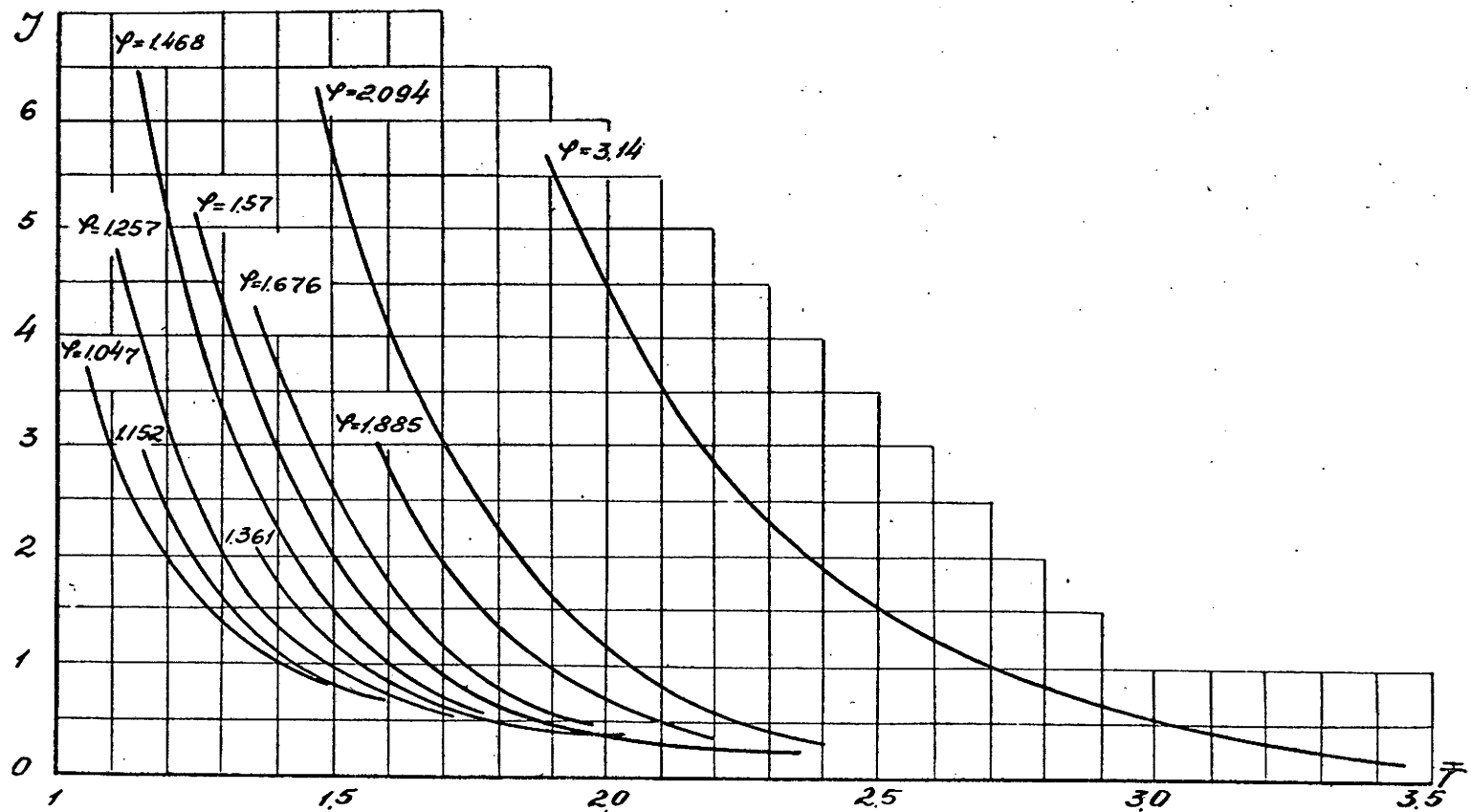
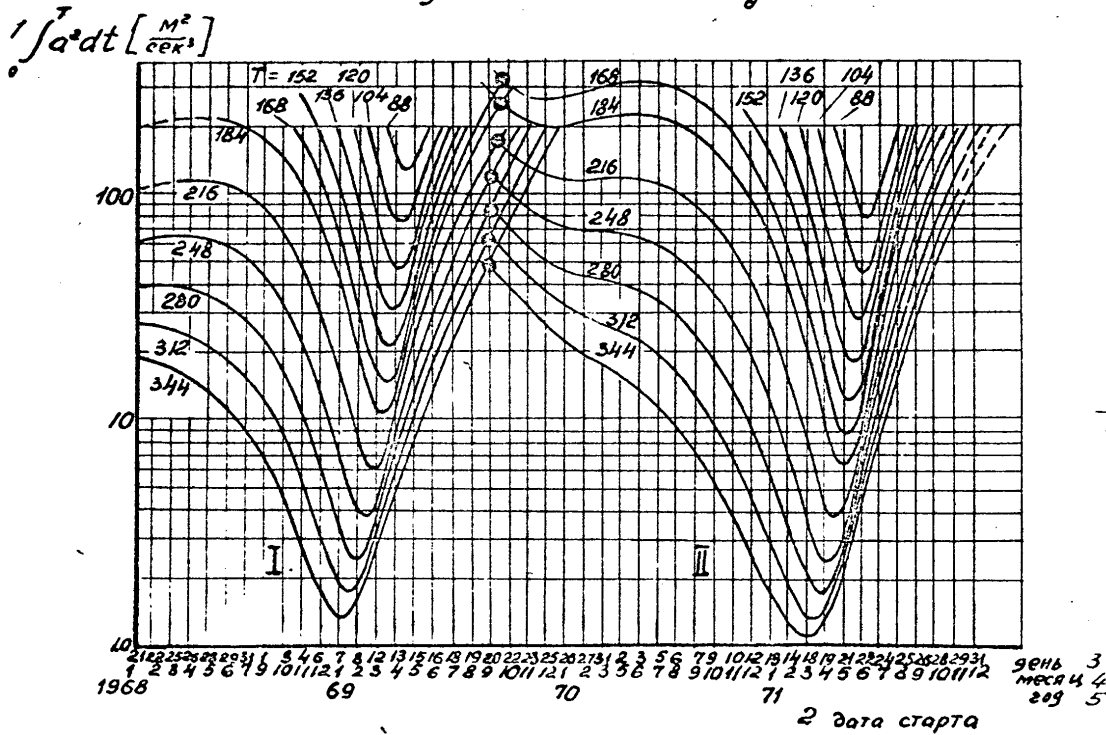


Fig 29

1.  $\int \alpha^2 dt [m^2/sec^3]$
2. Launch date.
3. Day.
4. Month
5. Year.



1. Apr. 8.5 1970
2. Oct. 6.5 1969

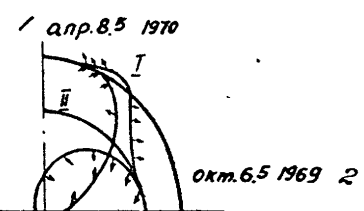


Fig. 31

Fig. 30

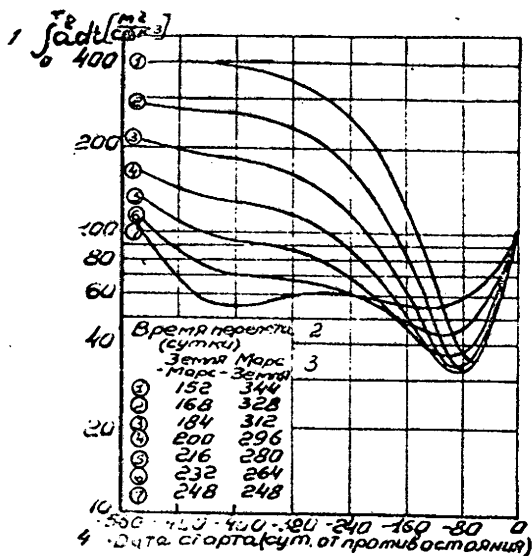
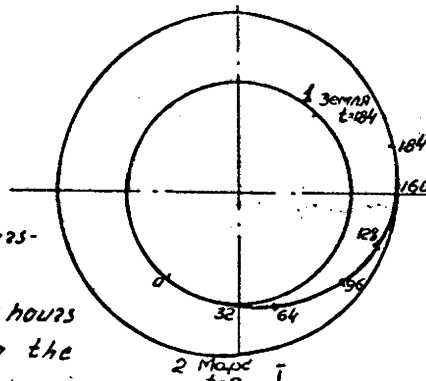


Fig. 32

1.  $\int a^2 dt \text{ m}^2/\text{sec}^3$
2. Transfer time (24 hours)
3. Earth-Mars-Mars-Earth
4. Launch date (24 hours with reference to the opposition.)



1. Earth.
2. Mars.
3.  $T_{opp} = 48$  hours
4. Earth
5. Mars.

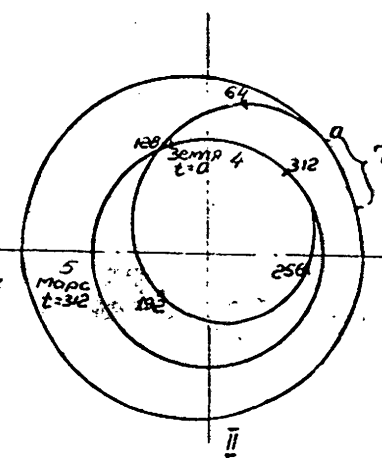


Fig. 33

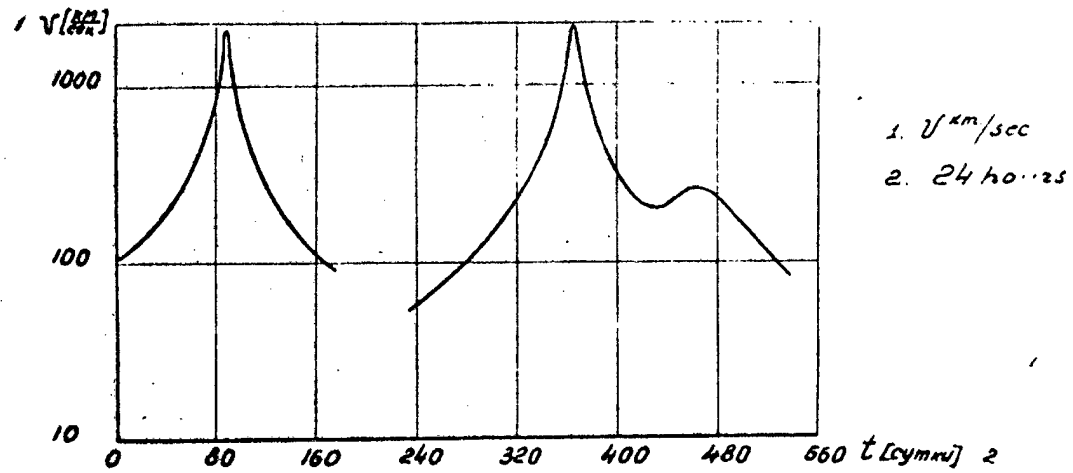


Fig. 34

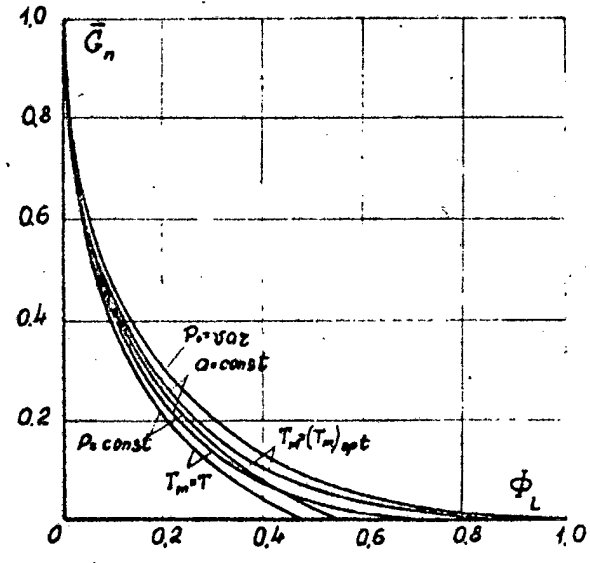
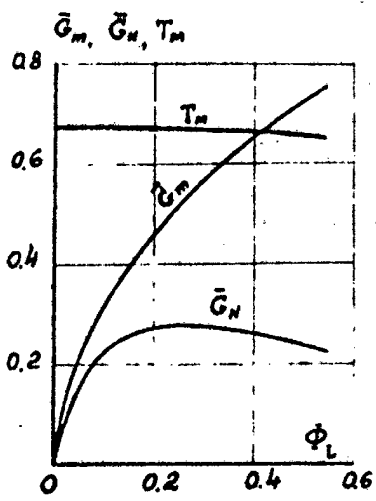


Fig. 35

1. SEC.
2. Earth - Mars
3. 24 hours
4.  $\text{kg}/\text{kwt}$

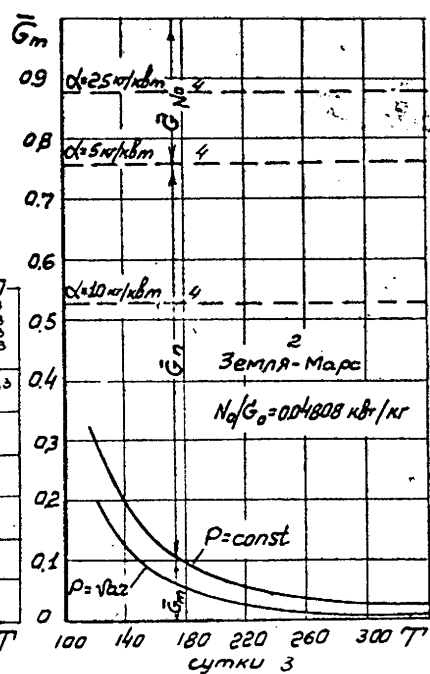
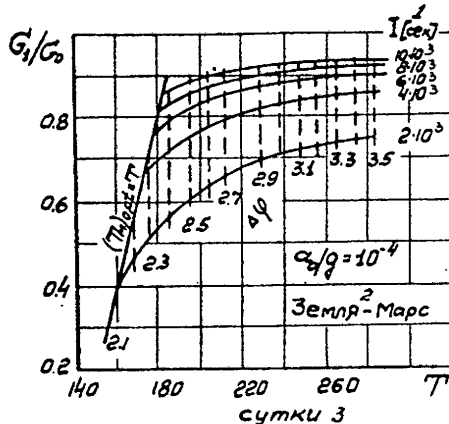


Fig. 36

1. Earth - Mars
2.  $V = 50 \text{ km/sec}$ .
3. 24 hours
4.  $J [m^2/\text{sec}^3]$

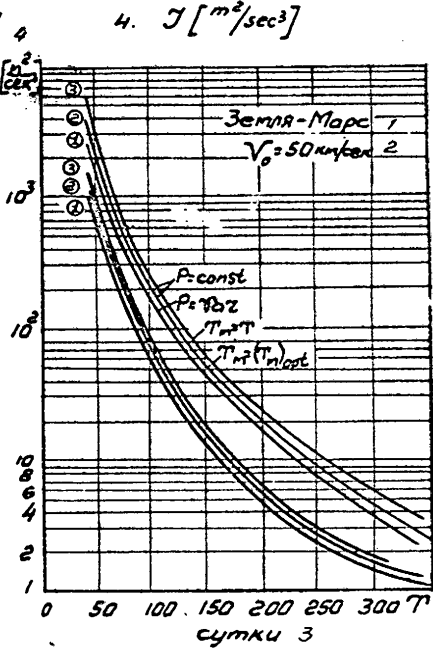


Fig. 37

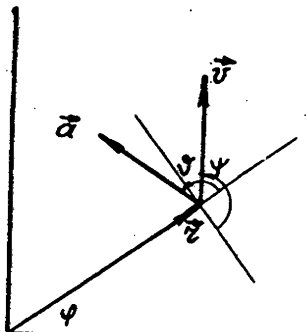


Fig. 38

$$z = (\psi + \pi/2 - \varphi)$$

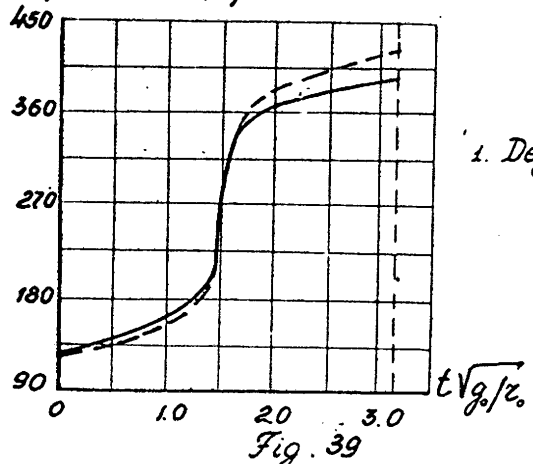


Fig. 39

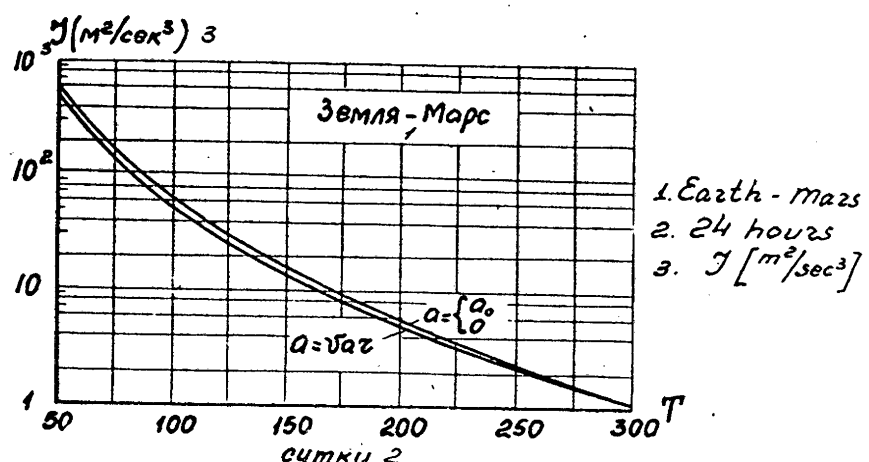


Fig. 40

1. Degrees

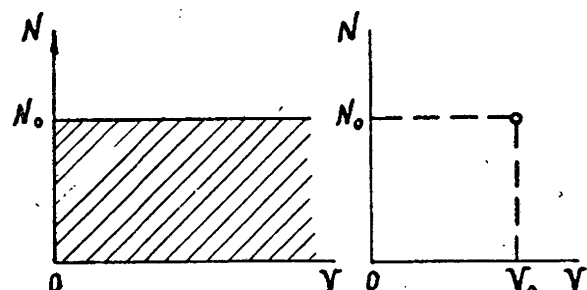


Fig. 41

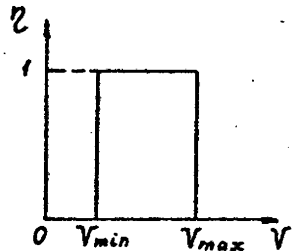


Fig. 42

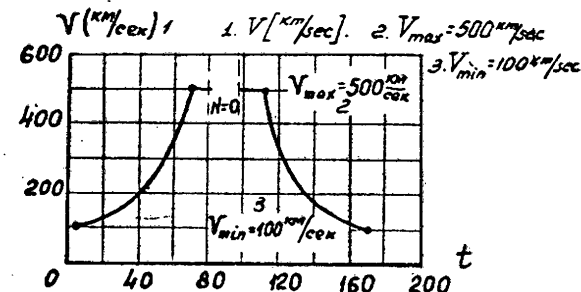
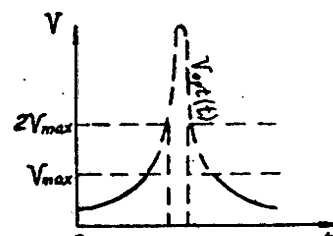
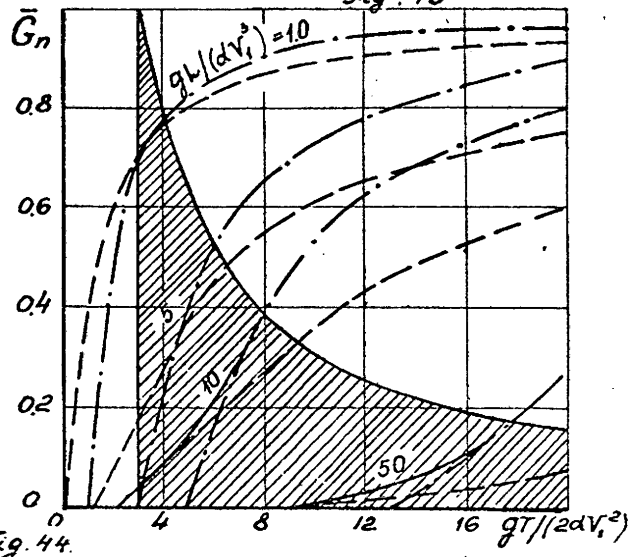
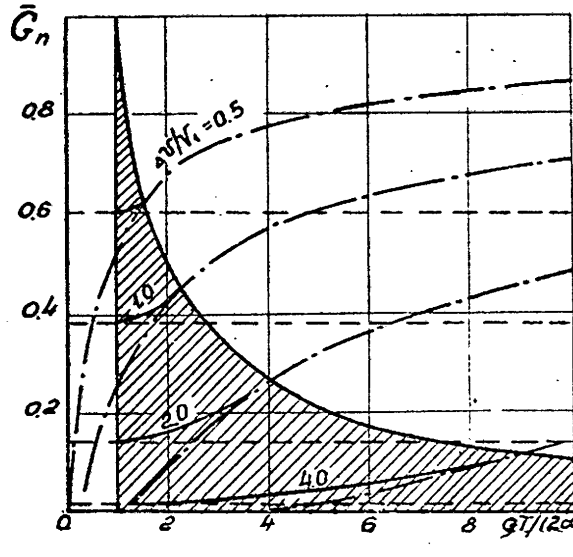


Fig. 43



БИБЛИОГРАФИЯ

1. Э.Л.АКИМ, Т.М. ЭНЕЕВ. "Космические исследования" т.1. №1, 1963 г.
2. С.Г.АЛЕКСАНДРОВ, Р.Е.ФЕДОРОВ. "Советские спутники и космические ракеты" Изд-во АН СССР, м., 1959 г.
3. В.В.БЕЛЕЦКИЙ, В.А.ЕГОРОВ. "Космические исследования" № 2, 1964 г.
4. В.В.БЕЛЕЦКИЙ, В.А.ЕГОРОВ. "Космические исследования" № 8, 1964 г.
5. В.В.БЕЛЕЦКИЙ, В.А.ЕГОРОВ, В.Г.ЕРОШОВ. "Космические исследования", №3, 1964 г.
6. В.В.БЕЛЕЦКИЙ "Космические исследования" №3, 1964 г.
7. И.С.БЕРЕЗИН, Н.П.ЖИДКОВ. "Методы вычислений", т.2. Физматгиз, 1960 г.
8. М.Ш.БИРМАН. "Успехи математических наук", т.5. №3(37), 1950 г.
9. Н.Н.БОГОЛОУБОВ, Ю.А.МИТРОПОЛЮСКИЙ. "Асимптотические методы в теории линейных колебаний". Физматгиз, 1958 г.
10. Н.Н.БОГОЛОУБОВ, Д.Н.ЗУБАРЕВ. "Укр.матем.журнал", УП, 1955 г.
11. В.А.БРУМБЕРГ. "Бюлл.ин-та теор.астрономии", т.8. № 4, 1962 г.
12. В.М.ВОЛОСОВ, Ж.Вычисл.матем.и матем.физ., т.3. №1, 1963 г.
13. М.К.ГАВУРИН. "Изв.выш.учебн.завед." Вып.5, 1958 г.
14. И.М.ГЕЛЬФАНД, С.В.Фомин "Вариационное исчисление", Физматгиз, 1961 г.
15. Г.Л.ГРОДЗОВСКИЙ, Ю.Н.ИВАНОВ, В.В.ТОКАРЕВ. "Докл.АН СССР, т.137, №5, 1961; XII IAF Congress
16. Г.Л.ГРОДЗОВСКИЙ. Acta Astronautica, VIII, 1962, XII IAF Congress, 1961.
17. Г.Л.ГРОДЗОВСКИЙ, Ю.Н.Иванов, В.В.Токарев, XIII IAE Congress, 1962.
18. Г.Л.ГРОДЗОВСКИЙ. "Изв.АН СССР", ОТН, №5, 1962 г.
19. Г.Л.ГРОДЗОВСКИЙ. "Изв.АН СССР", ОТН, Э и А, №6, 1962 г.
20. Г.Л.ГРОДЗОВСКИЙ, В.В.ФРОЛОВ, XIII IAE Congress, 1962.
21. Г.Л.ГРОДЗОВСКИЙ, Ю.Н.ИВАНОВ, В.В.ТОКАРЕВ. XIV IAE Congress, 1962.
22. Г.Л.ГРОДЗОВСКИЙ, А.Л.СТАСЕНКО.
23. Г.Л.ГРОДЗОВСКИЙ, Ю.Н.ИВАНОВ, В.В.ТОКАРЕВ. "II Всесоюзный съезд по механике" 1964 г.
24. Г.Л.ГРОДЗОВСКИЙ, Ю.Н.ИВАНОВ, В.В.ТОКАРЕВ. "Механика космического полета с малой тягой." Инженерный журнал АН СССР т.ш Вып.3 и 4, 1963 г. т.1у Вып.1 и 2, 1964 г.
25. Ю.П.ГУСКОВ, ПММ, т.27. №3, 1963 г.
26. Г.Н.ДУБОШИН. "Небесная механика" Физматгиз, 1963 г.
27. В.А.ЕГОРОВ. "Прикладная математика и механика" т.22. II, 1958 г.
28. А.Н.ЖУКОВ, В.Н.ЛЕБЕДЕВ. Сб. "Искусственные спутники Земли" №10, 1963 г.
29. Ю.Н.ИВАНОВ "Прикл.матем.и механ." т.26, №4, 1962 г.
30. Ю.Н.ИВАНОВ. "Прикл.матем.и механ." т.27, №5, 1963 г.
31. Ю.Н.ИВАНОВ. "Прикл.матем.и механ." т.28, №1, 1964 г.
32. Ю.Н.ИВАНОВ. "Изв. АН СССР" Отд.техн.наук "Механика и машиностроение" №2, 1964 г.
33. Ю.Н.ИВАНОВ. "Прикл.матем.и механ." т.28, №3, 1964 г.
34. Ю.Н.ИВАНОВ, В.В.ТОКАРЕВ, В.В.ШАЛАЕВ. "Космические исследования" №3 1964 г.

35. Ю.Н.ИВАНОВ, Ю.В.ШАЛАЕВ. "Космические исследования", №3, 1964 г.
36. Ю.Н.ИВАНОВ. "П Всесоюзный съезд по механике", 1964 г.
37. В.Ф.ИЛЛАРИОНОВ, Л.М.ШКАДОВ. "НММ", т.26, №1 1962 г.
38. В.К.ИСАЕВ. "Автоматика и телемеханика", т.22, №8 1961 г. Т.23 №1, 1962 г.
39. В.К.ИСАЕВ, В.В.СОНИН. "Автоматика и телемеханика", т.23, №9, 1962 г.
40. В.К.ИСАЕВ, В.В.СОНИН. "Журн.вычисл.матем.и матем.физ.", т.3, №6, 1963г.
41. Исследование оптимальных режимов движения ракет. Сб.под ред.И.Н.Савдовского. Оборонгиз, М., 1959 г.
42. Ионные, плазменные и дуговые ракетных двигатели. Сб.перев., Госатомиздат, М., 1961 г.
43. А.Ю.ИШЛИНСКИЙ. Доклады АН СССР, т.53, №7, 1946 г.
44. Л.В.КАНТОРОВИЧ, В.Н.КРЫЛОВ. Приближенные методы высшего анализа. Гостехиздат, 1941 г.
45. Л.В.Канторович. Доклад АН СССР, т.48, №7, 1945 г.
46. Л.В.КАНТОРОВИЧ. Доклад АН СССР, т.56, № 3 1947 г.
47. Л.В.КАНТОРОВИЧ. Успехи матем.наук, т.3, №6, 1948 г.
48. А.А.КАРЫМОВ. Прикл.матем.и механ., т.26, №5, 1962 г.
49. У.КОРЛИСС. Ракетные двигатели для космических полетов. Ил., М., 1962 г.
50. И.А.КРЫЛОВ, Ф.Л.ЧЕРНОУСЬКО. Журн.вычисл.матем.и матем.физ., т.2, №6 1962 г.
51. Н.М.КРЫЛОВ, Н.Н.БОГОЛОБОВ. Введение в нелинейную механику. Изд. АН УССР, 1937 г.
52. Р.КУРАНТ. Принцип Дирихле, конформное отображение и минимальные поверхности, Ил. 1963 г.
53. Г.Е.КУЗМАК, Ю.М.КОПНИН. Журн.вычисл.матем.и матем.физ., т.3, №4, 1968
54. В.В.ЛАРИЧЕВА, М.В.РЕИН. Журн.вычисл.матем.и матем.физ. (в печати)
55. В.В.ЛАРИЧЕВА, М.В.РЕИН. Асимптотика уравнений небесной механики, пригодная при большом диапазоне изменения эксцентриситета. Космические исследования (в печати)
56. В.В.ЛАРИЧЕВА, М.В.РЕИН. Замечания об осреднении уравнений возмущенного движения в оскулирующих элементах при изменении эксцентриситета в широких пределах. Космические исследования (в печати).
57. В.Н.ЛЕБЕДЕВ, Б.Н.РУМИНЦЕВ. Сб. "Искусственные спутники Земли" Вып.16, 1963 г.
58. В.Н.ЛЕБЕДЕВ. Вычисл.матем.и матем.физ. т.4, №3, 1964 г.
59. В.Н.ЛЕБЕДЕВ. Журн.вычисл.матем.и матем.физ. (в печати).
60. А.И.ЛУРЬЕ, М.К.ЧЕРЕМСИН. Сб. "Искусственные спутники Земли" №16 Изд-во АН СССР, 1963 г.
61. А.И.ЛУРЬЕ. Прикл.матем.и механ., т.23, №2, 1959 г., см.также сб. "Искусственные спутники Земли", вып.4, 1960 г.
62. С.Г.МИХАЛИН. Прямые методы математической физики. Гостехтеориадат, 1950г.
63. Н.Н.МОИСЕЕВ. N.N.MOISEYEV, XIII IAF Congress 1962.
64. Д.Е.ОХОЦИМСКИЙ. Прикл.матем.и механ. т.10, №2 1946 г.
65. Д.Е.ОХОЦИМСКИЙ, Т.М.ЭНЕЕВ. Успехи физ.наук. т.63, вып.1а, 1957 г.
66. Ю.И.ПАРАЕВ. Автоматика и телемеханика, т.23, №9 1962 г.
67. Л.С.ПОНТРИГИН, В.Г.БОЛТЯНСКИЙ, Е.Ф.МИЩЕНКО, Р.В.ГАМКРЕЛИДЗЕ. Математическая теория оптимальных процессов. Физматгиз, 1961 г.

68. В.С.ПУГАЧЕВ. Теория случайных функций и ее приложение к задачам автоматического управления. Физматгиз, 1960 г.
69. Л.И.РОЗЕНФОР. Автоматика и телемеханика, т.20, № 10-12, 1959 г.
70. Б.А.САМОКИШ. Успехи матем.наук, т.12, № 1(3), 1957 г.
71. Л.А.СИМОНОВ. Космические исследования, 1964 г. (в печати)
72. Ф.СМИТ. Ракетная техника, №II, 1961 г.
73. Р.СТЕЭНСИЛ, Л.КУЛАКОВСКИЙ. Ракетная техника, №7, 1961 г.  
(J. Amer. Soc. vol. 31, № 7, 1961.)
74. А.Л.СТАСЕНКО. Изв.АН СССР, ОТН №6, 1962 г.
75. И.Я.СТАВИССКИЙ, А.Л.БОНДАРЕНКО, В.И.КРОТОВ, С.Я.ЛЕБЕДЕВ, В.Я.ПУНКО, Э.А.СТУМБУР. Журн.техн.физ. т.29, №8, 1959 г.
76. М.Ф.СУББОТИН. Курс небесной механики. т.1. Гостехтеоретиздат, 1933 г., т.2, ОНТИ, 1937 г., т.3, ОНТИ, 1949 г.
77. В.В.ТОКАРЕВ. Прикл.матем.и механ., т.26, №4, 1962 г.
78. В.В.Токарев. Прикл.матем.и механ. т.27, № 1, 1963 г.
79. В.В.ТОКАРЕВ. Прикладн.матем.и механ. т.27, №4, 1963 г.
80. В.В.ТОКАРЕВ. II Всесоюзный съезд по механике, 1964 г.
81. Ч.Б.ТОМИКИНС. Сб. "Современная математика для инженеров" (под ред. Э.Ф.БЕККЕНБАХА), Ил. 1959 г.
82. В.В.ФРОЛОВ. Изв. АН СССР.,ОТН, Э и А, №6, 1962 г.
83. А.Я.ХИНИН. Тр.МИ. АН СССР, т.59, 1955 г.
84. Ф.А.ЦАНДЕР. Сб."Ракетная техника", №I, 1936 г.
85. Ф.А.ЦАНДЕР. Межпланетные путешествия. Оборонгиз, М., 1961 г.
86. Ю.В.ШАЛАЕВ, Ю.Н.ИВАНОВ. Космические исследования, 1964 г. (в печати)
87. Л.И.ШАТРОВСКИЙ. Журнал вычисл.матем.и матем.физ. т.2, №3 1962 г.
88. Т.М.ЭНЕЕВ, А.К.ПЛАТОНОВ, Р.К.КАЗАКОВА. Сб."Искусственные спутники Земли", № 4, Изд-во АН СССР, 1960 г.
89. Т.М.ЭНЕЕВ. Доклад на Всесоюзном симпозиуме по многоэкстремальным задачам. Вильнюс, 13-15 июня, 1963 г.
90. M.L.ANTHONY, C.J.NADAY, Prepr.Amer.Astronaut.Soc. No.102, 21, 1961.
91. P.D.ARTHUR, H.K.KARRENBERG, H.L.STARK. J.Amer.Rock.Soc. vol.50, No.7. 1960.
92. G.AU. J.Amer.Rock.Soc., vol.50. No.7. 1960.
93. G.AU. Raketenmechanik und Raumfahrtforschung, B.V.No.2. 1961.
94. G.F.AU. Lufttransittechnik, vol.7. N1. 1961.
95. G.F.AU. Raketenmechanik und Raumfahrtforschung, B.V./. N1, 1962.
96. R.H.BACON. Amer.J.Phys., vol.27, p.164-165, 1959.
97. Y.G.BANTAS, W.H.SELLENS. Trans.ASME. Ser.C.I. of Heat Transfer, 82, 1960.
98. D.J.BENNEY. J.Amer.Rock.Soc., vol.28, No.5, 1958.
99. P.BLANC. Memorial de L'Artillerie Francaise, vol.35, N1, 1961.
100. G.A.BLISS. Univ.of Chicago Press, Chicago, 1946.
101. R.H.BODEN. Internat.Astronaut.Congr. 1959, Wien, 1960.
102. R.H.BODEN. Adv.Prop.Techn. 1960, Oxford, 1961.
103. R.H.BODEN. II.Intern.Symp. on Rockets and Astronaut. Tokyo, 1960.  
Tokyo, 1961.

104. J.V.BREAKWELL. J.Soc.Industrial and Appl. Math., vol.7. p.215-247, 1959.
105. J.V.BREAKWELL. Proc. of the Symp.on Vehicle Syst.Optim., N.Y. 1961.
106. H.BROWN, J.R.NELSON. J.Amer.Rock.Soc., vol.30, No.7, 1960.
107. H.Brown, H.E.NICOLL. A.I.A.A. J. vol.J. N2, 1963.
108. A.E.BRYSON, W.F.DENHAM. Proc.of the Symp.on Vehicle Syst.Optim., N.Y., 1961.
109. A.E.BRYSON, W.F.DENHAM, F.J.CARROLL, K.NIKAMI. JASS, vol.29,N4, 1962.
110. A.E.BRYSON, W.F.DENHAM. Trans.ASME, No.2, 1962.
111. R.M.BUSSURD. J.Brit.Interpl.Soc., vol.15, No, 1956.
112. M.CAMAC. J.Amer.Roc.Soc., vol.30, N1., 1960.
113. S.J.Citron. J.Amer.Rock.Soc.,vol.31. N12, 1961.
114. R.CORNIG. Uistas in Astronaut., vol.1. N.Y.,1958.
115. R.COURANT. Calculus or variations and supplementary notes and exercises, N.Y.Univers.,Institute of Mathematical Sci.,1945-1946, revised and amended by J.Moser, 1956-1957.
116. J.COPELAND. J.Amer.Rock.Soc., vol.29, No.4, 1959.
117. L.CROCCO. Proc.Seminar Adv.on Astronaut. Prop., 1960. Milan,1962.
118. S.T.DEMETRIADES. Prepr.Pecir.Gen.Meet.Amer.Inst.Electr.Eng., 1960.
119. S.T.DEMETRIADES. J.Brit.Interpl.Soc., vol.18,p.392, 1961-62; XI Internat.Astronaut.Cong.r., 1960, Vien,1961.
120. A.DOBROWOLSKI. J.Amer.Prock.Soc., vol.28, p.687-689, 1958.
121. T.N.EDELBAUM. Prepr.Amer.Astronaut.Soc., No.104, 1961.
122. T.N.EDELBAUM. J.Amer.Rock.Soc., vol.31, No.8., 1961.
123. K.A.EHRICKE. Space flight, vol.1. Environment and celestial mechanics, o.6., Perturbations, Princeton, von Nostrand,1960.
124. D.L.ESCHNER. SAE Journ. vol.66, No.8, 1958.
125. C.R.FAULDERS. J.Amer.Rock.Soc.,v.10. No.30, 1960.
126. C.R.FAULDERS. Astronaut.Auta, v.7.No.1. 1961.
127. E.P.TRENCH. Prepr.Techn.Ses.Amer.Astronaut.Soc., No.9.1960.
128. W.R.FIMBLE. J.Amer.Rou.Soc., vol.32, No.6.1962.
129. G.F.FORBES. J.Brit.Interpl.Soc., vol.9.1950.
130. R.H.FOX. J.Astronaut.Sci., vol.6. No.1. 1959.
131. R.H.FOX. J.Amer.Rou.Soc., vol.31, No.1. 1961.
132. R.H.FOX. J.Amer.Roc.Soc.,vol.31. No.7.1961.
133. R.L.GARWIN. J.Prop., vol.28, No.3, 1958.
134. S.HERRICK. Space Technology, o.5.ed.Scifert, N.Y.,1959.
135. S.HERRICK. Astrodynamics. Princeton, N.Y.,1959.
136. S.HERRICK. Handbook of Astronaut.End., o.4. Mc.Graw-Hill, N.Y.,1961.
137. J.V.HUGHES,G.N.NOMIVAS. Planet Space Sci.,No.7.,1961.
138. W.E.JAHSMAN. J.Amer.Roc.Soc., vol.30, No.3.,1960.
139. J.H.IRVING, E.K.BLUM. Uistas in Astronaut., vol.II.,N.Y.,1959.
140. J.H.IRVING. Space Technol. o.10.,N.Y.,1959.
141. St.JUROVICS. J.Amer.Rouk.Soc.,vol.31, No.4.,1961.
142. St.A.JUROVIĆ, J.E.MCINTYRE. J.Amer.Rouk.Soc.,vol.32, No.9.,1962.
143. U.K.KARRENBERG. J.Amer.Rouk.Soc.,vol.30.,No.1.1960.
144. H.J.KELLEY. J.Amer.Rouk.Soc.,vol.30, No.10,1960.

145. H.J.KELLEY, R.E.KOPP, H.G.MOYER. Proc.of the Symp.on Vehicle Syst.Optim., N.Y. 1961.
146. H.J.KELLEY. G.6.Bu.G.Leitman, Acad.Press, N.Y.1962.
147. L.J.KULAKOWSKI, R.T.STANCIL. J.Amer.Rock.Soc., vol.50, p.612-619, 1960.
148. D.B.LANGMUIR. Space Technol., v.9. N.Y., 1959.
149. H.LASS, J.LORREL. Space Technol., v.9. N.Y., vol.51, No.1.1961.
150. H.LASS, G.B.SOLLOWAY. J.Amer.Rock.Soc., vol.52, No.1.1962.
151. D.F.LAWDEN. Astroneut.Acta. vol.1.p.41-56, 1955.
152. D.F.LAWDEN. Astroneut.Acta. vol.4. No.3, 1958.
153. D.F.LAWDEN. Astroneut.Acta. vol.6., No.4, 1960.
154. G.LEITMANN. J.Brit.Interpl.Soc., vol.16, No.10, 1958.
155. G.LEITMANN. XI Internat.Astronaut.Congr. 1960, Vien, 1961; J.Appl.Mech.Traps.ASME, v.E.28.No.2, 1961.
156. G.LEITMANN. Amer.Astronaut.Soc., No.20, 1961.
157. G.LEITMANN, S.ROSS. Proc.JAS Symp. "Vehicle Syst.Optim." N.Y., 1961.
158. G.LEITMANN. Progr.in Astronaut.Sci., v.I.Amsterdam, 1962.
159. E.LEVIN. ASME Prepr. 59-AV-2, March, 1959.
160. E.LEVIN. Handbook of Astronaut.Eng., McGraw-Hill, N.Y., 1961.
161. W.LINDORFER, A.NATHAN. Proc.of the Symp.on Vehicle Syst.Optim. N.Y., 1961.
162. W.LINDORFER, H.G.MOYER. J.Amer.Rock.Soc., vol.52 No.2, 1962.
163. H.S.LONDON. J.Amer.Roc.Soc., vol.30, No.2., 1960.
164. D.L.LUKES. Proc.of the Symp.on Vehicle Syst. Optim. N.Y., 1961.
165. J.S.MACKAY, L.G.ROSSA, A.V.ZIMMERMAN. Proc.JAS Symp. "Vehicle Syst.Optim"., N.Y., 1961.
166. J.MARTELLY. IRE Trans.on Nuclear Sci., vol.NS-9, No.1, 1962.
167. W.G.MELBOURNE. J.Amer.Rock.Soc., v.51.No.12, 1961.
168. W.G.MELBOURNE,C.G.SAUER, D.E.RICHARDSON. Proc.JAS Symp. "Vehicle Syst.Optim."., N.Y., 1961.
169. W.G.MELBOURNE,C.G.SAUER. Astronaut. Acta. v.8., No.4.1962.
170. W.G.MELBOURNE,C.G.SAUER. AIAA J., v.1.No.1.1963.
171. W.G.MELBOURNE,C.G.SAUER. Progr.in Astronaut.and Aeronaut., vol.9. Electrio.Prop.Devel., N.Y., 1963.
172. H.F.MICHEISEN. Astronaut. Acta, vol.3., No.2.1957.
173. H.F.MICHEISEN. Proc.Amer.Astronaut.Soc., Western.Reg.Meet., v.3.1958.
174. J.E.MCLNTYRE, St.A.JUROVICS, W.P.GARDILL, B.JOHNSON. Proc.of the Symp.on Vehicle Syst.Optim., N.Y., 1961.
175. W.E.MOECKEL. I Internat.Astronaut.Congr., Madrid., 1968.
176. W.E.MOECKEL. NASA TRR-53, 1959.
177. W.E.MOECKEL. Astronaut.ACTA. v.7. No.566, 1961.
178. W.E.MOECKEL. NASA. R-79, Wash., 1961.
179. F.R.MOULTON. An introduction to celestial mechanics, Mc.Millan, N.Y., 1914.
180. E.N.NILSON, R.GURRY. JASS, v.27, No.2.1960.
181. R.R.NEWTON. Jet Prop., v.1.20, p.752, 1958.
182. R.R.NEWTON. J.Amer.Roc.Soc., vol.51, No.2. 1961.

183. B.PAIWONSKY. X.Internat.Astronaut.congr. London, 1959.
184. F.M.PERKINS. JASS, vol.26, No.5, 1959.
185. C.W.PETTY. J.Amer.Rouk.Soc., vol.53, No.9, 1961.
186. C.G.PFEIFFER. Proc.of the Symp.on Vehicle Syst.
187. S.PINES. IAS Paper No.61-7; 29 Ann.Meet. JAS. N.Y.1961.
188. A.POZZI. Missili, vol.3, No.5, 1961.
189. A.POZZI, L.SOCIO. J.Amer.Rouk.Soc. vol.31, No.8, 1961.
190. H.PRESTON - THOMAS. J.Brit.Interpl.Soc., vol.11, No.4, 1952.
191. H.PRESTON - THOMAS. V.Internat.Astronaut.congr., 1954. Wien, 1955.
192. H.PRESTON - THOMAS. Realities of Space Travel, London, 1957.
193. H.PRESTON-THOMAS. J.Brit.Interpl.Soc., v.16, No.9, 1958.
194. H.PRESTON - THOMAS. J.Brit.Interpl.Soc., vol.16, No.10, 1958.
195. H.PRESTON - THOMAS. J.Brit.Interpl.Soc., vol.17, No.3, 4, 1959.
196. L.REIFFEL. J.Amer.Rouk.Soc., vol.30, No.5, 1960.
197. L.RIDER. J.Amer.Rouk.Soc., vol.30, No.7, 1960.
198. RODRIGUER. J.Amer.Rouk.Soc., vol.29, No.10, 1959.
199. P.C.ROSENBLUM. Proc.of the Sixth Symp. in Appl.Math.of the Amer.Math.Soc., McGraw-Hill, 1950.
200. G.SALTZER, R.CRAIG, C.FETHEROFF. Proc.of IRE, v.48, No.4, 1960.
201. G.SALTZER, C.W.FETHEROFF. Astronaut.Auta. vol.1, No.1, 1961.
202. N.SANDS. J.Amer.Rouk.Soc., vol.31, No.4, 1961.
203. H.S.SEIPERT. J.Prop. v.27, No.12, 1957.
204. L.R.SHEPHERD, A.V.GLEAVER, J.Brit.Interpl.Soc., vol.7, No.1, 1948, vol.8, No.2, 1949. Realities of Space Travel. London, 1957.
205. L.R.SHEPHERD. J.Brit.Interpl.Soc. vol.11, No.4, 1952. Realities of Space Travel, London, 1957.
206. B.SHERMAN. Proc.of the Symp.on Vehicle Syst.Optim. N.Y.1961.
207. L.SOCIO. Missili, vol.3, No.3, 1961.
208. E.M.SPARROW, E.R.G.ECKERT, T.E.IRVING. JASS, v.28, No.10, 1961.
209. H.M.STANK, P.D.ARTHUR, JASS, vol.28, No.11, 1961.
210. J.W.STEARNS. Astronautics, v.1, No.3, 1962.
211. K.R.STEHLING. Aviation Age, vol.28, No.1, 1958.
212. M.L.STEIN. Nat.Bur.Standards. J.Res. vol.50, No.5, 1955.
213. P.A.E.STEWART. Raketentechnik und Raumfahrtforschung, Bd.7, No.1, 1965.
214. E-STUHLINGER. V IAF Congress, 1954.
215. E.S-STUHLINGER. J.Astronaut.Sci., No.4, Winter, 1955; No.1, Spring, 1956; No.2, Summer, 1956.
216. E-STUHLINGER. JET Prop. vol.27, No.4, 1957.
217. E-STUHLINGER. VIII IAF Congress, 1957.
218. E-STUHLINGER. IX.IAF Congress, 1958.
219. E-STUHLINGER. XI IAF Congress, 1960.
220. E-STUHLINGER, R.F.SEITZ. Adv.Space Sci., vol.II-N.Y.-London, 1960.
221. F.D.SULL, V.W.SHILL. SAE Prep., No.1050, 1961.
222. J.GURUGUE, R.Le-CHIVES. Nucleus, No.5, 1962.
223. V.O.SZEBEHELY. XI IAF Congress, 1960.
224. H.S.TSIEN. J.Amer.Rouk.Soc., vol.23, No.4, 1955.

225. T.C.TSU. J.Amer.Roc.Soc., vol.29, No.6., 1959.
226. T.C.TSU. Proc. VI Ann.Meet.Amer.Astronaut.Soc., 1960.  
Adv. Astronaut.Sci., vol.6. N.Y. 1961.
227. G.ULAM. Rev.Franc. d'Astronaut., vol.1. p.23, 1958.
228. R.C.WEATHERSTON, W.E.SMITH. AER J. III, v.50. No.5, 1960.
229. Y.B.WILKINS. JASS, v.27, No.2.1960.
230. Y.B.WILKINS. J.Soc.Ind.and Appl.Math.8. No.4.XII, 1960.
231. M.J.WILLINSKI. Aviation Week, vol.67, No.14, 1957.
232. M.J.WILLINSKI. Jet Prop., vol.28, No.11. 1958.
233. P.WONG. J.Amer.Rock.Soc., vol.32, No.2, 1962.

(2)

G.L.GODZOVSKY <sup>x/</sup>, A.L. STASSENKO <sup>xx/</sup>, V.V.FROLOV <sup>xx/</sup>

ON THE SHAPE OF HEAT REJECTING ELEMENTS COOLED  
BY RADIATION.

PART IV. THE EQUILIBRIUM FORMS AND SMALL  
VIBRATIONS OF A FLEXIBLE THREAD ROTATING IN THE  
FORCELESS FIELD. THE LIMITARY CHARACTERISTICS OF  
A BELT RADIATOR WITH MUTUAL IRRADIATION. THE  
OPTIMUM SYSTEM OF HEAT REJECTING FINS WITH MUTUAL  
IRRADIATION.

---

<sup>x/</sup> Doctor of Physics and Mathematics; professor of Moscow Institute of Physics and Technology; editor, R.J.Mechanika, Academy of Sciences of the USSR, Baltijskaya 14, Moscow, USSR

<sup>xx/</sup> Leading Engineer, Moscow Institute of Physics and Technology

The previous parts (I-III) of the work dealt with determining of the form of a flexible heat exchange belt (a flexible thread) in the centrifugal force field and of the optimum contour heat rejecting lines provided the emissivity is unit and the base prism surface radiant flux is negligible  $\chi$ .

This paper presents the development of the investigations of the problems.

All the equilibrium forms of the rotating flexible belt are discussed and the domain of parameters within which the thread has no cross-points is outlined.

Small vibrations about the equilibrium form are also considered.

It is shown that the equation for the proper functions is that of Lamé, if the angle is of small curvature and the tension is large. For the straight equilibrium form of the thread the equation reduces to the equation of Legendre and the proper functions are written in integral form.

The limiting optimum heat transfer characteristics, corresponding to the two limiting cases of radiant intensities are presented.

The characteristics depend only on two dimensionless parameters and all the rest characteristics are placed between the two.

The two-dimensional variational problem of optimum contour of thin heat rejecting lines is considered, taking mutual regulation and the interaction between the lines and the base prism surface for any emissivity value taken into account.

- 
- 4/ See: Grodzovsky G.L., Report at the XII IAF Congress,  
Grodzovsky G.L., Feulov V.V., Report at the XIII IAF Congress  
Grodzovsky G.L., Staszenko A.S. Report at the XIV IAF Congress.

THE EQUILIBRIUM FORMS AND SMALL VIBRATIONS  
OF A FLEXIBLE THREAD ROTATING IN THE GRAVITY  
FIELD

A series of works [1 - 4] dealt with the investigation of a belt vibration.

In ref.[2], for instance, the equilibrium form of a free flexible belt, rotating in the forceless field and pressed to the surface of a rotating drum by centrifugal forces, has been defined. The main object of this paper is to investigate all the equilibrium forms of a rotating flexible thread (including a thread with cross-points), to determine the conditions under which the thread is convex and to consider the equation of small vibrations of the thread about the equilibrium form.

1. Let the thread with the length  $L$  and linear density  $M$  rotate with a constant angular velocity  $\bar{\omega}$  and simultaneously move with a constant tangential velocity  $\bar{v}$ , around one or several drums of radius  $\bar{r}_0$ , which revolve with angular velocity  $\omega_0$  (fig.1). In the case of assuming a slip between the drums and the thread we have

$$V = \bar{r}_0(\omega_0 - \omega). \quad (1.1)$$

The thread element, having  $\bar{r}$  as a radius vector with respect to the point of rotation is affected by the inertial force, equal to

$$\bar{\phi} = \mu \omega^2 \bar{r} + (2\mu v \omega + \mu v^2 \alpha) \bar{n}_0, \quad (1.2)$$

where  $\alpha$  - thread curvature,  $\bar{n}_0$  - unit vector of the normal to the element. As is known, the equilibrium form of a free flexible thread is described by the equation

$$\bar{\phi} + \frac{d}{ds} (\lambda \bar{r}_0) = 0, \quad (1.3)$$

where  $s$  - arc length,  $\bar{r}_0$  - unit vector of a tangent,  $\lambda$  - thread tension. Introducing non-dimensional values

$$\rho = \frac{r}{r_0}; \quad \theta = \frac{s}{r_0}; \quad \ell = \frac{l}{r_0}, \quad K = \alpha r_0.$$

$$\lambda = \frac{\lambda_0}{\sqrt{\mu \omega^2 r_0^2}}, \quad a = \frac{\lambda_0}{\sqrt{\mu \omega^2 r_0^2}}, \quad \theta = \frac{2v}{\omega r_0}, \quad (1.4)$$

where  $\lambda_0$  - the tension in the contact point of the thread with the drum; now we shall write the equation (1.3) in the projections onto the axes  $\bar{r}_0, \bar{n}_0$ .

$$\frac{d\lambda}{d\theta} + \bar{p} \bar{r}_0 = 0, \quad \bar{p} \bar{r}_0 = \frac{(f')'}{(f^2 + f'^2)^{1/2}}. \quad (1.5)$$

$$\bar{p} \bar{n}_0 + 2\theta + \frac{f''}{2} K - \lambda K = 0, \quad K = \frac{f^2 + 2f'^2 - ff''}{(f^2 + f'^2)^{3/2}}. \quad (1.6)$$

3.

After integrating (1.5) we have

$$\Lambda = \gamma - \rho^2 \quad (1.7)$$

where  $\gamma$  - integration constant.

On the basis of the derived relationships the symmetry with respect to  $\varphi$  is seen.

$$\text{in terms of new variables} \quad \rho^2 = \xi \quad (1.8)$$

$$\frac{\rho}{(\rho^2 + \rho'^2)^{1/2}} = \eta \quad (1.9)$$

using the equation (1.7), we can rewrite (1.6) in the form

$$\gamma + \delta - (\gamma - \frac{1}{2}\delta^2 - \xi) \frac{d\xi}{d\xi} = 0, \quad K = 2 \frac{d\xi}{d\xi}. \quad (1.10)$$

From

$$\gamma + \delta = C(\gamma - \frac{1}{2}\delta^2 - \xi)^{-1} \quad (1.11)$$

here  $C$  - integration constant

On the grounds of (1.10) we have

$$K = 2C(\frac{1}{2} - \xi)^{-2} \quad (1.12)$$

thus, the thread curvature will be a continuous not decreasing with respect to a module, having a constant sign function. It is clear, that at the point of contact with the drum the thread curvature cannot be superior to the drum curvature,  $K_0 \leq 1$ ; the sign of equality takes place only when the thread length  $l$  is equal to  $l_{\min}$ .

2. In the case of considering only one drum  $l_{\min} = 2\pi$ . and

$$a_{\min} = 2(1 + \frac{1}{2}\delta)^2 \quad (2.1)$$

On the plane ab all the threads must lie (fig.2) above the parabola (2.1). The initial conditions in the case of one drum are as follows:

$$\rho = 1, \rho' = 0 \quad (\text{at the point } \varphi = \varphi_0) \quad (2.2)$$

then, by defining the integration constants  $\gamma$  and  $C$  from the equations (1.1) and (1.11), we get expressions for momentary tensions and thread curvatures

$$\Lambda = a + 1 - \rho^2 \quad (2.3)$$

$$K = \frac{2(1+\delta)(a - \frac{1}{2}\delta^2)}{(a - \frac{1}{2}\delta^2 + 1 - \rho^2)} \quad (2.4)$$

$$K_0 = K(1) = \frac{2(1+\delta)}{a - \frac{1}{2}\delta^2} \quad (2.5)$$

4

$K(b)$  as a function of the parameter  $b$  is presented in Fig. 1. By integrating (2.4), we shall get the equation of the curve by means of a quadrature

$$\int \frac{[(a-\frac{1}{2}b^2) + b(\beta^2-1)] d\beta}{\beta \sqrt{\beta^2[(a-\frac{1}{2}b^2) - (\beta^2-1)]^2 - [(a-\frac{1}{2}b^2) + b(\beta^2-1)]^2}} \quad (2.6)$$

Let  $R$  be the maximum thread radius vector, satisfying the condition

$$\rho \geq 0, \quad \varphi = \pi \quad (2.7)$$

then power polynomial with respect to  $\rho^2$  in the radicand of the equation (2.6) has the following roots

$$\rho_1^2 = 1 \quad (2.8)$$

$$\rho_{12}^2 = (a - \frac{1}{2}b^2) + \gamma_2(\beta^2+1) \mp \gamma_2(1+b)\sqrt{4(a - \frac{1}{2}b^2) + (1-b^2)} \quad (2.9)$$

The sign before the root is chosen so that  $\rho_1^2 \leq \rho_2^2$ . This means that the thread contacts with the drum (see the initial conditions (2.2)). For all  $b > -1$  in the interval  $\rho_1^2 < \rho^2 < \rho_2^2$  the investigated third power polynomial is negative; therefore  $\rho = R$  and defines the largest relative radius, so that

$$1 \leq \rho \leq R, \quad \varphi_0 \leq \varphi \leq \pi \quad (2.10)$$

Besides,  $k(b) > 0$  for  $b > -1$  (Fig. 2) (the signs of equality are reached only at the boundary value  $b = -1$ ). Consequently, at  $b > -1$  the thread is convex, does not contain cross-points and its form is described by the integral (2.6), which is reduced to the sum of elliptical integrals of the first and the third kinds  $F(\psi, k)$  and  $\Pi(\psi, h, k)$

$$\varphi - \varphi_0 = \frac{b}{\sqrt{\rho_2^2 - 1}} F(\psi, k) + \frac{a - \frac{1}{2}b^2 - b}{\sqrt{\rho_2^2 - 1}} \Pi(\psi, h, k) \quad (2.11)$$

$$\sin^2 \psi = \frac{\rho^2 - 1}{\rho_2^2 - 1}, \quad h = \frac{\rho_2^2 - 1}{\rho^2 - 1}, \quad k^2 = \frac{\rho_2^2 - 1}{\rho^2 - 1}$$

The angle  $\psi_0$  is determined by the condition  $\varphi_0 = \pi$  at  $\rho = R$  and is expressed by means of the elliptical integrals

$$\pi - \varphi_0 = \frac{b}{\sqrt{\rho_2^2 - 1}} K(k) + \frac{a - \frac{1}{2}b^2 - b}{\sqrt{\rho_2^2 - 1}} \Pi(h, k) \quad (2.12)$$

The ratio

$$\gamma_1 l = \varphi_0 + \frac{a - (\rho_2^2 - 1)}{\sqrt{\rho_2^2 - 1}} K(k) + \sqrt{\rho_2^2 - 1} E(k) \quad (2.13)$$

where  $E(k)$  is the elliptical integral of the second kind, contains the non-dimensional initial tension  $\gamma_1$  with the thread length  $l$ .

At  $b < -1$  the thread curvature becomes negative, and the cross-points

$\varphi_0, \varphi_\infty = \pi$  is found on the basis of the condition

$$\pi - \varphi_0 = \int_1^{R_0} \frac{[(a - \frac{1}{2}b^2) + b(\beta^2-1)] d\beta}{\beta \sqrt{\beta^2[(a - \frac{1}{2}b^2) - (\beta^2-1)]^2 - [(a - \frac{1}{2}b^2) + b(\beta^2-1)]^2}} \quad (2.14)$$

The thread form may be also expressed in terms of special functions, which are connected with elliptical integrals (for example, by Jacobi-function or by Weierstrasse-function).

The dependence of the curved form on  $b$  for  $\ell = 25,0$  is shown in fig.4.

3. Let us consider  $N$  similar drums with mass  $M_0$ , embraced by one belt and situated symmetrically about the centre of inertia  $O$  of the system. Angle  $06\varphi \in \pi/N$  is measured from the ray  $OO_1$ . In the region  $2\psi$ , the belt contacts the drum (fig.5). The initial conditions, of contact at the point A have the form

$$\varrho = \varrho_1, \quad \varrho' = -\varrho_1 \tan(\psi_0 - \varphi_0) \quad (\varrho_1 = \tau_1/\omega_0) \quad \text{at } \varphi = \varphi_0. \quad (3.1)$$

For the point B the symmetry condition gives

$$\varrho = \varrho_{\min}, \quad \varrho' = 0 \quad \text{at } \varphi = \pi/N \quad (3.2)$$

By integrating the equation (1.12) with regard for (1.7) and (3.1) we get the following expression for the tension

$$\Lambda = a + \varrho_1^2 - \varrho^2 \quad (3.3)$$

and the equation of thread in the form of the following quadrature in the domain  $\varphi - \varphi_0$

$$= \int_{\varphi_0}^{\varphi} \frac{[(a - \frac{1}{2}b^2)\varrho, \cos(\psi_0 - \varphi_0) - b(\varrho_1^2 - \varrho^2)] d\varrho}{\varrho, \sqrt{\varrho^2[(a - \frac{1}{2}b^2)^2 + (\varrho_1^2 - \varrho^2)]^2 - [(a - \frac{1}{2}b^2)\varrho, \cos(\psi_0 - \varphi_0) + b(\varrho_1^2 - \varrho^2)]^2}} \quad (3.4)$$

In order to define the terms  $a, \varrho_1, \psi_0, \varphi_0$  and  $P$  where  $P$  is equal to the ratio of  $0O_1$ , shown in fig.5, to the radius  $\tau_0$ , we shall make use of the following three geometrical and force conditions:

the condition (3.2) and

$$\begin{aligned} \varrho_1^2 &= 1 + P^2 + 2P \cos \psi_0, \quad 1 = \varrho_1^2 + P^2 - 2\varrho_1 P \cos \psi_0 \\ \ell &= 2N(\psi_0 + \int_{\varphi_0}^{\pi/N} d\varphi) \quad \text{as } \sin \psi_0 = MF, \\ M &= \frac{M_0 P_0 \omega^2}{J \omega^2 \tau_0^2} \end{aligned} \quad (3.5)$$

Here  $P_0$  - radius-vector of the point of application of the centrifugal force, acting on the drum; and the second term in the right part of the last equation (3.5) is the  $0O_1$  projection of the forces, acting on the part of the thread, lying on the drum. Since  $Q < \infty$  it follows from the last equation (3.5), that  $\psi_0$  never equals zero. Consequently,  $\psi_0 - \varphi_0 > 0, \varrho' < 0$ , and the thread is entirely within the round, describes about the system of drums.

It is of interest to pay attention to some particular cases (fig.6).

1) Straight thread. Physically it means, that the normal component of the centrifugal force is constant and equal to the coriolis force, so that

$$b = -\varrho_{\min} \quad (3.6)$$

Here the equation of the curved (3.4) has the form

$$\varrho = \frac{\varrho_{\min}}{\cos(\pi/N - \varphi)} \quad (3.7)$$

and geometrical parameters are defined by the ratios

$$\ell = 2\pi + 2NP \sin \pi/N, \quad \varrho_{\min} = 1 + P \cos \pi/N, \quad \psi_0 = \pi/N$$

$$\varrho_1^2 = 1 + P^2 + 2P \cos \pi/N, \quad \cos(\pi/N - \varphi_0) = \varrho_{\min}/\varrho_1 \quad (3.8)$$

6

2) Boundary of the uniqueness of the immersion. This belongs to the thread at A passes through the centre of symmetry of the system

... here

$$\Psi_0 - \varphi_0 = \frac{1}{2}\pi \quad \sin\varphi_0 = \frac{1}{P}, \quad (2.4)$$

$$\varphi - \varphi_0 = -\frac{g}{2} \int_{\varphi_0}^{\varphi} \frac{(\varphi_i^2 - \varphi^2) d\varphi^2}{\sqrt{g^2[(a - \varphi_i b^2) + (P^2 - P_i^2)]^2 - b^2(P_i^2 - \varphi^2)^2}} \quad (2.4)$$

3) At a certain increase of  $\Psi_0$  the thread curvature becomes negative, with  $0 < \varphi_0 < \arcsin \frac{1}{P}$

$$\varphi_i^2 - \varphi^2 = \frac{P_i \cos(\varphi_0 - \varphi_0)(a - \varphi_i b^2)}{b - P_i \cos(\varphi_0 - \varphi)} \leq \varphi_i^2 \quad (2.4)$$

$\varphi_{\text{cr}}$  - the point, where the curvature  $\varphi' = 0$  is realized.

The case for  $\varphi_0 = \arcsin \frac{1}{P}$ ,  $\varphi_0 = \varphi_i$  corresponds to the boundary of uniqueness, considered above. The case of  $\varphi_0 = 0$  when the thread coincides the radius-vector of the axis centre, is a limiting one in the sense, that with further increase of  $\Psi_0$  the thread cross-points appear and the thread cannot be considered as the real model.

4. Consider small vibrations of a thread around the equilibrium form  $\bar{\varphi}^0(\varphi)$  (all the values, characterizing the equilibrium form, will be denoted by an index 0). The radius-vector of a vibrating thread-point with a coordinate  $\xi$  (non-dimensional arc length) at the time moment  $t = \bar{\tau}_0$  is represented as

$$\bar{\varphi}(\xi, t) = \bar{\varphi}^0(\xi) + n(\xi, t) \bar{n}^0. \quad (4.1)$$

We shall consider the smallness of vibrations in the usual sense

$$|\frac{d^n}{dx^n}| < \varepsilon, \quad (4.2)$$

where  $\varepsilon > 0$  - a small constant quantity.

Let  $\bar{t}^0$  and  $\bar{n}^0$  be the unit vectors of the tangent and of the normal to the vibrating thread. The force of inertia, acting on a unit segment of the vibrating thread is equal to

$$\bar{\Phi} = \mu \omega^2 \bar{x}_0 \left\{ \bar{p} + \left( \frac{g}{2} \right)^2 k - b \right\} \bar{n}^0 - \frac{d^2}{dx^2} \bar{n}^0 + 2 \frac{d}{dx} \bar{t}^0 \}. \quad (4.3)$$

In this equation the last two terms denote a non-dimensional inertial force, corresponding to acceleration  $(\frac{d^2}{dx^2} \bar{x}_0) \bar{n}^0$ , and to the Coriolis force, resulting from the motion in the rotating system with a relative velocity

$(\omega \bar{x}_0) \bar{n}^0$  represent the tension in the form

$$\Lambda(\xi, t) = \Lambda^0(\xi) + \Lambda^1(\xi, t), \quad (4.4)$$

where  $\Lambda^1$  - perturbation.

By writing (4.3) in the projections on the axis  $\bar{t}^0$  and  $\bar{n}^0$ , we get two systems: an undisturbed one (4.5), (4.6) and a system, describing small vibrations

$$\frac{1}{2} \cdot \frac{d^2 \Lambda^1}{d\xi^2} + \left[ \frac{1}{2} \left( \Lambda - \frac{1}{2} b^2 k - b \right) \frac{d^2 \Lambda^0}{d\xi^2} + 2 \frac{d^2}{d\xi^2} \right] = 0 \quad (4.5)$$

$$n - \frac{d^2 n}{d\xi^2} + \frac{1}{2} \frac{d}{d\xi} \left( \Lambda \frac{d^2 n}{d\xi^2} - \frac{1}{2} (\Lambda - \Lambda^0) k^2 + \left( \frac{g}{2} \right)^2 (k - k^0) \right) = 0 \quad (4.6)$$

The set of two equations (4.4), and (4.5) is nonlinear. We linearize it assuming the curvatures to be small  $|k^0(\epsilon)| < \epsilon$  and the solution to be rather large  $\Lambda^0 \gg |\Lambda^1|$ . These conditions may take place in the case when the unit moves around two or more steady curves. Then the equation (4.4) is satisfied in the form

$$\eta - \frac{\partial^2 \eta}{\partial \zeta^2} + \epsilon \frac{\partial}{\partial \zeta} \left[ (\Lambda^0 - \frac{1}{2} \beta^2) \cdot \frac{\partial^2 \eta}{\partial \zeta^2} \right] = 0 \quad (4.4)$$

and will not depend on  $\Lambda^1$ . Having solved it we may find  $\Lambda^1$  from (4.5) with the help of the quadrature.

We shall search the solution to (4.4) in the form  $\eta(\zeta, \tau) = S(\zeta) T(\tau)$  then for  $T_1(\tau)$  we shall find

$$T_1 = C_{11} \exp(i\sqrt{\epsilon} \tau) + C_{21} \exp(-i\sqrt{\epsilon} \tau) \quad (4.5)$$

and for definition of  $S(\zeta)$  we shall find the equation

$$\frac{d}{d\zeta} \left[ (\Lambda^0 - \frac{1}{2} \beta^2) \frac{dS}{d\zeta} \right] + y S' = 0 \quad (4.6)$$

With the help of the ratio  $x = F(y, k)$

$$x = \int \frac{d\zeta^2 \sqrt{\zeta_3^2 - \zeta_1^2}}{2 \sqrt{\zeta^2 [(\alpha - \frac{1}{2} \beta^2) + (\rho^2 - \rho^1)]^2 - [(\alpha - \frac{1}{2} \beta^2) \rho_1 \cos(\psi_0 - \psi_1) - \beta(\rho^2 - \rho^1)]^2}} \quad (4.7)$$

$$\sin^2 \psi = \frac{\zeta^2 - \zeta_1^2}{\zeta_1^2 - \zeta_2^2}, \quad k = \frac{\zeta_1^2 - \zeta_2^2}{\zeta_1^2 - \zeta_3^2}$$

we introduce a new variable.

here  $\zeta_1^2, \zeta_2^2, \zeta_3^2$  - the roots of the denominator in the ratio (4.7).

Then the equation (4.6) is in the form

$$\frac{d^2 S}{dx^2} = y \left[ k^2 \sin^2 x - \frac{\alpha - \frac{1}{2} \beta^2 - \rho_1^2 - \zeta_1^2}{\zeta_3^2 - \zeta_1^2} \right] S \quad (4.8)$$

In the particular case of  $\beta = -\rho_{min}$  we get the following equation of Legendre.

$$\frac{d}{d\zeta} \left[ (1 - \zeta_1^2) \cdot \frac{dS}{d\zeta} \right] + y S = 0 \quad (4.9)$$

$$\zeta_1 = \frac{\sqrt{\rho_1^2 - \rho_{min}^2} - \beta}{\sqrt{\alpha - \frac{1}{2} \beta^2 + \rho_1^2 - \rho_{min}^2}}$$

The equations (4.8) and (4.9) with  $y = m(m+1)$ ,  $m > 0$  integer have the solutions, called lame functions  $Y_l^m$  and legendre polynomial, respectively. In particular, the equation of lame was considered for  $M = 100$ , when it is equal to an integer plus one half  $l + \frac{1}{2}$ . As in our case, the proper values themselves must be determined, the equation (4.8) was been being solved numerically. In fig. 7 several first proper values for the problem with uniform boundary conditions are represented

The equation (4.12) in the general case has the following fundamental solutions  $Y_l^m$ :

$$S_{1y}(d) = 4 \int_0^\infty \frac{\cos \sqrt{1+d^2} z}{\sqrt{\cos z + \sin d}} dz = S_{2y}(-d) \quad (4.10)$$

$$d = \arcsin \theta,$$

We shall write the proper functions in the form of linear combinations of these fundamental solutions

$$S_y = A_y S_{1y} + B_y S_{2y} \quad (4.14)$$

and proper values will be found from the equation

$$\begin{vmatrix} S_{1y}(d_1) & S_{2y}(d_1) \\ S_{1y}(-d_1) & S_{2y}(-d_1) \end{vmatrix} = 0 \quad (4.15)$$

$d_1 = \arcsin \frac{\sqrt{s_1^2 - g_{min}^2}}{\sqrt{a - b^2 + g_1^2 - g_{min}^2}}$

The constant  $B_y$  is equal to

$$B_y = - \frac{S_{1y}(d_1)}{S_{2y}(d_1)}$$

The constant  $A_y$  is determined from the normalization condition

$$\int_{-d_1}^{d_1} S_y^2 ds = 1$$

#### B. Limiting characteristics of a belt radiator with mutual irradiation

In refs./1,2,4/, which dealt with the investigation of a belt radiator, the effect of the belt mutual irradiation on the radiator characteristics was not considered. It was only mentioned, that if it would be made into a mobile strip, the mutual irradiation would be increased; an attempt was made to use "the effective belt width" in the temperature distribution with length  $T(s)$ , got in the case when mutual irradiation was neglected. If it is taken into account the form of the very function  $T(s,z)$ , determined by integral-differential equation with a kernel, depending on the belt form and, consequently, on many concrete parameters, is changed. However, the quantities, depending only on two parameters, on the domain, in the limit of which the belt radiator characteristics (such as temperature distribution, mass and typical dimensions) at any belt form will be situated, may be marked.

The determination of this domain is the main object of the paper.

Let the belt with the length  $L$  move over the drum, with the radius  $\chi_0$ , which is being cooled; by contacting it the belt is being heated in the interval of temperatures from  $T_1$  to  $T_2 > T_1$ . Assume that:

- 1) the belt is physically thin,  $\delta/\lambda \rightarrow 0$  ( $\delta$  - belt thickness,  $\lambda$  - thermal conductivity);
- 2)  $\chi_0 \ll L$  then the temperature distribution equation and the equation of the accumulated and released energy balance may be given in the form

$$\frac{\rho c \delta V}{\delta s} = -2E_0 T^4(s,z) + \Phi(s,z) = -Q_{y_1}(s,z) \quad (1)$$

$$\Phi(s,z) = \int_0^L \int_{-\chi_0/2}^{\chi_0/2} H(s,z; s_0, z_0) dS_0 dz_0 \quad (2)$$

$$Q = M_L C \frac{V}{L} \cdot \frac{1}{\delta} \int_{g_1}^{g_2} [T_2(z) - T_1(z)] dz \quad Q = \int_0^L \int_{-\chi_0/2}^{\chi_0/2} q(s,z) dS dz \quad (3)$$

Here  $\rho, C$  - density and unit specific heat,  
 $\delta, B, M$  - thickness, width and mass of the belt,  
 $V$  - linear velocity,  
 $\epsilon$  - surface emissivity,  
 $\sigma_0$  - Stefan - Boltzmann constant,  
 $H$  - effective radiation flow,  
 $K$  - the kernel, depending on the belt form,  
 $Q$  - heat, conducted from the surface per unit time.

The two addends in the right half of the equation (1) describe radiant flows from the outer and inner (with mutual irradiation) surfaces of the belt. It may be shown, that

$$2\epsilon \left( \frac{\rho}{\sigma_0} \right) > T_2^4 > (\epsilon \tau^*(s) - \frac{1}{2\epsilon-1} [\tau^*(1-s) - \tau^*(s)]) = \epsilon \langle \tau^* \rangle \quad (4)$$

$$\tau = \frac{T}{T_2}, \quad S = \frac{s}{L}, \quad \langle f \rangle = \int_0^1 f(s) ds$$

The left half of inequality (4) corresponds to the belt without mutual irradiation, the right one corresponds to a rotated flat belt of any finite width (fig. 6), with the elements moving parallel and towards each other at an infinitely close distance (for one and two urums temperature distribution is evidently similar). In these two limiting cases the temperature distribution across the belt is described by the following equations

$$\alpha \frac{d\tau}{ds} = -\Omega \epsilon [\tau^*(s)]^4 \quad (5)$$

$$\alpha \frac{d\tau}{ds} = -\epsilon \left( 1 + \frac{1}{2-\epsilon} \right) \tau^*(s) + \frac{\epsilon}{2-\epsilon} \tau^*(1-\epsilon)$$

$$\alpha = \frac{\rho c \delta V}{\sigma_0 T_2^3 L} \quad (6)$$

The initial condition is

$$\tau^*(0) = \tau(0) = 1 \quad (7)$$

The equation (5) is being integrated in the final form /4/ and determines one-parametric family of curves.

$$\tau^*(s, \alpha/\epsilon) = \left( 1 + \frac{6\epsilon}{\alpha} s \right)^{-\frac{1}{3}} \quad (8)$$

The equation (6) was solved numerically with the help of the iteration method, with the function  $T_{n+1}(s) = k[\tau_{n+1}(s) - \tau_n(s)]$  substituted into the right half of the equation for determining  $\frac{d\tau}{ds}$ . At 5.9 and 6.8 the example of a convergence process depending on  $k$ . Let  $\delta_{n,n-1} = \left[ \int_0^1 (\tau_n - \tau_{n-1})^2 ds \right]^{\frac{1}{2}}$  be root-mean-square error. The process was stopped when the condition  $\delta_{n,N-1} \leq \omega$  ( $N$  - a full number of assumptions,  $\omega$  - relative accuracy) for calculations it was chosen:

$$T_1 \equiv T_0 \equiv \tau^*(s), \quad k = \frac{1}{4}, \quad \omega = 10^{-4}, \quad \Delta s = 10^{-2}, \quad 10^{-1} \leq \alpha/\epsilon \leq 10, \quad \frac{1}{2} \Delta \alpha = 10^1,$$

$$10^{-1} \leq \epsilon \leq 1, \quad \Delta \epsilon = 10^1$$

10

In fig. 10 a two-parametric family of the curves  $\tau(S; d; \varepsilon)$  is represented. The qualitative difference between the moments of the belt  $\tau^*(S; d; \varepsilon)$  and  $\tau(S; d; \varepsilon)$  is in that the derivative of the last with respect to the angle, as to the sum of  $S=1$  the resulting value is negative again; it is always a positive total variation sign. In it we introduce the following non-dimensional terms:

$$m = \frac{M}{Q/BG_0 C V T_2^6} ; \quad \ell = \frac{L}{Q/BG_0 T_2^4} \quad (9)$$

$$\Delta = \frac{\delta}{Q/BG_0 V T_2} , \quad T_2 = \tau(L) = \frac{T_1}{T_2}$$

From the equations (2) and (3) we shall have

$$m = \alpha \ell \quad \ell = \langle q_2 \rangle^{-1} \quad (10)$$

$$\langle q \rangle = \frac{\langle q_2 \rangle}{G_0 T_2^4} , \quad \Delta = (1 - \ell_2)^{-1} . \quad \text{From (4) it follows}$$

$$\langle q \rangle = \varepsilon \langle \tau^* \rangle , \quad \langle q^* \rangle = 2\varepsilon \langle \tau^* \rangle^4$$

11. With the help of (6), we neglect mutual irradiation, we have

$$m^* = \left( \frac{1}{\ell_2^4} - 1 \right) / 6\varepsilon (1 - \ell_2)^2 \quad (11)$$

$$\ell^* = \left( \frac{1}{\ell_2^4} - 1 \right) / 6\varepsilon (1 - \ell_2^*)$$

The functions  $\tau_2(d, \varepsilon)$ ,  $\ell(d, \varepsilon)$ ,  $\Delta(d, \varepsilon)$ ,  $m(d, \varepsilon)$  (non-dimensional mass of the belt)  $M(d, \varepsilon) = m/m^*$  and  $\eta(d, \varepsilon) = \langle q \rangle$  (coefficient of mutual irradiation) are shown in fig. 11-15. It is seen, that there exists min  $M$  with respect to  $d(\varepsilon)$

As  $\tau_2 = \tau_2(d, \varepsilon)$ , the optimum  $\tau_2^*(\varepsilon)$ , ensuring min  $M$ , exists. The optimum limiting values, corresponding to the very best and worse to the worst belts are given in fig. 10-10. Here it is seen, that the ratio  $\tau_2^*(\varepsilon)$  is represented by a straight line  $\tau_2^* \approx 0,69$ , according to the figure, that the solution of the equation (5) contains only one parameter  $\varepsilon/2\varepsilon$  (the corresponding optimum value is  $\varepsilon/2\varepsilon = 1,47$ ). We may get this value  $\varepsilon/2\varepsilon$  by differentiating (11) with respect to  $\ell_2^*$ ; as a result we have the fourth power equation

$$(\ell_2^*)^4 - 5/2\ell_2^* - 3/2 = 0 \quad (12)$$

in which one of the roots, satisfying to a physically clear requirement  $0 < \ell_2^* < 1$  is equal to  $\ell_2^* \approx 0,69$ .

At  $0.1 \leq \varepsilon \leq 1$  the ratio of the optimum limiting masses is monotonically changing from 2.00 to 2.50. It can be shown, that "one-blade" belt, radiating only from the outer surface [4], has the mass and the length, that is exactly twice the length in the case of neglecting mutual irradiation; subsequently, it lies in the limits of the motion of limiting characteristics, that has been already said. The temperature distribution is simply connected with  $\varepsilon^2$ :

$$\tau^*(S, \varepsilon) = \tau^*(S, \varepsilon^2)$$

Optimum system of heat rejecting fins

The consideration of the questions of cooling a vehicle in space vacuum leads to the problem of finding optimum shapes of the heat irradiating surfaces. In recent years such problems have been attracting the greater and greater attention.

The simplest problem of cooling a heat rejecting thin plate of rectangular cross-section was considered in refs. /6,9/. In these papers the efficiency of first heat rejecting fins, combined with tube radiators was investigated.

The optimum (in regard to the minimum cross-section area) form of a single heat rejecting triangular fin, uniformly heated from one end, was soon found in paper /10/. At the same time the problem of the optimum contour of a single heat rejecting fin in the family of curves expressed by the power law /11/, was also considered.

In papers /12-15/ the variational problem of the optimum profile of a single fin was considered and solved. In /13/ a fin with a trapezoidal profile was considered.

Papers /6-15/ dealt with a single fin. The problem of cooling a heat radiating cylinder by means of several fins (more than two) leads to the necessity of taking into account the fins mutual irradiation; in this case the temperature distribution across the fin width is found as the solution of a non-linear integro-differential equation. In papers /16-17/ the problem of the optimum number and contours of thin rectangular radiating fins was also investigated. A more general problem, concerning the optimum contours and number of thin trapezoidal fins, was soon solved in ref. /18/.

A little bit earlier, in paper /19/ the variational problem concerning the optimum profile and number of fins for radiating surfaces of finite emissivity was given.

All the mentioned problems were considered as two-dimensional. In the problems of /10-19/ the base cylinder or prism surface was assumed to be small in comparison with the fin radiating surface; therefore, the base surface radiation and the interference of the surface with the fins could be neglected.

In this paper the two-dimensional variational problem of the optimum profile of heat rejecting fins with base prism interaction for different surfaces emissivities, is considered. Notice, in /19/, this problem was considered only for the particular case of cooling a heat rejecting baffle, i.e. for  $X_0=0$  (fig.20), by black radiating surfaces of the fins.

In paper /20/ the optimum contour and number of thin triangular fins problem was considered, the interference of the fins with the base surface of the cooled regular prism for different surfaces' emissivities was soon taken into account.

Let us consider the two-dimensional problem of cooling a regular prism, radiating prismatic heat flow  $W$  from the prism with vertical and having a prescribed constant surface temperature  $T_s$ . As is usual, the cooling fins

12

are assumed to be thin and slope, in the sense that the transversal heat flow in the film is negligible as compared to the longitudinal one, and that each film does not irradiate itself. (8-18)

With these assumptions in view, the thermal conductivity equation and the irradiation-rejection law are:

$$Q(x) = -2\lambda y(x) \frac{dT}{dx} \quad (1)$$

$$dQ(x) = -2q(x)dx \quad (2)$$

where  $Q(x)$  = heat flow passing through the film cross-section at the point  $x$ ,

$y(x)$  = unit fall of the film thickness,

$q(x)$  = resultant rejection from a film side surface.

$\lambda$  = film material thermal conductivity.

for  $\epsilon < 1$   $Q(x)$  is found as the solution of the following integral equation

$$Q(x) = Q_0(x) + (1-\epsilon) \int_{F_1}^{F_2} Q(\xi) G(x\xi) dF_\xi \quad (3)$$

where

$$Q(x) = \epsilon G T^*(x) - \epsilon \int_{F_1}^{F_2} \epsilon G T^*(\xi) K(x\xi) dF_\xi - \int_{F_1}^{F_2} \epsilon G T^*(\xi) K(x\xi) dF_\xi - \int_{F_1}^{F_2} (1-\epsilon) \left[ \int_{F_1}^{F_2} \epsilon G T^*(\zeta) [K_1(z\xi) + K_2(z\xi)] dF_\zeta \right] K(x\xi) dF_\xi$$

$$\epsilon = \text{surface emissivity}; \quad G(x\xi) = K(x\xi) + (1-\epsilon) \int_{F_1}^{F_2} [K_1(z\xi) + K_2(z\xi)] K(z\xi) dF_z$$

$$G = \text{Stefan-Boltzmann constant};$$

$K(x\xi) = \frac{\cos \theta_x \cos \theta_\xi}{\pi \gamma^*(x\xi)}$  - the well known kernel of integral equations in radiation problems (see Fig. 20).

The integrals in (3) are taken with respect to the surfaces in and prism surfaces, "seen" from the point  $x$ .

The following variational problem should be solved to determine the cross-section profile  $y(x)$  and the number  $n$  of films, having the minimum total weight, i.e.

$x_0$  = prescribed prism size,

$T_0$  = prism surface temperature,

$W$  = total heat flow to be removed.

This is the problem of minimizing the functional

$$F_x = 2n \int_{x_0}^{x_1} y(x) dx \quad (4)$$

with the ties (1), (2), (3) and under the isoperimetric condition

$$W = n(Q_0 + Q') \quad (5)$$

here  $Q_0$  and  $Q'$  = heat flows, radiated by one film and one prism surface respectively. We have:

$$Q' = \int_{-z_0}^{z_1} \left[ \epsilon G T^*(z) - \int_{F_1}^{F_2} \epsilon G T^*(\xi) K(z\xi) dF_\xi + \int_{F_1}^{F_2} (1-\epsilon) Q(\xi) K(z\xi) dF_\xi \right] dz \quad (6)$$

The solution of the equation (5) may be written in the form

$$Q(x) = Q_0(x) + (1-\epsilon) \int_{F_1}^{F_2} \Gamma(x\xi) Q_0(\xi) dF_\xi \quad (7)$$

73

$$\text{where } \Gamma(x_t) = \sum_{j=0}^{\infty} (1-\varepsilon)^j G_j(x_t) \quad \rightarrow \text{the relation to the equation (2)}$$

$$G_0(x_t) \leq G(x_t); \quad G_j(x_t) = \int_{F_t}^x G_0(\xi) G_{j-1}(\xi) dF_\xi$$

Substituting  $Q_p(x)$  from (7) into (2) and integrating the latter we receive

$$Q(x) = Q_0 - 2 \int_{x_0}^x [Q_p(x) + (1-\varepsilon) \int_{F_t}^x \Gamma(x_t) Q_p(\xi) dF_\xi] dx \quad (8)$$

Using (5), (6) and (1) we shall find the expression for  $\bar{Q}(x)$ :

$$Q(x) = \frac{\int_x^{\infty} [Q_p(x) + (1-\varepsilon) \int_{F_t}^x \Gamma(x_t) Q_p(\xi) dF_\xi] dx - \frac{1}{2} (\frac{W}{n} - Q')}{\lambda T'(x)} \quad (9)$$

thus the (1), (2), (3) and the isoperimetric condition (5) have been satisfied. The problem remains to determine the function  $\bar{T}(x)$  depending only on  $T(x)$ ; here we have the same, that after substituting  $Q_p(x)$  from (7) into (8) we obtain  $Q$  after substituting  $Q$  only on  $T(x)$ .

Let us first make some simplification and transformation of the variables:

$$\bar{Q} = \frac{Q}{W}; \quad \bar{Q}' = \frac{Q'}{W}; \quad \bar{T} = \frac{T}{T_0}; \quad \bar{x} = \frac{x}{x_0}; \quad \bar{\xi} = \frac{\xi}{x_0}; \quad \bar{y} = \frac{y}{y_0}$$

$$\bar{Q}_p = \frac{Q_p}{\varepsilon \bar{E} \bar{T}_0^4}; \quad \bar{F} = \frac{F}{\bar{F}_0}$$

where

$$W = \frac{W}{n}; \quad x^* = \frac{W}{\varepsilon \bar{E} \bar{T}_0^4}; \quad y^* = \frac{W x^*}{\lambda \bar{T}_0} \quad F^* = \frac{2 W^3}{\lambda \bar{E}^2 \bar{T}_0^6}$$

In terms of the new variables the functional (10) can be rewritten in the form:

$$\bar{F} = \frac{n}{\varepsilon^2} \int_{\bar{x}_0}^{\bar{x}_1} \bar{y} [\bar{T}(\bar{x}), \bar{x}, n, \varepsilon] d\bar{x} \quad (10)$$

The unknown extremal  $\bar{T}(\bar{x})$  must satisfy the following boundary conditions

$$\bar{T}(\bar{x}_0) = 1 \quad \bar{T}(\bar{x}_1) = \bar{T}_1 \quad (11)$$

The optimum value  $\bar{T}_1$  (as the rim width is not preselected) will be found from the equation

$$n \int_{\bar{x}_0}^{\bar{x}_1} [\bar{Q}_p(\bar{x}) + (1-\varepsilon) \int_{F_t}^{\bar{x}} \Gamma(\bar{x}_t) \bar{Q}_p(\bar{\xi}) dF_{\bar{\xi}}] d\bar{x} - \frac{1}{2} (1 - \bar{Q}') = 0 \quad (12)$$

The condition (12) meets the natural physical requirement  $\bar{Q}(\bar{x}_1) = 0$

The solution to the problem (11-12) has been realized with the help of an electronic computer.

The numerical solution to the problem was carried out by the following relaxation method: the root  $\bar{x}_1^{(0)}$  of the equation (12) is found on the basis of an arbitrary initial approximation  $\bar{T}^{(0)}(\bar{x})$ , satisfying the condition (12), then the first improved approximation  $\bar{T}^{(1)}(\bar{x})$  to the extremal is found by means of the steepest descent method /21,22/. The iteration process is continued until

14

two subsequent approximations  $\bar{T}^{(i)}(\bar{x})$ ,  $\bar{x}_i^{(i)}$  and  $\bar{T}^{(i+1)}(\bar{x})$ ,  $\bar{x}_i^{(i+1)}$  differ by less than a prescribed magnitude.

In figs. 21+20 the examples of calculated curves for different values of  $\xi, \bar{x}_0, n, \bar{T}_0$  are presented. The dependence of the optimum film profile contour on the size  $\bar{x}_0$  of a cooled rectangular prism with  $\xi = 0,5$  and  $\bar{T}_0 = 0,5$  is plotted in fig. 21. Fig. 22 presents the dependence of the film profile on the number of lines with fixed magnitudes of the other parameters. As is seen in fig. 21, the quantity  $\bar{T}_0$  begins to affect the local weight of the system of lines only from the values  $0,65 + 0,75$ . As to the optimum film profile and especially its width  $\bar{x}_0 - \bar{x}_i$ , the influence has been revealed earlier (fig. 21). The temperature distribution across the film width is shown in fig. 24.

In general, the more the number of lines, the nearer the function  $\bar{T}(\bar{x})$  is to the linear one (if  $\bar{T}_0$  is not too small). For the systems of lines with  $n=3$  the temperature distribution is close to the curve  $T(x) = \sqrt{\frac{\bar{x}-\bar{x}_0}{\bar{x}_0-\bar{x}}}$ , corresponding to an optimum single line. In figures 25 and 26 the dependence of the curve  $\bar{Q}(\bar{x})$  on the number of lines and on the cooled prism size  $\bar{x}_0$  is shown. The correlations between  $\bar{F}$  and the number of heat rejecting lines for different  $\xi$  and the sizes  $\bar{x}_0$  of the cooled prism are represented in figs. 28+30. The continuous curves reflect the results of this paper. The dotted line corresponds to the most profitable lines of a triangular profile; it is built on the basis of the results of paper /4/. The long-dash line /4/ corresponds to the most profitable lines of a rectangular profile. The dots on this figure correspond to the results of paper /1/. The correlation  $\bar{F}(n) = 1$  meeting the case of negligible lines' mutual irradiation is also plotted on the graph.

To evaluate the applicability of the produced results to real systems it should be noted, that the characteristic linear dimensions of the problem, i.e. the dimensions within which the phenomenon develops, may be found from the relations

$$W \approx n x'' \xi \bar{T}_0 \quad \text{and} \quad W \approx y'' \lambda n \frac{\bar{T}_0}{x''}$$

Nondimensional variables, introduced by the correlations  $\bar{y} y'' = y$ ,  $\bar{x} x'' = x$  must be of the same order (of the order 1, as it is seen in the graphs, taking into account, that  $x'' = n x''$  and  $y'' = n^2 y''$ )

therefrom it follows

$$\frac{y_0}{\Delta x} \approx \frac{y''}{x''} = \frac{W}{n \lambda \bar{T}_0}$$

where  $\Delta x = x - x_0$ .

A film will be thin, if  $\frac{y_0}{\Delta x} \ll 1$ , i.e.  $W \ll n \lambda \bar{T}_0$ . It is seen that for the prescribed  $W$  and  $\bar{T}_0$  the validity of the obtained results increases with the increase of the number of lines.

15

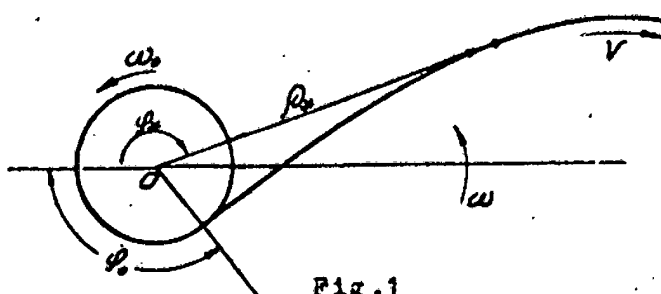


Fig. 1

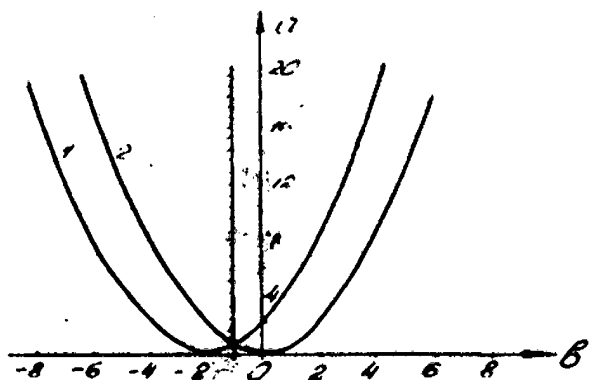


Fig. 2 1)  $\alpha = 2(1 + \frac{\beta}{2})$   
2)  $\alpha = \frac{6\beta}{2}$

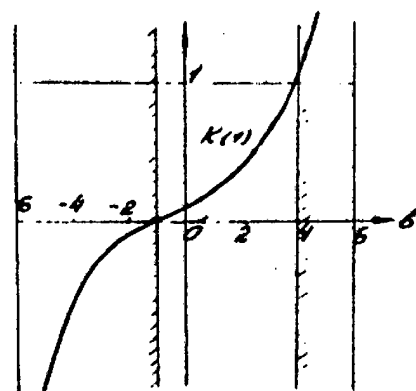
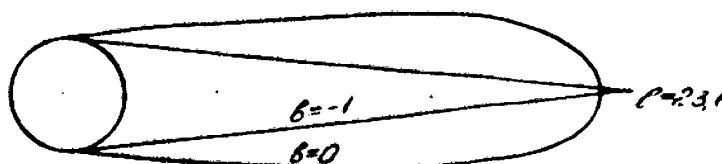
Fig. 3  $a = 18$ 

Fig. 4

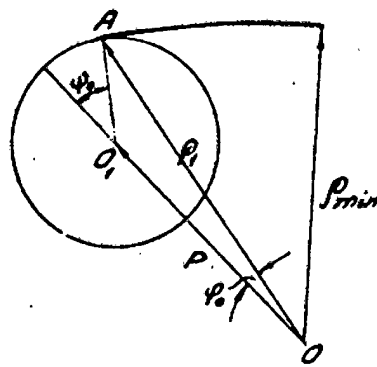


Fig. 5

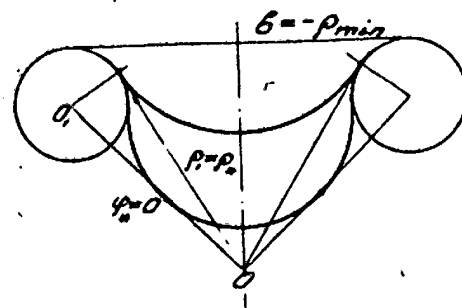


Fig. 6

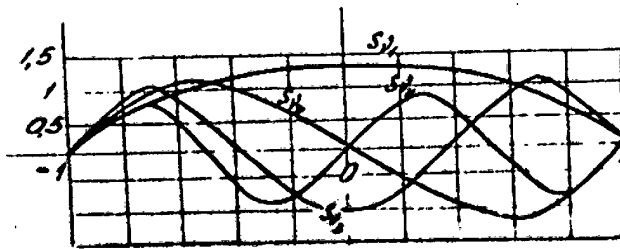


Fig. 7

$\alpha = 50$   
 $\beta = 5$   
 $\rho_0 = 10$   
 $P_{min} = 2$

16

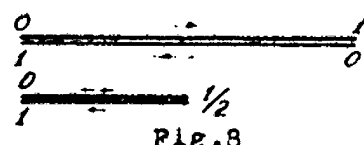


Fig. 8

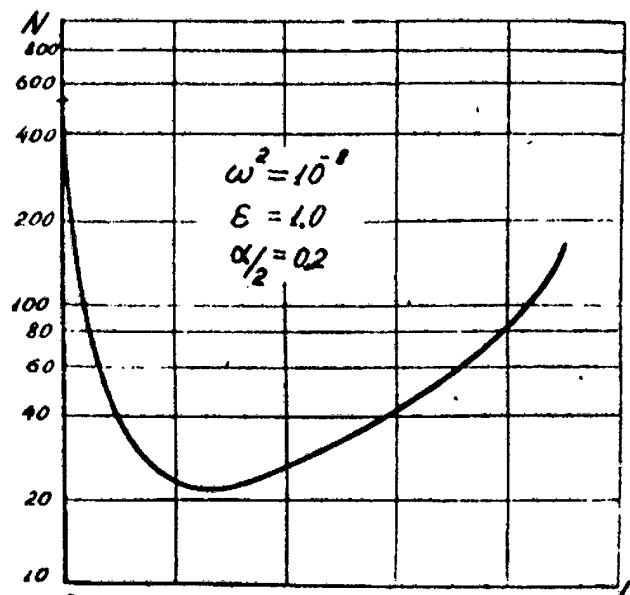


Fig. 9

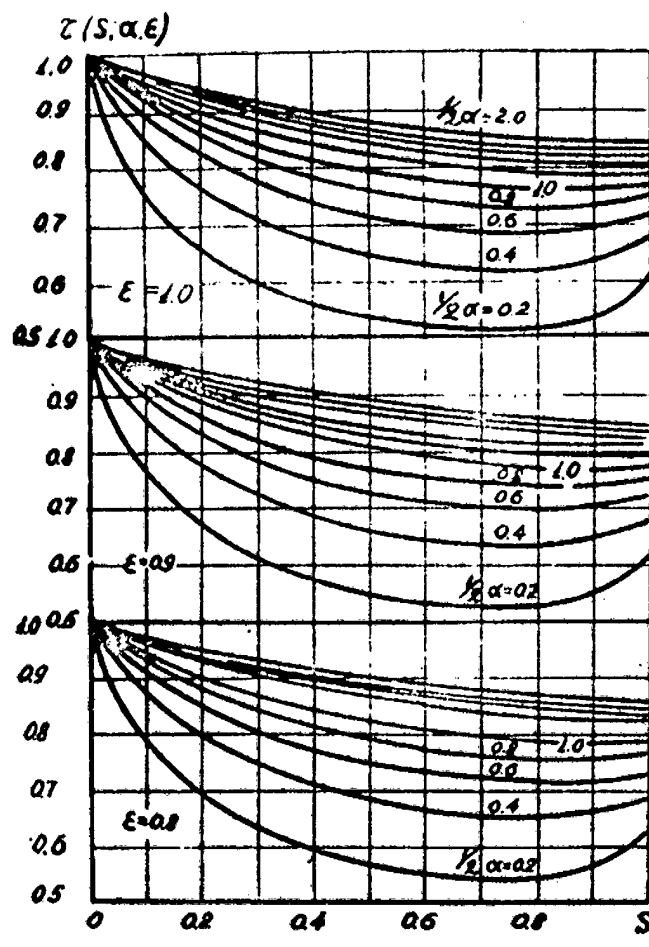


Fig. 10

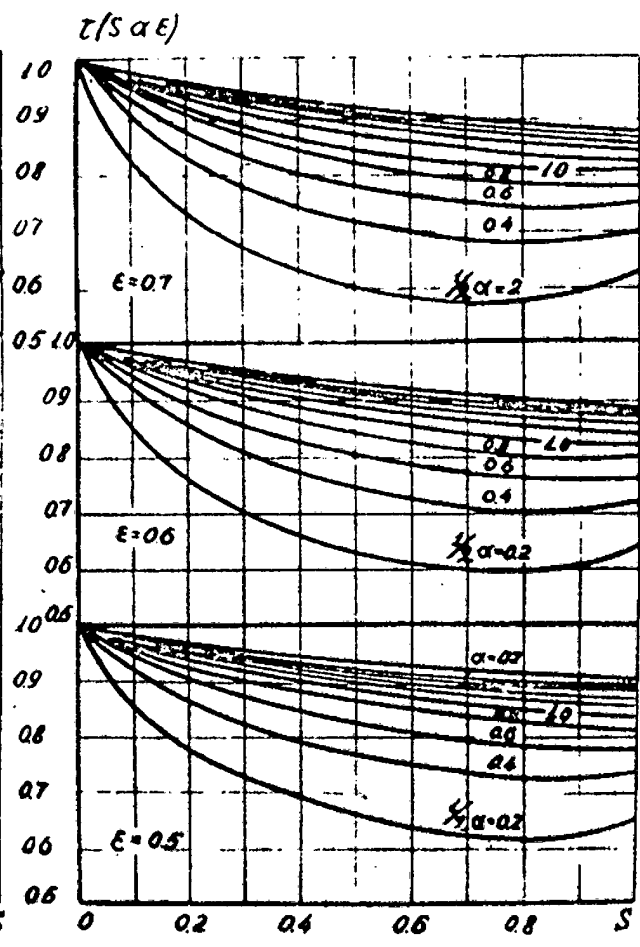


Fig. 11

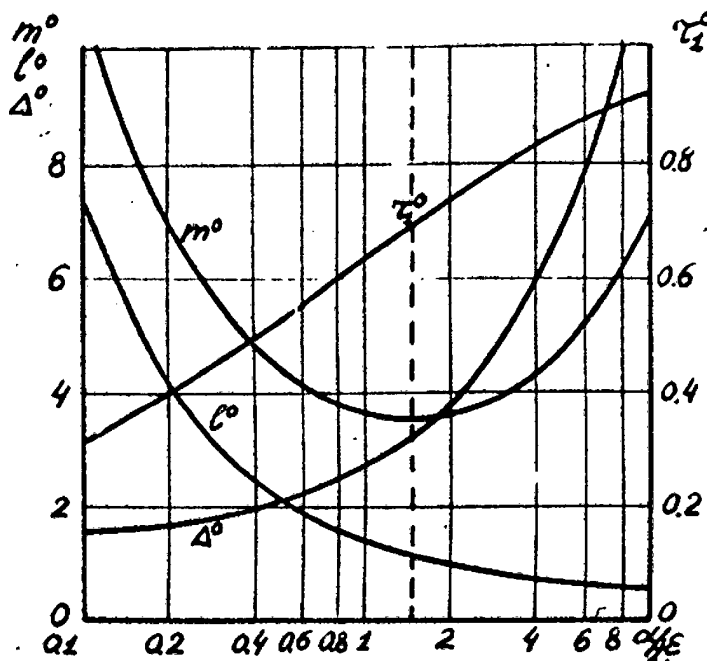


Fig. 12

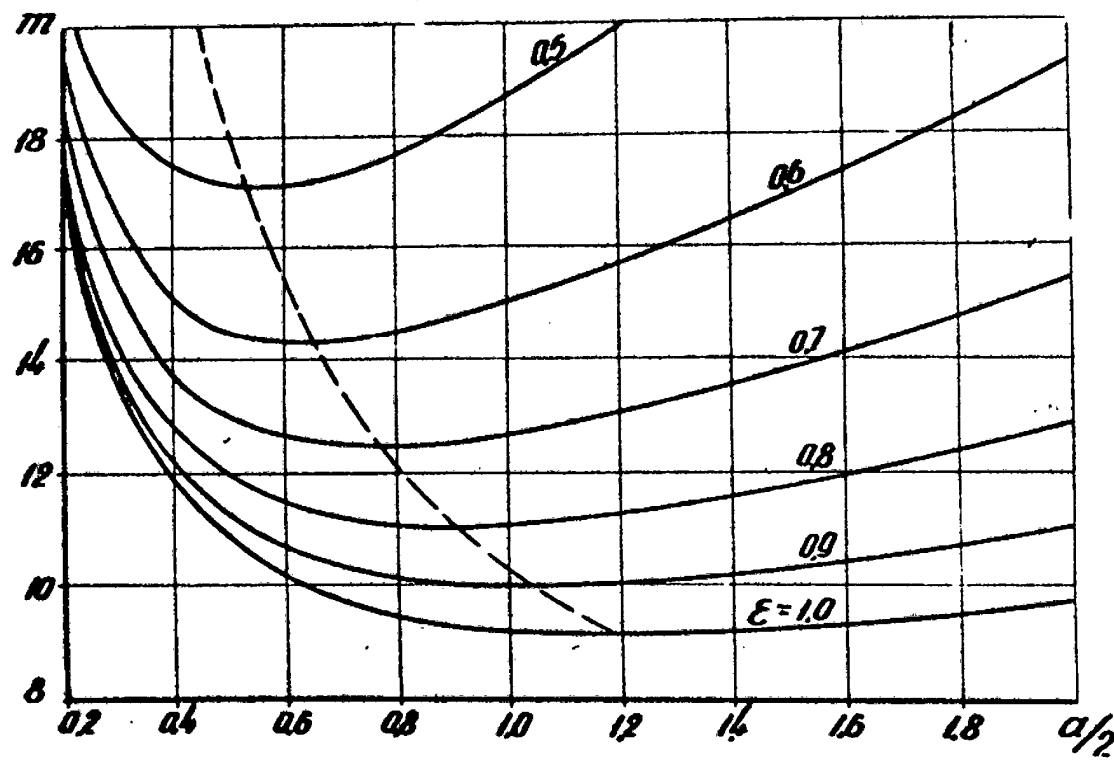


Fig. 13

'B

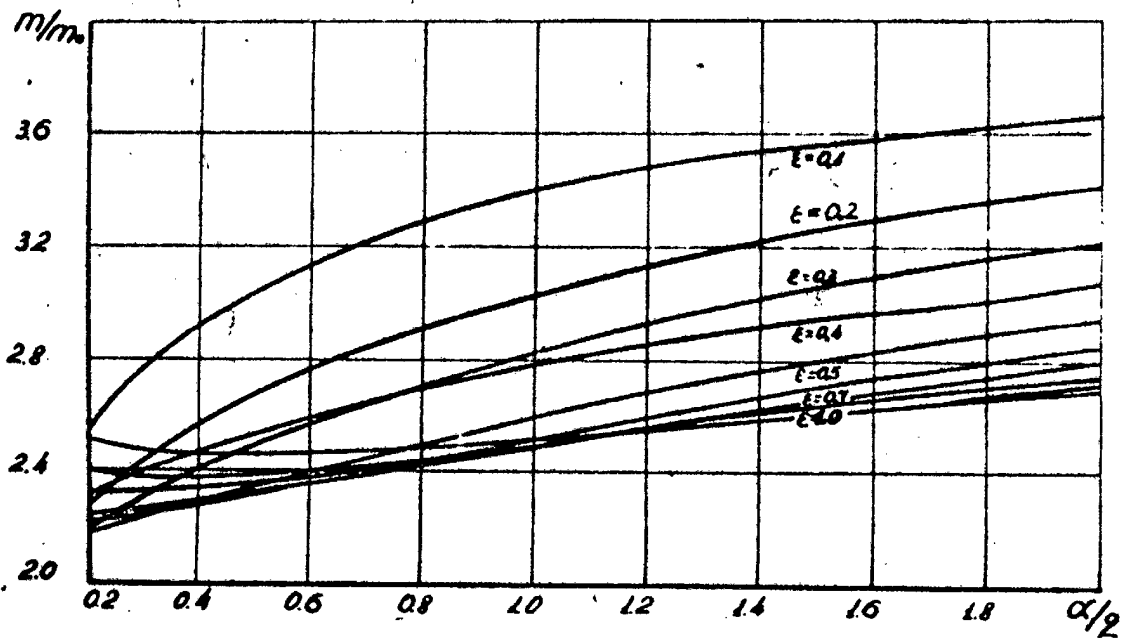


Fig. 14

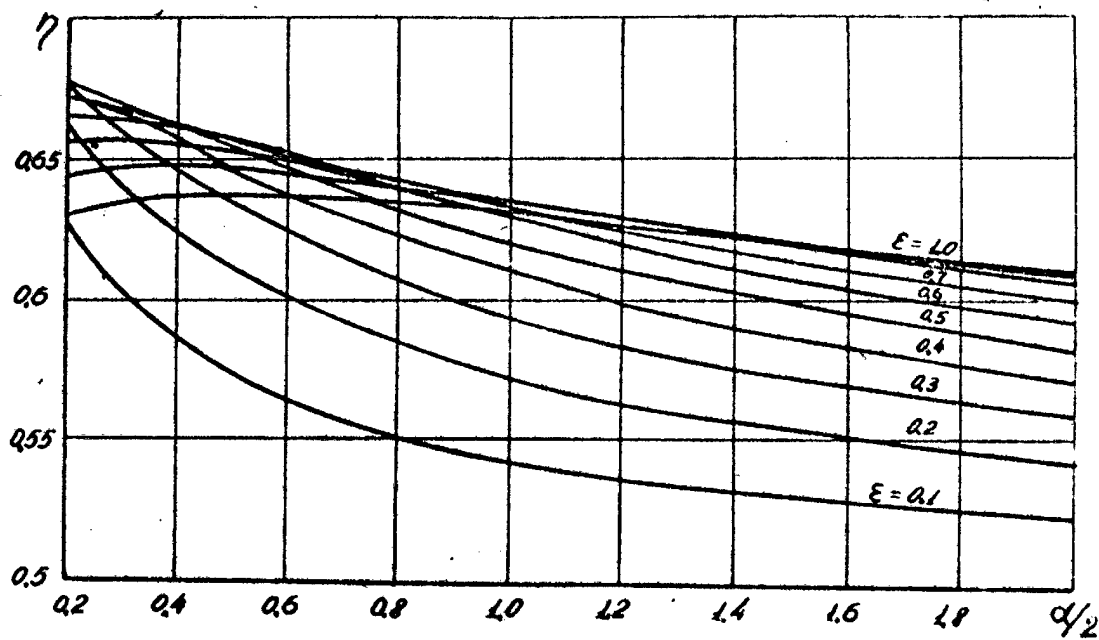


Fig. 15

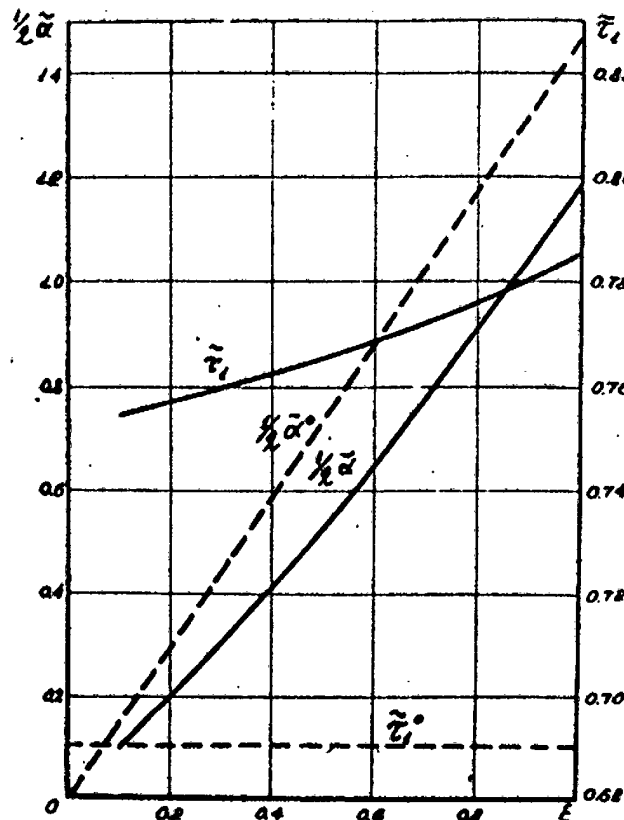


Fig. 16

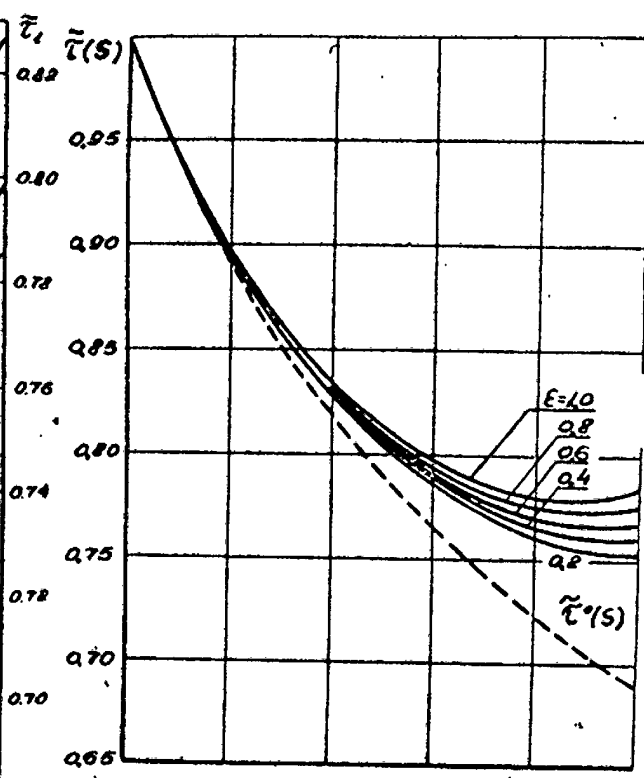


Fig. 17

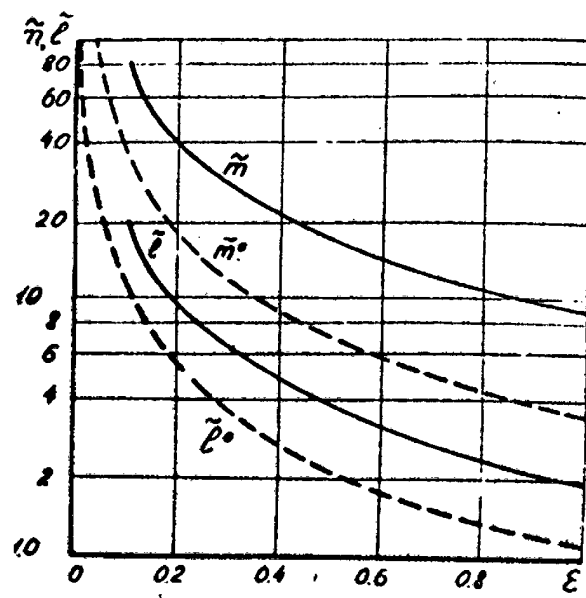


Fig. 18

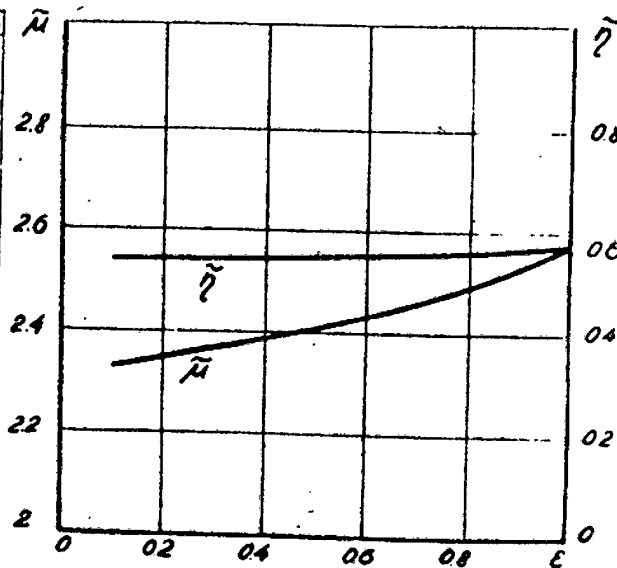


Fig. 19

20

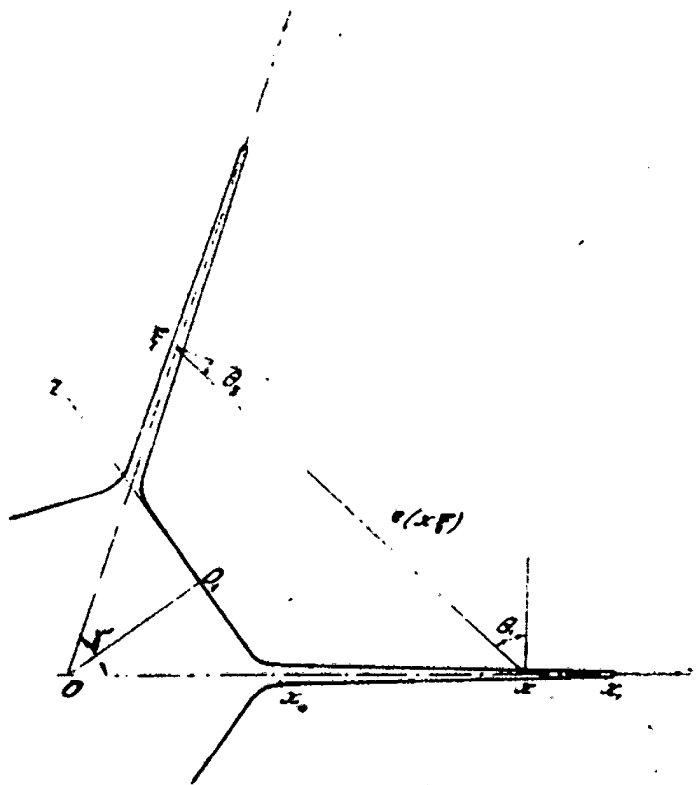


Fig. 20

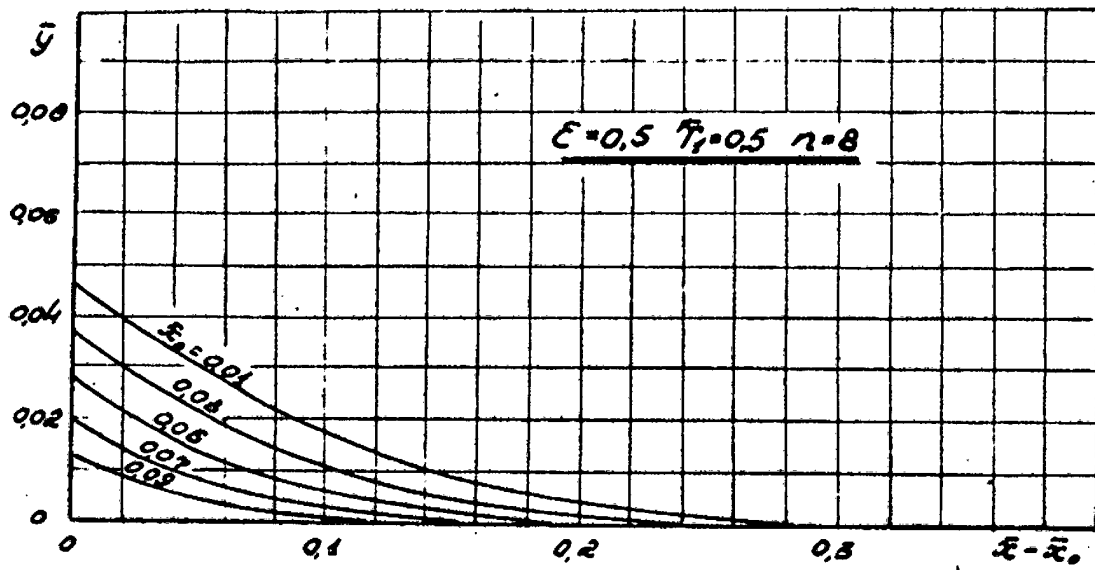
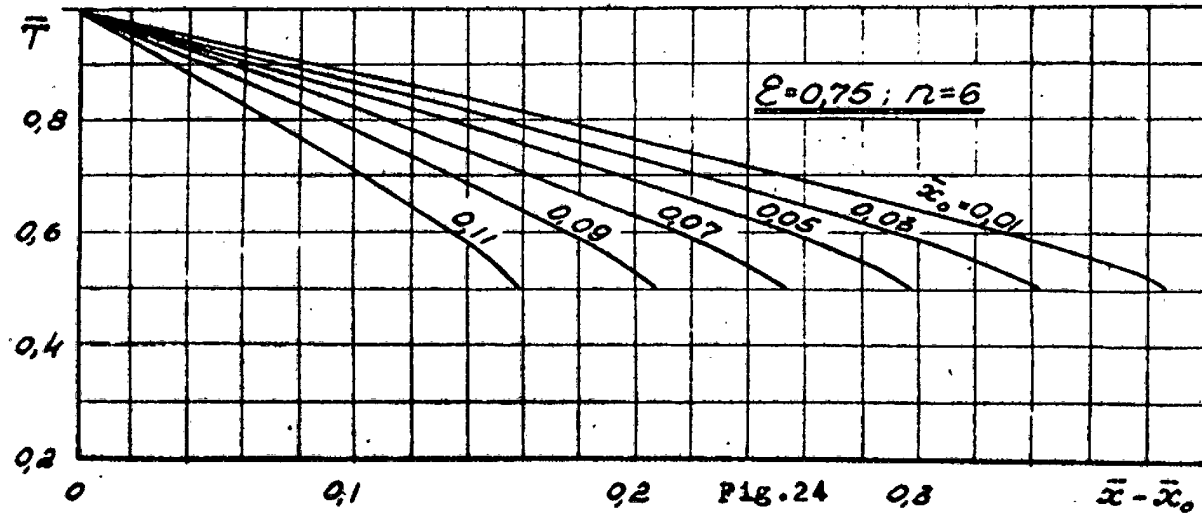
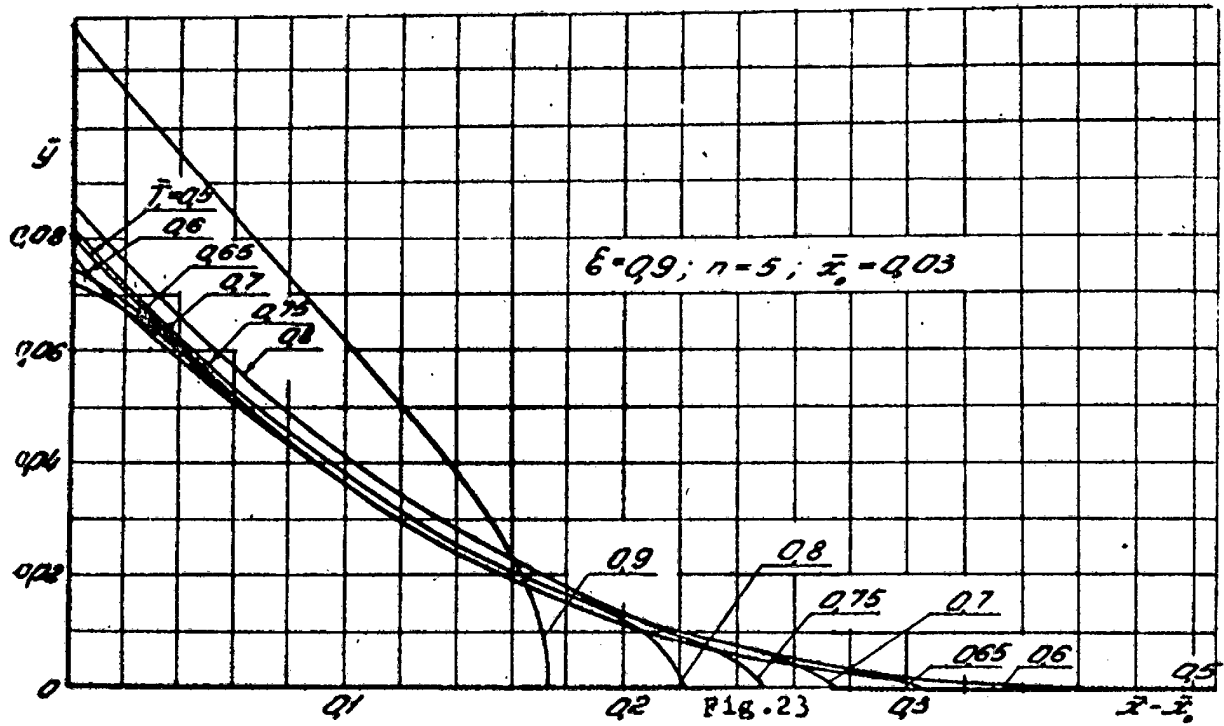
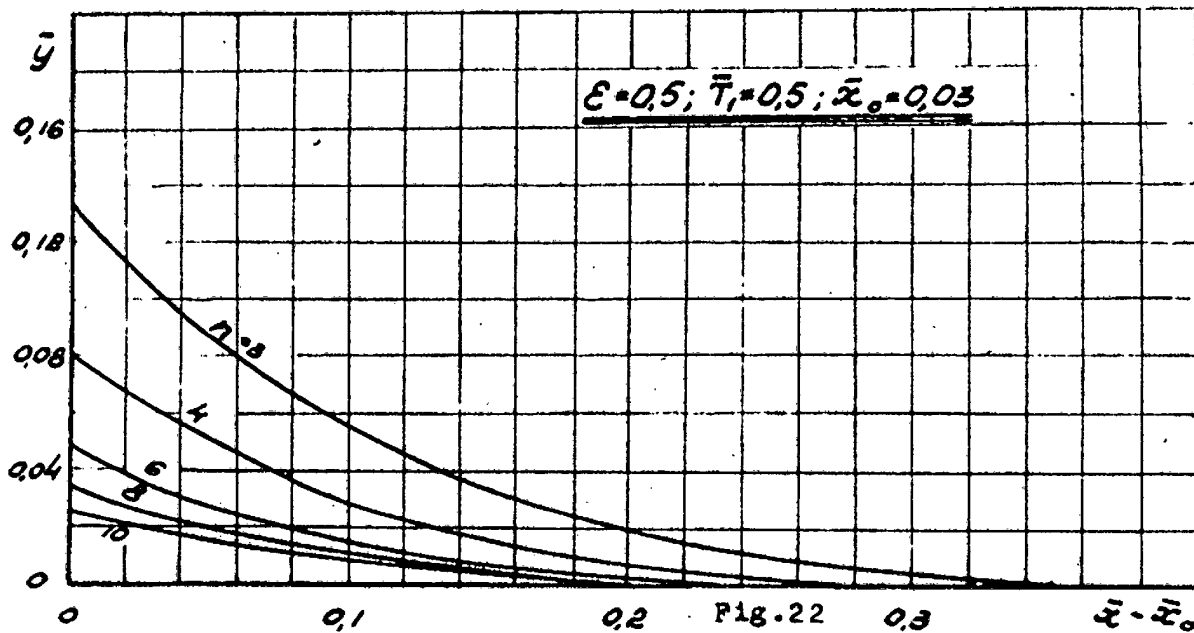


Fig. 21



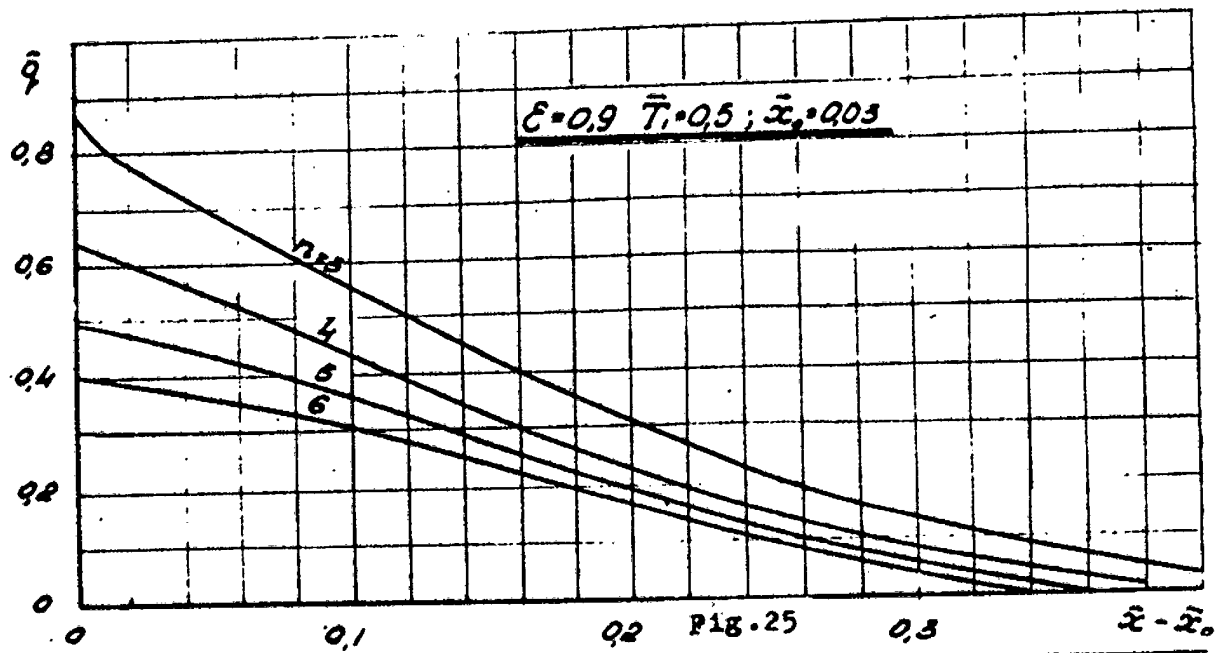


Fig. 25

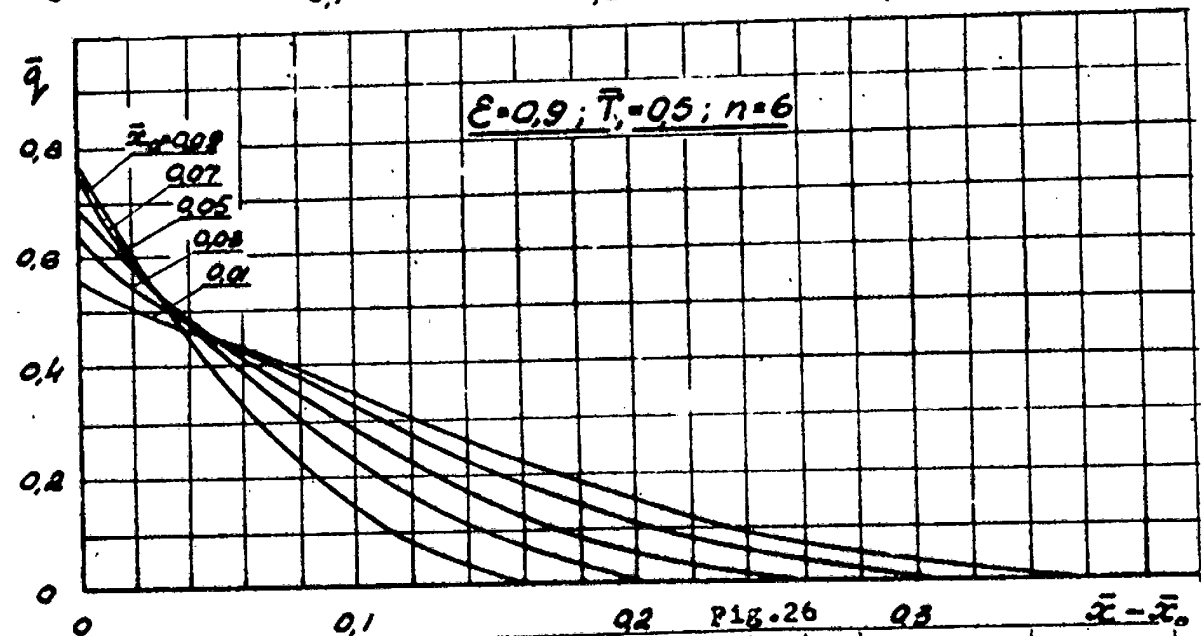


Fig. 26

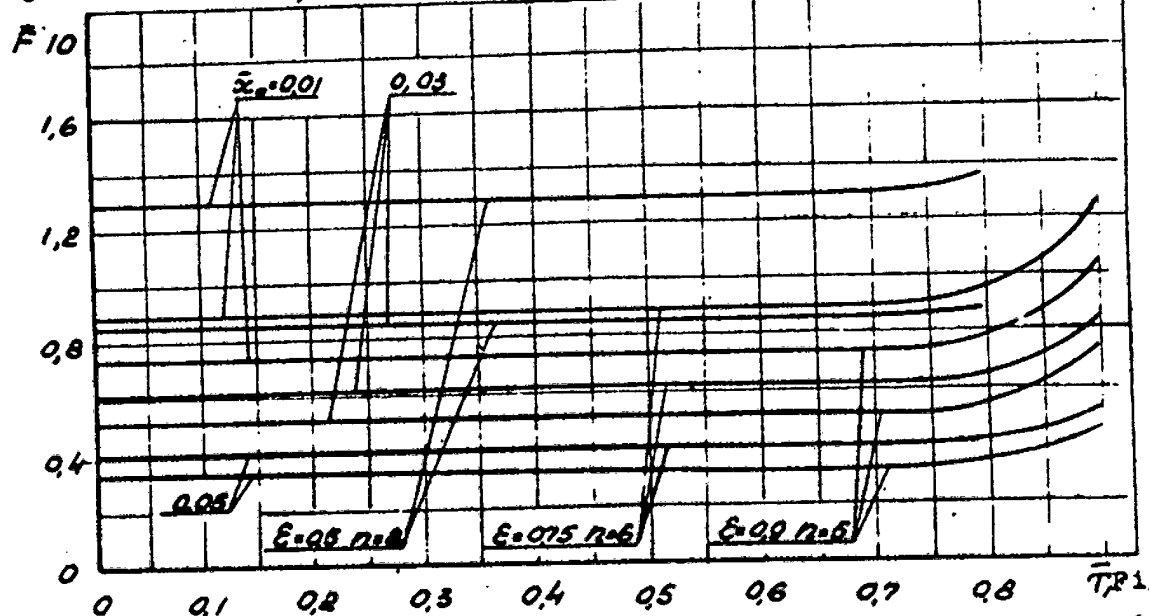


Fig. 27

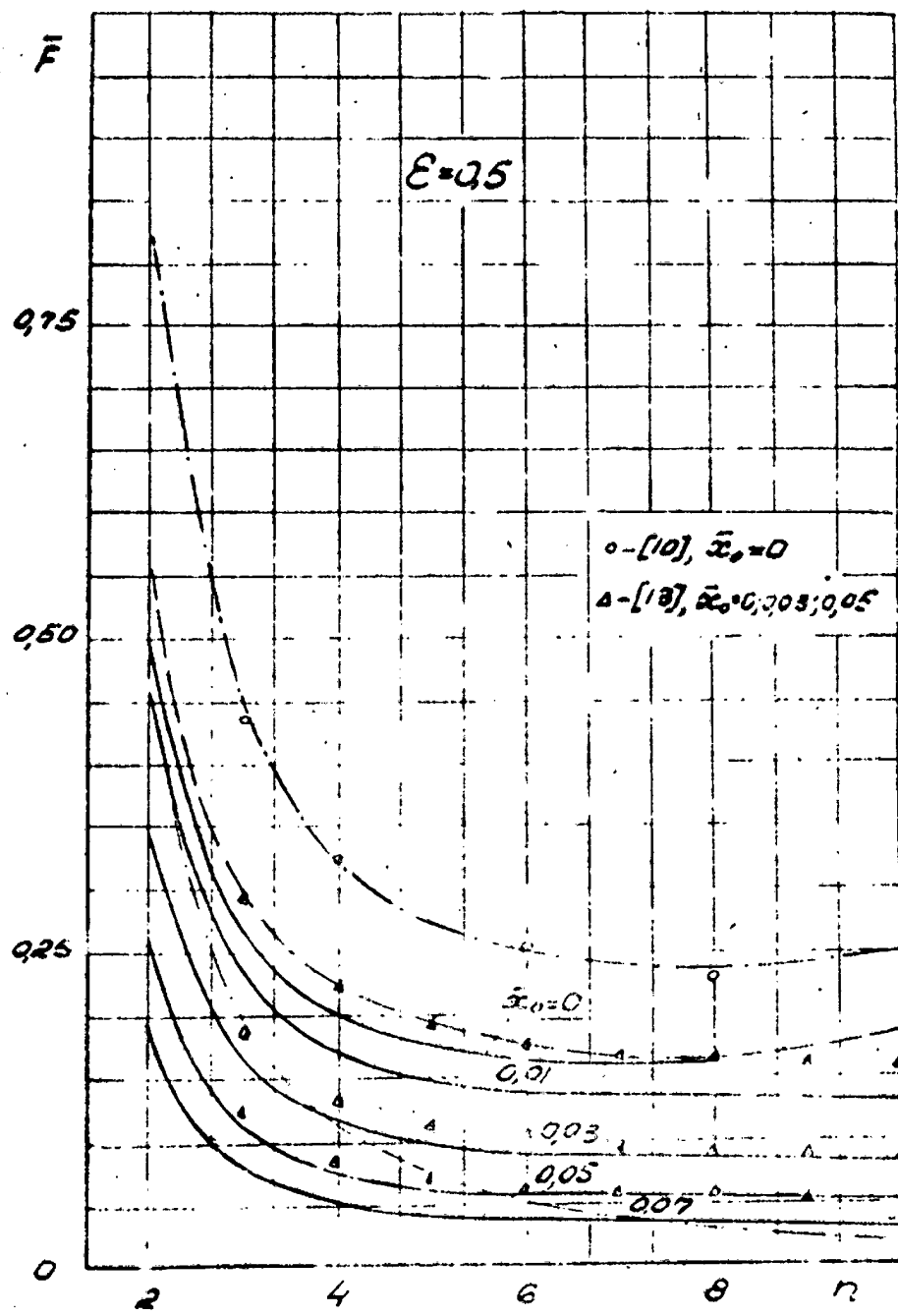


Fig. 28

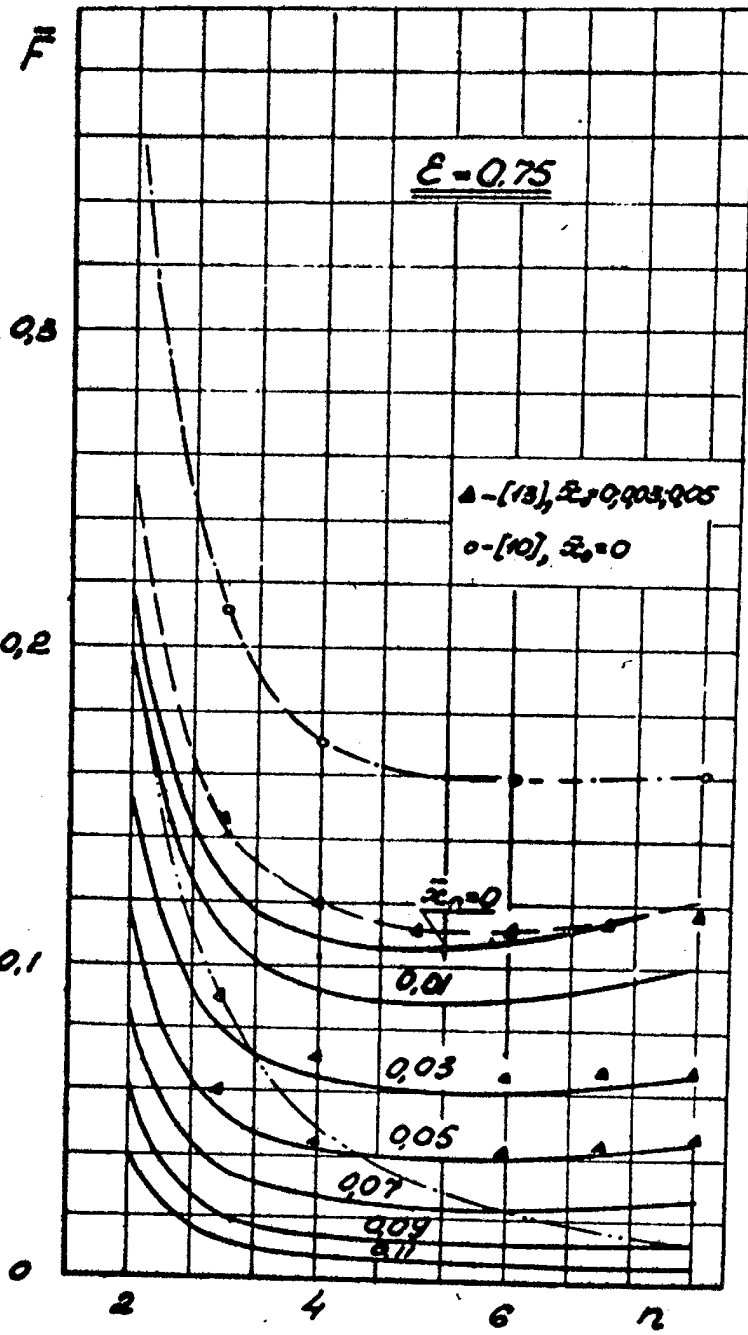


Fig. 29

25

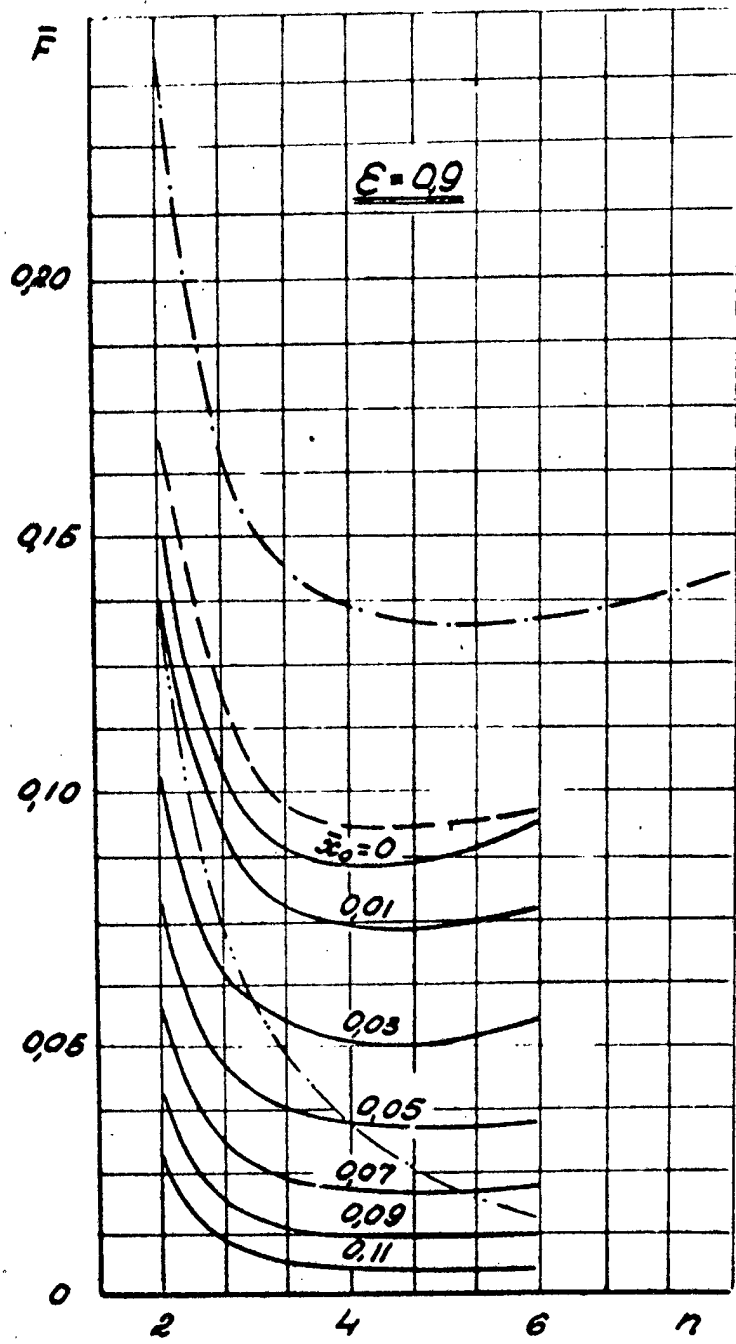


Fig. 30

## Л И Т Е Р А Т У Р А

1. WEATHERSTON, R.C., SMITH W.E. A method of heat rejection from space powerplants. ARS, 1960, vol.30, Nj.
2. WEATHERSTON, R.C., SMITH, W.E. A new type of thermal radiator for space vehicles. Aeronautical Eng., 1961, vol.20, N1.
3. СТАСЕНКО А.Л. Форма гибкой нити в поле центробежных сил. Изв. АН СССР, ОТН, Механика и машиностроение, 1962, №6.
4. BURGE H.L. Revolving belt space radiator. ARS, 1962, vol.32, N8.
5. APPEL P., LACOUR S. Principles de la theorie des fonctions elliptiques et leurs applications. Paris, 1922.
6. HALPHEN G.H. Fonctions elliptiques. II Paris, 1888.
7. ТИТЧАРШ Э.И. Разложения по собственным функциям, связанные с дифференциальными уравнениями второго порядка, I ИД 1960.
8. BARTAS, T.G., SELLENS, W.H. Radiation fin effectiveness. Transactions of ASME. JOURNAL of Heat Transfer, 81, 1 (1960).
9. CHEN, Y.L. On minimum weight rectangular fins. Journal of Aero/space Sciences, 27, 11 (1960).
10. NILSON E.N., CURRY, R. The minimum weight straight fins of triangular profile radiating to space. Journal of Aero/space sciences, 27, 2 (1960).
11. WILKINS J.E. Jr. Minimizing the mass of thin radiating fins. Journal of Aero/space sciences, 27, 2 (1960).
12. WILKINS, J.E.Jr. Minimizing mass fins, which transfer heat only by radiation to surrounding at absolute zero. Journal of the Society for Industrial and Appl. Mathematics. v.8, N4, Dec. 1960.
13. WILKINS, J.E. Jr. Minimum mass thin fins for space radiators. Proceedings of the Heat Transfer and Fluid Mechanics Institute, Stanford Univ. 1960.
14. WILKINS J.E. Jr. Minimum mass fins and constant gradient. Journal of the society for Industrial and Appl. Math., v.10, N1. 1962.
15. ПРОДЗОВСКИЙ Г.Л. Оптимальная форма теплоотводящих ребер, охлаждаемых излучением. Изв. АН СССР, ОТН. Энергетика и автоматика. №6, 1962.
16. ECKERT E.R.G., IRVING T.F.Jr., SPAHRON M. Analytical formulation for radiating fins with mutual irradiation. Journ. of the American Rocket Society, 30, 7, 1960.
17. SPAHRON M., ECKERT E.R.G., IRVING T.F.Jr. The effectiveness of radiating fins with mutual irradiation. Jour. Aero/space Sciences, 28, 10 (1960).

18. KARLEKAR B.V. and CHAO B.J. Mass minimisation of radiating trapezoidal fins with negligible base cylinder interaction. International Journal of Heat and Mass Transfer, v.6, N1, 1963.
  19. ФРОЛОВ В.В. Оптимальная форма теплоотводящих ребер с учетом взаимного облучения. Изв. АН СССР, ОТН. Энергетика и автоматика №6, 1962.
  20. ВАСАНОВ Ю.А., ЖУЛЕВ Ю.Г. Оптимальная форма треугольных теплоотводящих ребер с учетом взаимного облучения ребер и охлаждаемой поверхности. Изв. АН СССР. Энергетика и транспорт (в печати).
  21. КОНТОГОВИЧ Л.В. Успехи математических наук, 1948, т.3 вып.6.
  22. Своевременная математика для инженеров. Под ред. Э.Ф. БЕКЕНБАХ. пер. с англ. под ред. И.И. ВЕКУА. ИЛ. 1958.
-